

**INITIAL CHARACTERIZATION OF PEPTIDOGLYCAN
O-ACETYLATION AND THE EFFECTS ON COLONIZATION
FACTORS OF *CAMPYLOBACTER JEJUNI***

by

Reuben Danny Ha

H.B.Sc., Lakehead University, 2012

**A THESIS SUBMITTED IN PARTIAL FULFILLMENT OF THE
REQUIREMENTS FOR THE DEGREE OF**

MASTER OF SCIENCE

in

**The Faculty of Graduate and Postdoctoral Studies
(Microbiology and Immunology)**

**THE UNIVERSITY OF BRITISH COLUMBIA
(VANCOUVER)**

April, 2016

©Reuben Danny Ha, 2016

ABSTRACT

Campylobacter jejuni is a leading cause of bacterial gastroenteritis in the developed world. Despite its prevalence, its pathogenesis is poorly understood. It lacks clear virulence factors such as those described for other enteropathogens. The characteristic helical shape of *C. jejuni*, maintained by the peptidoglycan (PG) layer, is important for colonization and host-pathogen interactions. Therefore, changes in morphology and the underlying PG greatly affect the physiology and biology of the organism. O-Acetylation of Peptidoglycan (OAP) is a phenomenon by which bacteria acetylate the C6 hydroxyl group of N-acetylmuramic acid in the glycan backbone to confer resistance to lysozyme and control lytic transglycosylase activity. The OAP gene cluster consists of a transmembrane PG O-acetyltransferase A (*patA*) for translocation of acetate into the periplasm, a periplasmic PG O-acetyltransferase B (*patB*) responsible for O-acetylation of N-acetylmuramic acid (MurNAc), and an O-acetylpeptidoglycan esterase (*apeI*) for de-O-acetylation. Reduced OAP in $\Delta patA$ and $\Delta patB$ has a minimal effect on growth and fitness under the conditions tested. However, accumulation of OAP in $\Delta apeI$ results in marked differences in peptidoglycan biochemistry including changes in O-acetylation levels, anhydromuropeptide levels, and PG changes not expected to be a direct result of Ape1 activity. This suggests that OAP may be a form of substrate level regulation in PG metabolism. Ape1 acetyltransferase activity was confirmed *in vitro* using *p*-nitrophenyl acetate and O-acetylated PG as substrates. In addition, $\Delta apeI$ exhibits defects in pathogenesis-associated phenotypes including cell shape, motility, biofilm formation, and sodium deoxycholate sensitivity. The mutant is also impaired for chick colonization and adhesion, and invasion and intracellular survival in INT407 epithelial cells lines *in vitro*. The importance of Ape1 activity to *C. jejuni* biology makes it a good candidate as a novel antimicrobial target.

PREFACE

Initial conceptualization of the project was by supervisory author Dr. Erin Gaynor and Dr. Emilisa Frirdich and was carried out by me with guidance and training from Dr. Frirdich. Experiments were carried out by me at the Life Sciences Institute at the University of British Columbia under the UBC Research Ethics Board Biosafety Committee Certificate of Approval #B10-0061, unless otherwise stated. Initial deletion mutants were generated by Dr. Frirdich and complementation was performed by me. Samples were prepared for TEM by me and images were taken by Jenny Vermeulen at the Bioimaging Facility of UBC. Interpretation and analysis of research was performed by me with the help of the Gaynor research group and collaborators.

For the muropeptide composition analysis, samples were prepared by me using techniques established previously by Dr. Frirdich (1) and sent to Dr. Jacob Biboy in Dr. Waldemar Vollmer's research group at the Institute of Cell and Molecular Biosciences at Newcastle University in the United Kingdom for HPLC-MS analysis (2,3). Determination of O-acetylation levels was performed by PhD Candidate David Sychantha (MSc) in Dr. Anthony Clarke's research group in the Department of Molecular and Cellular Biology at the University of Guelph on samples prepared by me with the assistance of Jenny Vermeulen at UBC (4,5). Chick Colonization studies were performed at the University of Michigan Medical School with Dr. Michael Taveirne and Dr. Jeremiah Johnson in Dr. Victor DiRita's research group in the Department of Microbiology and Immunology in accordance with protocol 10462 approved by the University of Michigan Committee on Care and Use of Animals as described (1,6).

The research described in Chapter 3, has resulted in a manuscript that has been submitted. It was written and prepared by me with help in interpretation from primarily Dr. Frirdich and Dr. Gaynor and assistance from co-authors in interpreting research performed by collaborators as listed above.

TABLE OF CONTENTS

Abstract.....	ii
Preface	iii
Table of Contents.....	iv
List of Tables	vi
List of Figures.....	vii
List of Abbreviations	viii
Acknowledgements.....	xi
1. Introduction.....	1
1.1. <i>Campylobacter jejuni</i> : General Background.....	1
1.2. <i>Campylobacter</i> as a Genus.....	1
1.3. Campylobacteriosis: <i>Campylobacter</i> -mediated Infections	2
1.3.1. <i>Campylobacter</i> Enteritis	2
1.3.2. Medical Sequelae	4
1.3.3. Treatment and Prevention of <i>C. jejuni</i> Infections	8
1.4. Prevalence and Significance of <i>C. jejuni</i>	9
1.4.1. Epidemiology of <i>C. jejuni</i> Infection.....	9
1.4.2. Sources of Infection	11
1.5. <i>C. jejuni</i> Physiology in Survival, Transmission, and Host-Bacterial Interactions.....	11
1.5.1. Flagella, Motility, and Chemotaxis.....	12
1.5.2. Biofilm Formation.....	13
1.5.3. <i>C. jejuni</i> Association, Invasion, and Survival within Host Cell.....	13
1.5.4. Lipooligosaccharide and Capsule	14
1.6. Peptidoglycan: The Bacterial Cell Wall.....	15
1.6.1. Peptidoglycan Metabolism.....	16
1.6.2. Peptidoglycan, Cell Shape, and Pathogenesis.....	18
1.6.3. Significance of Peptidoglycan Signaling and its Role in Host-Response to Infection	18
1.6.4. Peptidoglycan as a Target for the Design of Antimicrobial Compounds.....	19
1.6.5. O-Acetylation of Peptidoglycan.....	20
1.7. Hypothesis and Research Objectives	23
1.7.1 Objectives (Aims) of the Project.....	23
2. Materials and Methods.....	24
2.1. Strains and Growth Conditions	24

2.2. Deletion and Complementation of OAP mutants.....	24
2.3. Cloning of Ape1 for Expression and Purification.....	26
2.4. PG Isolation and Assessment of O-Acetylation Levels	26
2.5. PG Isolation and Muropeptide Analysis	28
2.6. Expression, Purification, and Biochemical Assays of Ape1	29
2.7. Microscopy and Celltool Shape Analysis	31
2.8. Phenotypic Characterization of OAP Mutants: Motility, Biofilm, Cell Surface Hydrophobicity, and Minimum Inhibitory/Bactericidal Concentrations	32
2.9. Chick Colonization Studies.....	34
2.10. Gentamicin Protection Assay.....	34
2.11. Interleukin-8 Quantification.....	35
3. Results.....	36
3.1. <i>C. jejuni</i> OAP genes were identified by BLAST and insertion mutations were generated	36
3.2. O-acetylation levels of purified PG from deletion mutants reflect the putative functions of the <i>C. jejuni</i> OAP gene cluster	37
3.3. <i>C. jejuni</i> OAP mutants exhibit altered PG muropeptide profiles, with Δ <i>ape1</i> displaying the most dramatic changes from wild type	38
3.4. Recombinant Ape1 exhibits acetyltransferase activity <i>in vitro</i> on artificial substrate <i>p</i> -nitrophenylacetate and natural substrate O-Acetylated PG	42
3.5. Microscopy and Celltool analyses of <i>C. jejuni</i> Δ <i>ape1</i> population morphology reveal shape pleomorphism	45
3.6. Phenotypic analyses reveal the importance of O-acetylpeptidoglycan esterase activity on various aspects of <i>C. jejuni</i> physiology.	50
3.7. Ape1 is required for efficient <i>C. jejuni</i> bacterial-host interaction.....	52
4. Discussion and Conclusions.....	56
4.1 Future Directions	64
References.....	68
Appendix 1. Bacterial strains or plasmids used in this study.....	82
Appendix 2. List of primers used with underlined restriction sites in lowercase	84
Appendix 3. Muropeptide composition of <i>C. jejuni</i> wild-type 81-176, Δ <i>ape1</i> , Δ <i>patB</i> , and Δ <i>patA</i> showing relative abundance of muropeptides corresponding to peaks in HPLC chromatograms (Figure 3) of samples analyzed in January 2013.	86
Appendix 4. Muropeptide composition of <i>C. jejuni</i> wild-type 81-176, Δ <i>ape1</i> ^C , Δ <i>patB</i> ^C , Δ <i>patA</i> ^C , and Δ <i>oap</i> showing relative abundance of muropeptides corresponding to peaks in HPLC chromatograms (Figure 3) of samples analyzed in August 2013.....	87

LIST OF TABLES

Table 1. O-Acetylation levels of PG of *C. jejuni* 81-176, Δape , $\Delta apeI$ complement ($\Delta apeI^C$), $\Delta patB$, $\Delta patA$ and Δoap (a mutant in which the entire cluster was deleted: Δape , $\Delta patB$ and $\Delta patA$), as determined by base-catalyzed hydrolysis reported as a % of O-acetylation relative to MurNAc content.. 38

Table 2. Summary of PG mucopeptide composition for *C. jejuni* 81-176, Δape , $\Delta patB$, $\Delta patA$, $\Delta apeI^C$, $\Delta patB^C$, $\Delta patA^C$, and Δoap 41

Table 3. MIC₅₀ of *C. jejuni* OAP mutants determined by broth dilution.¹ 53

LIST OF FIGURES

Figure 1. Peptidoglycan is the structural component of the bacterial cellular envelope and is highly variable due to PG remodeling and modification machinery.....	22
Figure 2. OAP gene cluster in <i>C. jejuni</i> and design for deletion and complementation.	36
Figure 3. HPLC chromatograms of <i>C. jejuni</i> muropeptides and proposed structures.	39
Figure 4. Design of Ape1 expression construct and assays for acetyltransferase activity.....	43
Figure 5. DICM and TEM reveal shape heterogeneity in $\Delta ape1$	46
Figure 6. Celltool analysis of wild-type strain 81-176, $\Delta ape1$, $\Delta ape1^C$, $\Delta patB$, $\Delta patA$, and Δoap population morphology at early-log phase.....	47
Figure 7. Celltool analysis of wild-type strain 81-176, $\Delta ape1$, $\Delta ape1^C$, $\Delta patB$, $\Delta patA$, and Δoap population morphology at mid-log phase.	48
Figure 8. Motility, biofilm formation, and cell surface hydrophobicity of OAP mutants.	51
Figure 9. The effect of OAP levels on <i>C. jejuni</i> host-bacterial interactions.	54

LIST OF ABBREVIATIONS

(<u> </u>) ^R	Resistance to (antibiotic)
AIDS	Acquired immune deficiency syndrome
anhMP	Anhydromuropeptide
Ap	Ampicillin
<i>ape1</i>	<i>Cjj81176_0638</i> gene O-acetylpeptidoglycan esterase
<i>aphA-3</i>	aminoglycoside phosphotransferase type III
bp	Base pairs
C ₅₅	C55-isoprenyl pyrophosphate
C6-OH	Hydroxyl functional group of 6th Carbon in MurNAc
Caco-2	Human epithelial colorectal adenocarcinoma cells
CadF	Campylobacter adhesion to fibronectin
CAMP	Cationic antimicrobial peptides
CD4	Cluster of differentiation 4
cfu	Colony-forming units
Cia	Campylobacter invasion antigens
Cm	Chloramphenicol
CPS	Capsular polysaccharides
D-ala	D-alanine
DALY	Disability-adjusted life years
D-glu	D-glutamic acid
DICM	Differential interference contrast microscopy
FBS	Fetal bovine serum
GBS	Guillain-Barré syndrome
GlcNAc	N-acetylglucosamine
HIV	Human immunodeficiency virus
HPLC	High-performance liquid chromatography
IBD	Inflammatory Bowel Disease
INT-407	Originally derived from the jejunum and ileum but HeLa contaminant
IPTG	Isopropyl β -D-1-thiogalactopyranoside

Km	Kanamycin
L-ala	L-alanine
LB	Lysogeny broth
L-lys	L-lysine
LOS	Lipooligosaccharide
LPS	Lipopolysaccharide
Lys	lysozyme
LytTG	Lytic transglycosylase
MAMP	Microbe-associated molecular pattern
MBC	Minimum bactericidal concentration
MEM	Minimum essential medium
meso-DAP	meso-Diaminopimelic acid
MH	Mueller-Hinton
MIC	Minimum inhibitory concentration
MOI	Multiplicity of infection
<i>motA/B</i>	Motility Protein A/B
MS	Mass spectrometry
MurNAc	N-acetylmuramic acid
MWCO	Molecular weight cut-off
NF- κ B	Nuclear factor kappa-light-chain-enhancer of activated B cells
Ni-NTA	Nickel-nitrilotriacetic acid
NLR	NOD-like receptor
NOD	Nucleotide-binding oligomerization domain
OAP	O-acetylation of peptidoglycan
<i>oatA/B</i>	O-acetyltransferase A and B
OD ₆₀₀	Optical density measured at 600 nm
<i>patA</i>	<i>Cjj81176_0640</i> Peptidoglycan O-acetyltransferase A
<i>patB</i>	<i>Cjj81176_0639</i> Peptidoglycan O-acetyltransferase B
PBP	Penicillin binding protein
PC	Principal component
PCA	Principal component analysis

PCR	Polymerase chain reaction
pen/strep	Penicillin/streptomycin
PG	Peptidoglycan
PGBD	Peptidoglycan Binding Domain
<i>pgp1</i>	Peptidoglycan peptidase 1
<i>pgp2</i>	Peptidoglycan peptidase 2
PGRP	Peptidoglycan Recognition Protein
<i>pNPAc</i>	<i>p</i> -nitrophenylacetate
PRR	Pattern Recognition receptor
pRRC	Cm ^R cassette cloned into a fragment of rRNA gene cluster in a commercial plasmid pGEM-T
PWR	Power
RA	Reactive arthritis
RNA	Ribonucleic acid
rpm	Revolutions per minute
rRNA	Ribosomal RNA
RT-qPCR	Reverse transcriptase quantitative PCR
SDS	Sodium Dodecyl Sulphate
SDS-PAGE	SDS-polyacrylamide gel electrophoresis
Ser/Thr	Serine/ Threonine
T	Trimethoprim
TEM	Transmission electron microscopy
TLR	Toll-like receptor
Tris	Tris(hydroxymethyl)aminomethane
UDP	Uridine Diphosphate
UDP-GlcNAc	Uridine diphosphate -N-acetylglucosamine
UDP-MurNAc	Uridine diphosphate -N-acetylmuramic acid
V	Vancomycin

ACKNOWLEDGEMENTS

I would like to thank my supervisor Erin C. Gaynor for agreeing to take me in as an MSc student. None of this work could have been accomplished without the support throughout my experience here. I would also like to thank Emilisa Frirdich, my mentor and friend, for the on-hands guidance and knowledge that I will carry through into my future. I would like to thank the rest of the Gaynor research group for their assistance with heavily labour intensive experiments, valuable intellectual input, and for keeping me company during long-nights at the bench and desk. I would also like to thank Tom Beatty, Brett Finlay, and Michael Murphy for agreeing to be members of my Thesis and Supervisory Committees and for their constructive criticism, knowledgeable suggestions, and encouragement. I would also like to extend my gratitude to Dr. Jacob Biboy and Dr. Waldemar Vollmer at Newcastle University, David Sychantha and Dr. Anthony Clarke at the University of Guelph, and Dr. Michael Taveirne and Dr. Jeremiah Johnson in Dr. Victor DiRita at the University of Michigan Medical School for agreeing to collaborate with us to tell this story.

Additionally, I would like to thank the Canadian Institute for Health Research (CIHR) and Natural Sciences and Engineering Research Council (NSERC) for funding the Gaynor research group and for the Canada Graduate Scholarship-Master's Award, respectively.

Finally, I would like to thank my family and friends for their continued moral support. To my family, we celebrated during happy times and remained strong through difficult times, even though we are far apart. I look forward to a future where we will continue to support each other from wherever we may be. To my friends in UBC K-Wave and UBC Dance Horizons, thank you for giving me the chance to enjoy my non-academic time at UBC and making it a lot less lonely than it could have been and for the friendships that I will cherish for a lifetime.

1. INTRODUCTION

1.1. *Campylobacter jejuni*: General Background

Campylobacter jejuni is a helical, motile, Gram-negative bacterium from the class Epsilonproteobacteria and is now recognized as a major contributor to bacterial food-borne gastroenteritis in the developed world, as well as the most common antecedent to Guillain-Barré syndrome (7,8). Despite its prevalence, the pathogenesis mechanisms of this bacterium are poorly understood in part due to its relatively recent classification. Theodor Escherich made what was believed to be the first description of a member of the *Campylobacter* genus in 1886, describing it as a spiral organism associated with a “cholera-like” diarrheal disease in kittens that could not be isolated on solid media but would grow in broth (9). McFayden and Stockman later isolated a range of other “*Vibrio*-like” organisms from both healthy and symptomatic animals in 1913 but it was not until 1963 when Sebald and Véron re-classified *Vibrio fetus* and *Vibrio bubulus* as *Campylobacter fetus* and *Campylobacter bubulus* based on DNA base composition, microaerophilic growth, and non-fermentative metabolism that the *Campylobacter* genus was established (10). With the improvement of cultivation techniques for *Campylobacter spp.*, research quickly progressed in the 1980s, leading to descriptions of new *Campylobacter* organisms and a new-found appreciation for the significance of this zoonotic pathogen (11).

1.2. *Campylobacter* as a Genus

The genus *Campylobacter* contains a broad range of important zoonotic pathogens. Members of this genus can be found colonizing the intestinal tracts of numerous domestic and agriculturally significant animals asymptotically, including but not limited to cattle, various poultry, pigs, sheep, and pets such as dogs and cats (12). However, there are many examples of *Campylobacter spp.* associated with disease in animals. For instance, *C. fetus* causes septic

abortions or venereal disease leading to infertility in cattle and sheep. *C. hyointestinalis* and *C. mucosalis* cause a variety of porcine intestinal diseases (10).

In general, cells are 0.2 to 0.8 μm wide and 0.5 to 5 μm long, helical in shape (which transition to a coccoid form at late growth stages), with polar flagella at one or both ends (10). The genus is asaccharolytic, as in they are unable to metabolize glucose and complex carbohydrates through respiration or fermentation, and instead rely on the presence of tricarboxylic acids and amino acids as electron donors (10). *Campylobacter spp.* are fastidious, requiring a microaerophilic atmosphere (6% O_2 , 10% CO_2) and are thermotolerant (grow optimally at 38°C and 42°C, and do not grow below 30°C or above 50°C) (13). Disease is primarily caused by *C. jejuni* and *C. coli*. However, other *Campylobacter spp.* have also been isolated from patients with diarrheal disease. Of emerging importance are *C. concisus* and *C. upsaliensis* that together rival the incidence rates of *C. jejuni* subsp. *jejuni* enteritis (12). In addition, other *Campylobacter spp.*, such as *C. concisus*, *C. hominis*, *C. showae* and *C. ureolyticus*, are now appreciated in the initiation or exacerbation of inflammatory bowel diseases (IBD) (12).

1.3. Campylobacteriosis: *Campylobacter*-Mediated Infections

1.3.1. *Campylobacter* Enteritis

The term campylobacteriosis is used to describe the collective manifestation of disease due to an infection by any member of the *Campylobacter* genus (14). The most common and most significant outcome is *Campylobacter* enteritis, an acute diarrheal disease. The disease presents itself as a watery to bloody diarrhea accompanied by abdominal pain, and may include fever and vomiting. This is not unlike many other infectious enteritis and thus is often indistinguishable clinically from shigellosis or salmonellosis without culture confirmation (15).

Infection begins with ingestion of a relatively low number of *C. jejuni* cells. A study with human volunteers showed an infectious dose as low as 800 cells depending on the strain, and a case study in 1981 fulfilled Koch's postulates with as few as 500 cells (16). The experiment with human volunteers did not reveal a clear dose-dependence for virulence but did exhibit strain differences (17). After an average incubation period of three days, the onset of *Campylobacter* enteritis often begins with abdominal cramps and diarrhea. However, flu-like prodromal symptoms such as fever, headache, and dizziness may be experienced in patients that experience more severe disease states. Patients experience diarrhea for three to four days before recovery begins. In general, infection is self-limiting in healthy individuals but may require antibiotic intervention in the immunocompromised. Abdominal pain may persist for longer despite improvements to bowel movements. Even after the clinical symptoms of disease cease, bacteria may be shed for up to several weeks. The duration of illness is multi-factorial and is influenced by the strain, immune system of the patient, and exposure levels (15).

Immunocompromised patients often present more severe disease states. Case studies reveal that AIDS patients experience chronic infections with *C. jejuni* that are intensely debilitating and often relapse after cessation of antibiotic treatment giving rise to the development of antibiotic resistance strains (18,19). In addition to exacerbated enteritis, immunocompromised patients are more prone to bacteremia. A meta-analysis of hospital records from Fairfield Hospital in Melbourne Australia identified a total of 1006 patients with *C. jejuni* enteritis, of which 24 patients experienced bacteremia. The rates of bacteremia were significantly higher for HIV-positive patients (8.3% or 10/121) compared to non-HIV-infected patients (1.6% or 14/885). The mortality rate among HIV/bacteremia patients in this meta-analysis was significantly higher at 33% compared to bacteremia alone which did not occur in the study.

Patients whose death was attributed to the *C. jejuni* infection had CD4⁺ cell counts of <20/mm³ (18). This shows the importance of adaptive immunity in control of *C. jejuni* infection.

The most informative diagnostic technique is to culture *C. jejuni* from stool samples of symptomatic patients. Prior to isolation and culturing, tests can be run on the stool samples as indicators of infection. These include: Gram stain for Gram-negative helical bacteria, stool antigen tests to detect *Campylobacter* specific antigens, and molecular-based assays (Multiplex PCR analysis of enteric pathogens) which have been developed to assess the presence of not only *C. jejuni*, but other *Campylobacter spp* as well. (20,21) However, these techniques fail to generate viable cultures for downstream analysis, such as antibiotic susceptibility testing, which may be important for establishing treatment regimens.

1.3.2. Medical Sequelae

Infection by *C. jejuni* is now an appreciated medical antecedent to a number of autoimmune diseases including Guillain-Barré syndrome (GBS), reactive arthritis (RA), and inflammatory bowel disease (IBD). Using ELISA assays against *C. jejuni* OMP18 and P39 antigens, a recent case-control study found 34-49% of GBS, 44-62% of RA, and 23-40% of IBD cases could be associated with prior infection by *Campylobacter spp.*, and the seropositivity for *Campylobacter spp.* was greater than that of other infectious antecedents (22). The combination of culture and seropositivity would provide the greatest evidence to link *C. jejuni* to these sequelae, but because the infectious agent is often cleared prior to onset of these autoimmune disorders, serological tests alone are the next most reliable methodology.

GBS is an autoimmune disease characterized by acute neuromuscular paralysis attributable to cross-reactive antibodies against gangliosides that leads to complement-dependent nerve damage. It is described as a polyradiculoneuropathy and can damage nerves at both the

root and the periphery (23). The disease severity varies and can begin with numbness and develop over the course of the disease into symmetrical weakness of the limbs, paralysis, or in rare cases even respiratory failure and death. Symptoms plateau for two to four weeks as auto-antibody titres diminish before recovery begins, but complete recovery is rare and up to one-fifth of patients can retain permanent nerve damage and complications (23).

GBS is now classified as a post-infectious disease. Infection by *C. jejuni* is the most common antecedent to GBS, preceding up to 20 to 50% of GBS cases depending on the study and geographical location (23-25). There is evidence supporting this relation as causal in nature and a true example of molecular mimicry. Genetic screens identified the LOS biosynthesis gene cluster in *C. jejuni*, and in particular the gene *cstII* which encodes a sialyltransferase that was significantly associated with neuropathogenicity (26). Compelling studies on the cross-reactivity of anti-campylobacter antibodies against strain-specific lipooligosaccharide (LOS) and that of anti-ganglioside antibodies against GM1 gangliosides support the theory of molecular mimicry. In an investigation on GBS-related *C. jejuni* infections in Bangladesh, serum IgG from GBS patients interacted with both specific *C. jejuni* LOS structures and GM1 gangliosides, and anti-ganglioside antibodies from both GBS patients and murine mono-clonal antibodies against gangliosides cross-reacted to purified *C. jejuni* LOS. The LOS structure of *C. jejuni* strains from GBS patients were determined to have glycan structures identical to those of gangliosides on the basis of mass spectrometry (27), thus corroborating findings of previous studies (23).

Reactive arthritis (RA) is a condition characterized by inflammation of the large joints due to an autoimmune reaction following a gastrointestinal or urogenital infection (15). It has been associated with infections by *Yersinia spp.*, *Salmonella spp.*, *Shigella spp.*, *Chlamydia trachomatis*, *Neisseria gonorrhoea*, and many others. As a common gastrointestinal pathogen, it

is not surprising that *C. jejuni* may also correlate with RA. One difficulty with estimating the incidence of RA is that there are no universally accepted diagnostic criteria. A systematic review of the literature, that used an inclusion criterion to minimize the variation in the field, reports an incidence of post-campylobacteriosis RA to be 9 in every 1 000 infections (573 RA patients out of 63 206 campylobacteriosis patients) which was slightly lower than both *Salmonella*- and *Shigella*-associated RA (12 in every 1,000 infections) (28).

The inflammation of RA is often associated with impaired clearance of circulating bacterial antigens. In the case of *C. trachomatis* urogenital infections, bacterial components can be found in the synovial fluid which may perpetuate inflammation (29). However, *C. jejuni* antigens have not been found in synovial fluids despite being associated with RA. The pathology of RA as sequelae to campylobacteriosis is poorly understood. The class A LOS gene cluster in *C. jejuni* that imparts the ability to sialylate the LOS is implicated as a genetic marker for the development of RA. The high prevalence of the class A LOS is also associated with more severe disease states. A compromised epithelial barrier caused by severe disease may lead to greater antigen translocation and to cross-reactive antibodies (30).

IBD is driven by an imbalance or excessive immune responses in the gut directed towards the commensal gut microbiota and are primarily driven by activated T lymphocytes. This is supported by observations that animal models of IBD exhibit less severe disease states under germ-free conditions, inflammation is found along areas of the gastrointestinal tract with the greatest bacterial densities, antibiotics can alleviate disease symptoms, and a loss of immunological tolerance to commensal microflora (31). The disease is multi-factorial in nature so prior infection by a pathogen is just one of many contributing factors to the onset of IBD. Some of these risk factors include residents of the host intestinal microflora, environmental

influences such as diet or antibiotic treatment, the host immune response, and genetic predispositions such as the polymorphisms in *NOD2/CARD15* (31) that exhibit reduced or loss-of-function in recognizing microbial-associated molecular patterns (MAMPs) (32).

Despite the developing interest for *C. jejuni* and *Salmonella spp.* in the onset of IBD, the pathogenesis mechanisms have yet to be elucidated. Three prevailing hypotheses exist for development of IBD. The dysbiosis hypothesis suggests that there is an imbalance in the resident microflora that shifts the population towards the harmful bacterial population to elicit inflammation.(31) An investigation of colonization potential in mice found a positive correlation between concentration of *C. jejuni* and dysbiosis of the microbiota (33). The persistent infection hypothesis proposes that specific enteric pathogens may initiate disease or cause relapse in IBD patients. There is insufficient evidence to distinguish whether colonization of certain microbial species under both hypotheses, be it commensal or pathogenic, is a cause or result of IBD (31). The luminal antigen translocation hypothesis proposes that the intestinal epithelial barrier is in some way compromised leading to increased translocation of commensal antigens and loss of tolerance towards resident microbial species (31). Studies have shown *C. jejuni* can induce transcytosis of non-invasive *Escherichia coli* across epithelial monolayers (34,35). Mice infected with *C. jejuni* had commensal intestinal bacteria in the mesenteric lymph nodes, liver, and spleen (34). *C. jejuni* can also translocate across the epithelial cell barrier paracellularly (36). However, disruption of tight junctions was not observed and barrier integrity remained intact. Thus, paracellular trafficking may not contribute to antigen translocation (37,38).

C. concisus seems to be the major *Campylobacter* species involved as it has the greatest significant correlation with onset of IBD. Many of the pathogenesis-associated phenotypes of *C. concisus* overlap with those of *C. jejuni*. However, there are distinct factors found in *C. concisus*

that may explain its prevalence over *C. jejuni* in IBD. Genomic and proteomic approaches have identified candidate genes, such as exotoxin 9/DnaI, that were highly associated with adherent and invasive *C. concisus* and adherent/toxigenic *C. concisus* pathotypes. *C. concisus* can be isolated from healthy individuals as well which challenges its role in IBD and showcases the multifactorial nature of the disease (39).

1.3.3. Treatment and Prevention of *C. jejuni* Infections

There is no established treatment regimen for *Campylobacter*-associated gastritis other than replenishment of fluids and electrolytes. The gastrointestinal manifestation is often self-limiting in healthy individuals and does not require antibiotic treatment (13,15). An analysis of antibiotic intervention in gastrointestinal complications showed significant reduction in symptoms, severity of disease, and duration of morbidity. However, recovery was only 1.32 days shorter and only made a significant difference if administered early in illness (40). By the time infection is confirmed by stool culture, patients are often already recovering. Thus, the use of antibiotics remains controversial, especially in light of growing antibiotic resistance in *Campylobacter spp.* (41). In severe cases, which can develop in immunocompromised individuals such as the young, elderly, and HIV-positive demographics (13), macrolides are the antibiotics of choice, particularly erythromycin. Due to their broad-spectrum properties, fluoroquinolones may also be prescribed as they are a popular choice for enteric pathogens. However, resistance is now arising globally for both clinically important antibiotics classes (42).

Resistance to fluoroquinolones is believed to arise from the unwarranted use of antibiotics during treatment as well as in veterinary medicine and in the poultry industry (43). The spontaneous mutation in *gyrA* that confers resistance to fluoroquinolones does not have a significant fitness cost and can easily be maintained even in the absence of selective pressures.

Mutations in 23S rRNA confers resistance to macrolides, but the rate of mutations giving rise to macrolide resistance is much lower than for fluoroquinolone resistance in *C. jejuni* (42). Rather than approach *C. jejuni* from a treatment perspective, prevention tactics and intervention should be the focus (44). A national study in New Zealand has shown that implementation of food safety programs to prevent contamination of poultry meat was effective in decreasing both the incidence of *C. jejuni* enteritis (45) and GBS (46). The design of a vaccine to reduce *C. jejuni* colonization in chicks is a popular area of research. One study successfully used an attenuated *Salmonella* strain expressing a number of *Campylobacter* antigens as a vaccine and significantly reduced colonization of the chicks. Although the designed vaccines did not reach commercial efficacy, this study acts a proof of principle for live vector vaccines (47).

1.4. Prevalence and Significance of *C. jejuni*

1.4.1. Epidemiology of *C. jejuni* Infection

Under-reporting and under-diagnosis is a problem with foodborne diseases in general, attributable to cases not seeking medical attention, lack of sample submissions for laboratory tests, and under-reporting to surveillance systems. Estimates are made using pathogen-specific multipliers by considering factors such as the likelihood of seeking medical attention. An analysis based primarily on Canadian statistics of foodborne illnesses listed 10,344 laboratory-confirmed cases of *Campylobacter spp.*-related foodborne illnesses circa 2006 reported *Campylobacter spp.* as the leading bacterial cause of domestically acquired foodborne illness in Canada, with an estimated 447 cases per 100,000 which is greater than the estimated rate for non-typhoidal *Salmonella spp.* (48). Regardless of geographic location or method of estimation, *Campylobacter spp.* consistently remains one of the major bacterial contributors to foodborne illness in developed nations, ranking first in Canada (48), second for incidence rates in the USA

from a 2013 report by FoodNet (49), and first in reported numbers in Europe since 2005 in accordance with the European Centre for Disease Prevention and Control (50).

A recent report of disability-adjusted life years (DALY) has estimated *Campylobacter* enteritis is responsible for 109 DALY per 100,000 population in 2010 out of 1,299 DALY lost to diarrheal diseases globally (51). Monetary costs were recently estimated to be up to \$1.7 billion in the United States (52). Altogether, the costs of infection are a significant socioeconomic burden that include, but are not limited to, medical expenses, lost wages, and product recalls, making it both an economic issue and a health care concern (13).

Incidence rates increase in the spring and peak in the months of June and July, before falling in the winter months (53). The trend is most observable in climates where there is a more pronounced difference in seasons. Although the true reason for this is unknown, a few investigations looking at the carriage rates in broiler chickens found an increase in the levels of contamination during the summer months (54). In addition to this, changes in human behavior with shifts in seasons (travel and vacations, recreational activities such as barbecuing meat) may correlate with the increased incidence. In support of a more anthropogenic involvement in the observed seasonal variation, the trend is absent in developing nations (14,55). As such, the seasonal variations may be a combination of environmental and human factors.

Campylobacteriosis presents itself differently in developing countries. Firstly, *Campylobacter spp.* are endemic in many developing countries and infections are most prevalent in children less than 5 years of age. Incidence rates for children in the developing countries were estimated to be as high as 40,000 to 60,000 infections per 100,000 individuals. This is significantly higher than the estimated incidence rate of 300 per 100,000 in developed countries (14). In developing countries, *Campylobacter spp.* are isolated from healthy children in

comparable numbers to children expressing clinical disease and symptoms are often less severe as well (14,56). However, Campylobacters are still significantly associated with moderate-to-severe diarrhea (57). In addition, *Campylobacter spp.* infections were overrepresented in malnourished children in developing nations (56). Further research into campylobacteriosis in developing nations is still warranted despite reduced severity in gastrointestinal illness.

1.4.2. Sources of Infection

C. jejuni has been isolated from the intestinal tract or feces of a number of animals (12). Surveillance programs are important in the food industry as contamination can go unnoticed due to asymptomatic colonization. This is also a reason why there is no established reproducible disease model to date (58). However, recent studies show promising development of disease models in mice (59). Meat products, poultry meat in particular, are important sources of infection and intervention tactics focus on preventing contamination (44). Unpasteurized milk has also repeatedly been a source of *C. jejuni* outbreaks (60). Most *C. jejuni* infections are sporadic in the developed world and rarely environmentally acquired. However, outbreaks have occurred due to fecal contamination of drinking water such as the infamous Walkerton, Canada outbreak which was traced back to runoffs from a farm due to heavy rainfall leading to contamination of drinking water by both *E. coli* and *C. jejuni* (61). This, and its endemic nature in developing countries (56), shows that *C. jejuni* can be environmentally acquired.

1.5. *C. jejuni* Physiology in Survival, Transmission, and Host-Bacterial Interactions

Despite the prevalence of *C. jejuni*, relatively little is known about its pathogenesis in humans. Traditional virulence factors, such as secretion systems, are for the most part, absent in *C. jejuni*, (62-64). Since the sequencing of the genome, efforts to characterize non-canonical virulence mechanisms have provided insights into how the normal physiology of *C. jejuni*

impacts virulence. Some examples of these are signal recognition and regulation of gene expression under stress (65-67), metabolism (68,69), and maintenance of cell shape (1,68-70). Some candidates for true virulence factors have been identified including the pVir plasmid, which contains putative a putative type VI secretion system (71), and the only identified toxin in the genome, cytolethal distending toxin (62). However, the roles of these candidates in pathogenesis are debated (72-74). The following are well-established indicators of pathogenesis, virulence, and colonization potential.

1.5.1. Flagella, Motility, and Chemotaxis

Motility is an essential factor for *C. jejuni* colonization of day old chicks (6). A number of factors play roles in efficient *C. jejuni* motility. Flagella, multi-protein complexes composed of the hook-basal body and the extracellular filament, are responsible for motility of *C. jejuni* (75). The hook-basal body contains MotAB proteins that act as the stator to couple proton flow with generation of torque to rotate the extracellular filament. In the absence of the stator, the extracellular filament cannot rotate and thus the cell is immotile. The debate between whether motility or the flagellum itself is required for colonization has long been debated (76-78). Recent evidence using *C. jejuni* Δ *motAB* mutants suggests motility is a necessity for colonization but flagella still plays roles as an adhesin (77). In fact, flagella of *C. jejuni* have many potential roles in pathogenesis independent of motility, including secretion of *Campylobacter* invasion antigens (Cia) (79) as well as evasion of host immune responses, as *C. jejuni* flagellin does not activate the Toll-like receptor (TLR) 5 (80). In addition to the flagellum, chemotaxis (6,75) and cell shape (81) are important for proper motility and colonization efficiency.

1.5.2. Biofilm Formation

Due to its fastidious nature under laboratory conditions, *C. jejuni* is not expected to survive under aerobic conditions despite being one of the most prevalent foodborne pathogens. Biofilm formation is a proposed survival strategy important for transmission and general response to stress such as oxidative stress (82) and the presence of bile acids (83). In response to oxygen-enriched conditions, *C. jejuni* alters the proteins in its outer membrane, including the *Campylobacter* adhesion to fibronectin (CadF) protein, which may contribute to its ability to adhere to surfaces and initiate biofilm formation (82). A major component of the *C. jejuni* biofilm matrix is extracellular DNA that results from cell lysis (67). However, cell lysis and release of extracellular DNA alone are insufficient for initiation of biofilm formation and at the least, full length flagella, but not motility is a requirement (83). *C. jejuni* produces biofilms as unattached aggregates, pellicles at the air liquid interface, and on abiotic surfaces (84).

1.5.3. *C. jejuni* Association, Invasion, and Survival within Host Cell

C. jejuni adherence, invasion and intracellular survival have been thoroughly investigated and the invasion capabilities of *C. jejuni* are proposed as an indicator of strain virulence. Studies utilize gentamicin protection assays to assess interactions with intestinal epithelial cells *in vitro*. Important factors for adherence include CadF, JlpA, PEB1, FlpA, and flagellin (36,85). Motility has not been implicated for adherence to host cells *in vitro* and in fact, non-motile *C. jejuni* with full length flagella exhibits increased adherence to host cells. This is in stark contrast to its requirement in successful colonization of chick ceca due to host factors (e.g. peristalsis, mucus) that are absent in cell-line models (77). *Campylobacter* invasion mechanisms have been heavily debated and currently, actin- microtubule- independent and dependent mechanisms have all been described (38,86-88). The best characterized uptake mechanism studied thus far includes the

CadF/FlpA fibronectin signaling cascade that leads to uptake by actin-dependent membrane ruffling (86,87,89,90). However, basolateral invasion of Caco-2 cells was also observed to be actin/microtubule independent (38). The inconsistency in experimental results showcases the extensity and complexity of *C. jejuni* invasion and its contribution to disease. *C. jejuni* is able to survive within host intestinal epithelial cells (but not macrophages) by escaping the classical endocytic pathway after invasion and thus avoid phago-lysosomal fusion and reside near the Golgi-apparatus (88). In addition, secretion of Cia are now also implicated in both cell invasion and survival within host epithelial cells (86,91-94).

1.5.4. Lipooligosaccharide and Capsule

The outer membrane of *C. jejuni* is composed of lipooligosaccharides (LOS) as opposed to lipopolysaccharide (LPS) as it does not contain the O-antigen characteristic of other Gram-negative LPS structures. The LOS of *C. jejuni* is characterized by Lipid A membrane anchor bound to keto-deoxyoctulosonate and heptose moieties of the inner core, and an oligosaccharide outer core containing a variety of combinations of galactose, sialic acids, and N-acetylglucosamine (26). The LOS in *C. jejuni* contributes to resistance to complement proteins, cationic antimicrobial peptides (CAMPs), and bile acids and is necessary for successful host colonization as shown using LOS truncation experiments (95,96). The LOS of *C. jejuni* can also be modified to alter the host response. The Lipid A moiety is modified relative to *E. coli* in that two of the acyl chains are amide linked which significantly reduces recognition by TLR4 (97). Phosphoethanolamine can be added to Lipid A as well as to the first heptose sugar in the inner core to confer resistance to CAMPs and may play a role in activating TLR4-MD2 mediated responses (98). The LOS of *C. jejuni* is also implicated in the onset of GBS through biomimicry and is supported by experiments showing cross-reactivity between anti-gangliosidic and anti-*C.*

jejuni LOS antibodies (23,26,27). In addition to its role in GBS, *C. jejuni* strains that possess the ability to incorporate sialic acid into their LOS outer core (LOS A/B strains) correlates with severe gastroenteritis and reactive arthritis (30).

C. jejuni produces capsular polysaccharides (CPS) that are the major antigenic components recognized in the Penner serotyping method (99). The Penner serotyping scheme has identified upwards of 60 different serotypes, all of which in theory represent a different CPS structure. Indeed, great genetic diversity in the CPS locus of *C. jejuni* strains correlates with compositional differences (100). The CPS plays a role in resisting complement-mediated killing but offers limited protection against β -defensins (101). In addition, the *C. jejuni* CPS was shown to reduce the levels of TLR2 and TLR4 activation, likely due to shielding of their respective MAMPs (102). Conjugate vaccine trials using *C. jejuni* CPS conjugated to diphtheria toxin mutant CRM197 in non-human primates are promising and protected from diarrheal disease, (103). A more robust vaccine design that is multivalent is necessary considering the vastly different CPS structures; however, this is an initial proof of principle that conjugate vaccines may play an important role in control of *C. jejuni* in the future (103,104)

1.6. Peptidoglycan: The Bacterial Cell Wall

The bacterial cell envelope is an important anatomical feature made up of a number of components. Selectively permeable lipid bilayer membranes separate the interior of the cell from the environment. Imbedded in/spanning these membranes are proteins such as sensor kinases of two-component regulatory systems for sensing and responding to external stimuli, flagella and pili for motion, bacterial adhesins for attachment to surfaces, transport proteins, and many others. The structure of the cellular envelope is maintained by the peptidoglycan (PG) layer. The PG sacculus is a large heteropolymeric complex comprised of alternating residues of β -1-4 N-

acetylglucosamine (GlcNAc) and N-acetylmuramic acid (MurNAc) with associated cross-linked peptide side-chains. It is responsible for providing structural strength to resist turgor pressures and for maintaining cell shape. It also acts as an anchoring point for proteins of various functions including those that stabilize the outer membrane of Gram-negative bacteria (105-107). The bacterial cellular envelope follows two general patterns. Gram-negative bacteria contain two lipid bilayers (inner and outer membranes) with a thin layer of PG in between. Gram-positive bacterial cell envelopes are characterized by a single lipid bilayer membrane encompassed by a thick layer of PG (108) (Fig. 1A). This has major implications for antibiotic treatment regimens.

1.6.1. Peptidoglycan Metabolism

Although rigid, the PG sacculus is a dynamic structure that is constantly being synthesized, modified, and degraded. PG synthesis begins in the cytoplasm as the generation of the precursor uridine diphosphate (UDP)-MurNAc with a pentapeptide side-chain extending from the C3 position, consisting of L-ala- γ -D-glu-meso-DAP-D-ala-D-ala in Gram-negative bacteria and L-ala- γ -D-glu-L-lys-D-ala-D-ala in Gram-positive bacteria (108). However, there are notable exceptions such as *Bacillus spp.* which contain meso-DAP type PG (109,110). Synthesis of this precursor is performed by the Mur ligases (MurA-F). UDP-MurNAc is first attached to the C₅₅ lipid carrier via MraY and freeing UDP to form lipid I. UDP-GlcNAc is then attached by MurG releasing UDP and forming lipid II (111,112). The lipid II precursor with the muropeptide in the cytoplasm needs to be flipped into the periplasm via a flippase. This flippase was recently identified as MurJ (113) in *E. coli*. Incorporation of the new precursor is accomplished by bi-functional penicillin-binding proteins (PBP) in which the new disaccharide is added onto the reducing end of the pre-existing PG glycan backbone by the

glycosyltransferase function followed by the transpeptidation function to cross-link the side chain to a pre-existing side chain of a separate glycan strand (111).

A number of modifications are still possible (114). Different bacteria have unique repertoires of remodeling and modifying enzymes available in their genomes. The collective action of these enzymes leads to the generation of a structure that varies chemically (e.g. muropeptide compositional analysis by HPLC) (4), in structure (e.g. orientation of the glycan strands relative to the cell), architecture (e.g. subcellular structures and organization like cords, knobbls, and differential densities assessed by electron cryotomography and atomic force microscopy), and overall mechanics (e.g. cell division properties) which cumulate as a distinct bacterial shape (105,115).

As the cells grow, in addition to synthesis of new PG, small muropeptide fragments are released into the environment through lytic means that are necessary for division, remodeling, and repair (111,116). A major class of enzymes responsible for PG turnover are N-acetylmuramidases that cleave the β -1,4-glycosidic linkages. These are endogenous bacterial lytic enzymes that are either true muramidases that are similar mechanistically to lysozyme (hydrolytic activity) or lytic transglycosylases (LytTG) that lyses the glycosidic bond using the free hydroxyl functional group on the C6 carbon (C6-OH) in an intramolecular cyclization yielding a bicyclic anhydromuropeptide (anhMP) species (Fig. 1B). These play important roles in PG metabolism as they generate insertion sites for newly synthesized muropeptides during cell growth and division (117). In addition, the anhMP is a distinctly different muropeptide structure and is recognized by specialized permeases for import into the cytoplasm for recycling or for signaling. Turnover and recycling rates may differ between bacteria as well (116).

1.6.2. Peptidoglycan, Cell Shape, and Pathogenesis

PG maintains cell shape and therefore is modified to suit the needs of the organism that changes shape when moving from one to another environment (105,106,118). Changes to bacterial shape can be triggered by a number of different stimuli and are reflected as a change in the PG muropeptide composition, such as in sporulation, filamentation, and transitioning from helical to coccoid forms. Mutations in remodeling enzymes can affect interactions with the host and pathogenesis in a number of bacterial species. The most relevant example is the corkscrew motility of *C. jejuni* that is aided by its helical shape and polar flagella which are thought to be important in enhancing its ability in comparison to bacilli to move through viscous media, such as the mucus layer of the gastrointestinal tract (81,118). Deletion of PG remodeling enzymes peptidoglycan peptidase 1 (*pgp1*) and 2 (*pgp2*) in *C. jejuni* (1,70) results in a complete change in the morphology from helical to straight cells, with accompanying defects in traits associated with pathogenesis. PG remodeling has been shown to influence shape and pathogenic properties in numerous bacterial species including but not limited to *Mycobacterium tuberculosis*, *Proteus mirabilis*, and *Helicobacter pylori* (119-122).

1.6.3. Significance of Peptidoglycan Signaling and its Role in Host-Response to Infection

As PG is unique to bacteria, it is used as an indicator for the presence of bacteria. Proteins that contain PG recognition domains (e.g. lysine motif domain, penicillin binding proteins and Ser/Thr kinase-associated motif) are found in organisms across all kingdoms of life with the exception of Archaea. Many examples of bacterial resuscitation from dormancy (e.g. germination of *B. subtilis* spores) involve the quiescent body sensing muropeptide fragments shed from actively growing cells as an indication of improved growth conditions. PG signaling is also seen in eukaryotes, such as in the legume-rhizobium symbiosis for nitrogen fixation and the

Euprymna scolopes (bobtail squid) symbiosis with *V. fischeri* in the light organ (116). In addition, proteins of the PG recognition protein family have been implicated in immune tolerance to and control of commensal microbiota using a variety of mechanisms in studies with insects, fish, and mice (123). PG recognition is also a defense mechanism of host organisms for eliciting immune responses to pathogenic bacteria.

The innate immune system recognizes MAMPs using pattern recognition receptors (PRR). MAMPs are small molecules that are associated with foreign microbial organisms but not the host. Some common MAMPs are flagellin, lipoprotein, lipopolysaccharide, peptidoglycan, and CpG oligonucleotides. Of the known PRRs the best characterized are those of the TLR family. Each TLR has a leucine rich repeat domain that binds its agonist MAMP. Binding ultimately leads to downstream NF- κ B activation and transcription of genes to elicit an immune response (112). Some studies suggest that TLR-2 may recognize PG in complex with lipoproteins but this is still debated (124). Similar types of PRRs known as the nucleotide-binding oligomerization domain (NOD) -like receptors (NLR) are intracellular receptors for MAMPs. NOD1 and NOD2 recognize D-glu-meso-DAP and muramyl dipeptide as their cognate agonists respectively; both are components of PG. As NOD1 recognizes meso-DAP, it is more important for recognition of Gram-negative bacteria than most Gram-positive bacteria (125). Studies have shown that *C. jejuni* can elicit an immune response *in vitro* from epithelial cells through NOD1 activation (126).

1.6.4. Peptidoglycan as a Target for the Design of Antimicrobial Compounds

PG metabolism is a dynamic balance of synthesis, remodeling, and degradation. Inhibition of any process may shift the overall metabolic activity towards an unfavourable state that can be detrimental to the physiological condition of the cell (105,127). Given the essential

role of the bacterial cell wall, it is not surprising that antibiotics like β -lactam antibiotics target PG biosynthesis machinery. In fact, penicillin irreversibly inhibits the transpeptidase functions of high-molecular weight PBPs thus shifting PG metabolism towards degradation, leading to cell lysis and death (114). *C. jejuni* and other *Campylobacter* spp. are resistant to this class of antibiotics both intrinsically, due to the outer membrane and small pore size (128) (Fig. 1A) restricting access to PG, and through β -lactamase production in certain strains (42). Thus, understanding PG biosynthetic mechanisms may be advantageous to the development of new antimicrobials. A number of PG remodeling enzymes have been proposed as targets for antimicrobial design including LD-transpeptidases in *M. tuberculosis* (129,130) and N-acetylglucosamine de-acetylases in *Bacillus anthracis* (110). Recently, O-acetylation of PG machinery has garnered attention as a potential target.

1.6.5. O-Acetylation of Peptidoglycan

In addition to glycosyltransferase, transpeptidase, and hydrolase activities, PG can be biochemically modified in a number of manners, some of which contribute to pathogenesis and immune evasion. O-acetylation of peptidoglycan (OAP) is a phenomenon characterized by the acetylation of the C6-OH of MurNAc residues (117,131). OAP occurs in both Gram-positive (132,133) and Gram-negative (134,135) bacteria, and this modification confers resistance to lysozyme which degrades PG by cleaving the glycosidic bonds in the PG backbone (131). This modification contributes to lysozyme resistance in Gram-negative bacteria, as demonstrated in *H. pylori* mutants defective in O-acetylation and N-deacetylation exhibiting increased susceptibility to physiologically relevant concentrations of lysozyme in the presence of lactoferrin, which permeabilizes the cell membrane (136). The degradative activity of lysozymes is important for host immune defenses as they have antibacterial properties, generate NOD

agonists, and prevent circulation of large fragments of PG which has been linked to the development of rheumatoid arthritis (117,137). GlcNAc N-de-acetylation (110,138) and GlcNAc O-acetylation (139) also confer resistance to lysozyme. OAP is also believed to be involved in maintenance and regulation of PG turnover by preventing the activity of LytTGs that require the C6-OH moiety of MurNAc to cleave the glycosidic bond (Fig. 1B). Dysregulation of OAP has been shown to affect a number of physiological processes in multiple bacterial species. Factors influenced either directly by OAP or indirectly through LytTG inhibition (140) include cell division (141,142), anchoring of protein/glycoprotein complexes (142,143), cell morphology (109), glycan length regulation (144), and swarming motility (120).

The OAP gene cluster was discovered in *N. gonorrhoeae* and is primarily responsible for OAP in Gram-negative bacteria, but homologs are also found in addition to other OAP (*oatA/B*) machinery in some Gram-positive pathogens (131,145,146). Since the discovery of PatB and Ape1 in *N. gonorrhoeae* and *N. meningitidis*, these proteins have been well characterized biochemically including a description of the catalytic residues, the mechanism of enzyme action, and substrate specificity (145,147-151). Host interaction studies also lend support for their application as targets for antimicrobial design (144,152). *C. jejuni* encodes homologs of the OAP gene cluster: a putative transmembrane protein, **Peptidoglycan O-Acetyltransferase A** for translocation of acetate, a putative periplasmic transferase **Peptidoglycan O-Acetyltransferase B** for O-acetylation of MurNAc, and a putative O-Acetyl- **peptidoglycan Esterase** for de-O-acetylation. (Fig. 1C) These genes have yet to be characterized in *C. jejuni*, a species that relies on its helical form for host colonization.

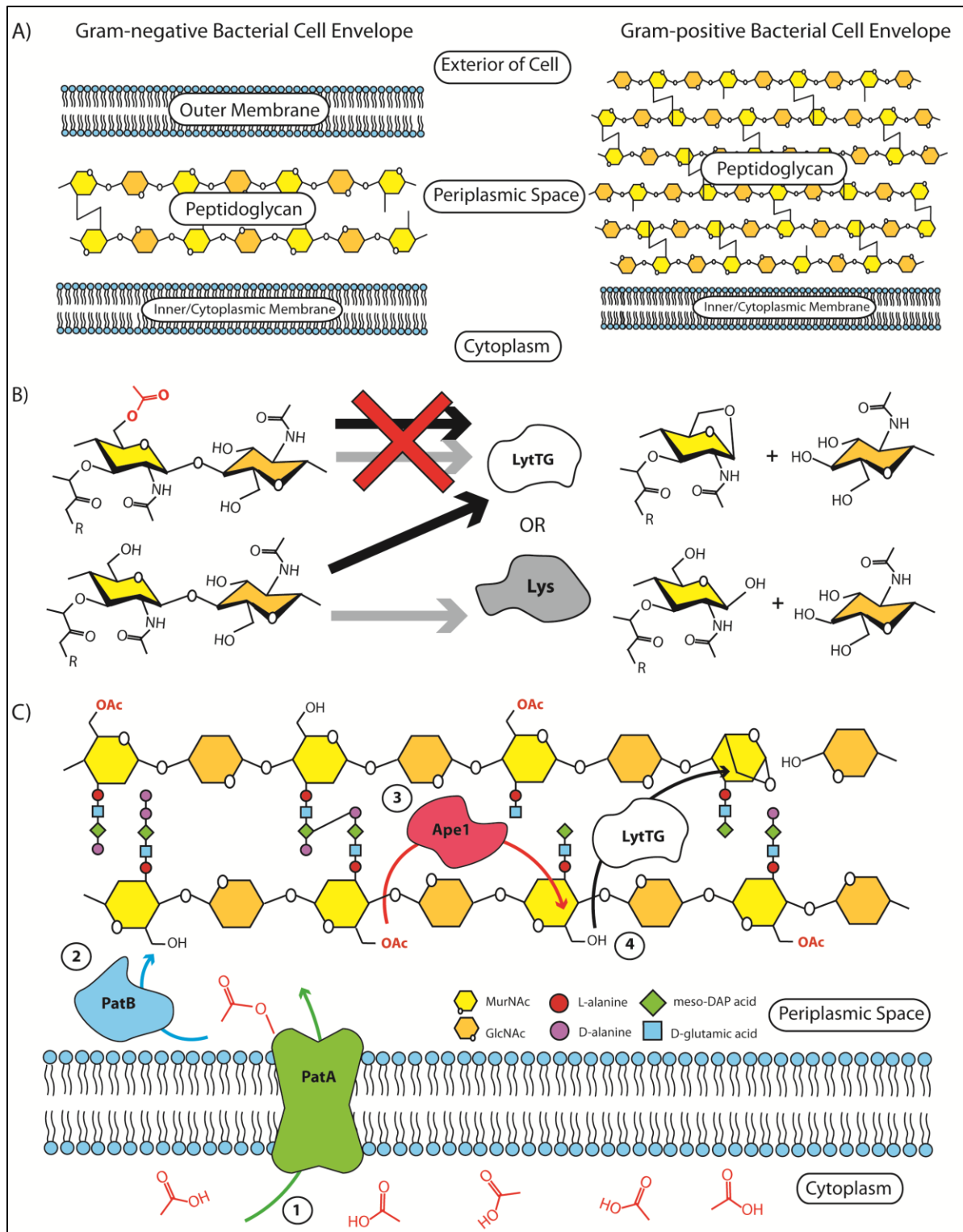


Figure 1. Peptidoglycan is the structural component of the bacterial cellular envelope and is highly variable due to PG remodeling and modification machinery.
 Complete figure caption can be found on page 23.

Figure 1. Peptidoglycan is the Structural Component of the Bacterial Cellular Envelope and is Highly Variable due to PG Remodeling and Modification Machinery.

A) Organization of the cellular envelopes of Gram-negative and Gram-positive bacteria. Gram-negative bacteria possess an outer membrane and a thin layer of peptidoglycan while Gram-positive bacteria that contain a thicker peptidoglycan layer and no outer membrane. B) O-acetylation of MurNAc inhibits the activity of N-acetylmuramidases. Lysozyme (Lys) activity is believed to be inhibited sterically due to the presence of the acetate at the C6-OH. OAP inhibits Lytic transglycosylase (LytTG) activity as it requires a free C6-OH to lyse the glycosidic bond. LytTG activity results in the formation of a bicyclic structure called an anhydromuropeptide. C) Proposed functions of the OAP machinery. C1) *patA* encodes peptidoglycan O-acetyltransferase A, a putative translocase responsible for translocation of acetate from the cytoplasm to the periplasm. The source of the acetate is currently unknown (?). C2) *patB* encodes peptidoglycan O-acetyltransferase B, the periplasmic protein that transfers acetate from PatA to the C6-OH of MurNAc. C3) *ape1* encodes O-acetylpeptidoglycan esterase, a periplasmic protein responsible for removing acetate from the C6 of MurNAc. De-O-acetylation must precede the activity of LytTG.

1.7. Hypothesis and Research Objectives

My thesis hypothesis was that the *C. jejuni* OAP gene cluster encodes a vital component of the PG biosynthetic machinery and is required for maintenance of cell integrity and pathogenesis-associated properties. The overall goals were to **1)** address how OAP genes affect PG structure; **2)** investigate the effect of OAP on *C. jejuni* physiology and host interaction

1.7.1 Objectives (Aims) of the Project

- A. Generate deletion mutants and complemented strains for each gene in the OAP gene cluster.
- B. Analyze the muropeptide profiles and O-acetylation levels of the OAP mutants.
- C. Biochemically characterize Ape1 and confirm its activity on purified PG *in vitro*.
- D. Characterize the virulence-associated phenotypes and shape changes of OAP mutants.

2. MATERIALS AND METHODS

2.1. Strains and Growth Conditions

A list of bacterial strains and plasmids used in this study can be found in Appendix 1 and a description of their construction below. *C. jejuni* strains, unless otherwise stated, were grown in Mueller-Hinton (as directed by the manufacturer) (MH; Oxoid) broth or agar (1.7 % w/v) supplemented with vancomycin (V; 10 µg/ml) and trimethoprim (T; 5 µg/ml) and when appropriate kanamycin (Km; 50 µg/ml) and chloramphenicol (Cm; 25 µg/ml). Standard laboratory conditions for *C. jejuni* growth were 38°C under microaerophilic conditions (12% CO₂, 6% O₂ in N₂) in a Sanyo tri-gas incubator for MH agar or for standing MH broth cultures. For shaking MH broth cultures, *C. jejuni* were cultured in airtight jars using the Oxoid CampyGen Atmosphere generation system with shaking at 200 rpm. $\Delta apeI$ was standardized to 2X the OD₆₀₀ of wild-type 81-176 to achieve identical CFU counts. Experiments were performed on log-phase cultures obtained from 16-18 h shaking broth-grown cultures initiated at OD₆₀₀ 0.002 in 10 mL MH-TV (OD~0.2-0.3 at harvest with a doubling time of approximately 2.5 hrs, not shown). For plasmid construction and protein purification, *Escherichia coli* (DH5- α or BL21) strains were grown at 37°C in Luria-Bertani (LB; Sigma) broth or LB agar (7.5 % w/v) supplemented with ampicillin (Ap; 100 µg/ml), Km (25 µg/ml) or Cm (15 µg/ml) as required.

2.2. Deletion and Complementation of OAP mutants

Genes were PCR amplified using iProof™ (Bio-Rad) with primers designed to include 500-600 bp of flanking DNA on either side of each gene (for the sequence of PCR primers used for each gene, refer to Appendix 2). PCR products were adenylated at the 3'-ends using Taq DNA Polymerase (Invitrogen) and ligated to commercial cloning vector pGEM-T (Promega), resulting in pGEM-T-0638, pGEM-T-0639, and pGEM-T-0640. Vectors were transformed into

E. coli DH5- α and selected for Ap^R resistance and blue/white screening. All constructs were verified by sequencing and restriction digestion. The resulting constructs were inverse PCR amplified using primers designed to amplify the flanking regions and pGEM-T vector without the target gene save for the sequences used for primer design at the 5' and 3' ends of each gene. Inverse PCR products were restriction digested where appropriate by cutting at sites encoded within the primers, and ligated to the non-polar Km^R cassette (*aphA-3*) digested out of pUC18K-2 (153) with *KpnI* and *HincII* to form the deletion-constructs pGEM-0638::*aphA-3*, pGEM-0639::*aphA-3*, and pGEM-0640::*aphA-3*. To generate the pGEM-0638-40::*aphA-3* deletion construct, the primers 0637-1/0638-1(*KpnI*) and 0641-1(*NcoI*)/0641-2(*KpnI*) were used to amplify the regions downstream and upstream of the OAP operon, respectively. The downstream PCR product was adenylated, ligated to pGEM-T, digested with *KpnI* and *NcoI* and ligated to the upstream PCR product (digested with *KpnI* and *NcoI*) generating pGEM-T-0637+0641. The *aphA-3* from pUC18K-2 (*KpnI* and *HincII* digested) was ligated to pGEM-T-0637+0641 digested with *KpnI* and *SmaI* resulting in pGEM-T-0638-40Km^R. *C. jejuni* 81-176 was naturally transformed with each deletion construct. Mutant strains were selected by Km^R and verified by PCR, restriction digestion, and sequencing (Fig. 2B).

Genes were complemented using the pRRC system for gene delivery and expression (154). The genes *cjj81176_0638*, *cjj81176_0639*, and *cjj81176_0640* were each individually PCR amplified using the complementation primers (denoted with a C in the primer name after the gene designation in Appendix 2). PCR products and pRRC vectors were restriction digested with *MfeI/NheI* and *XbaI/NheI*, respectively and ligated together. The resultant complementation constructs were transformed into *E. coli* DH5 α , selected for resistance to Cm^R on LB-Cm^R agar plates and confirmed by PCR and sequencing. Complementation constructs were naturally

transformed into their respective mutants with the exception of pRRC-0638 which was first methylated before transformation into Δ *ape1*. Successful transformants were confirmed by PCR (Cat-2 and corresponding reverse complement primers designated with C2, Appendix 2) (1) and the rRNA locus of each insertion was confirmed using ak233, ak234 and ak235 primers specific to each of the three ribosomal spacer regions with the C2 primers (Appendix 2) (154).

2.3. Cloning of Ape1 for Expression and Purification

The *ape1* gene was PCR amplified using primer pairs 0638-His-NF/0638-His-NR and 0638-His-CF/0638-His-CR for insertion into pET28a(+) in frame with the encoded N-terminal and C-terminal 6xHis tags, respectively to yield pHis₆-0638 and p0638-His₆ respectively. Primer 0638-His-NF was designed with an *NheI* restriction site for insertion downstream of pET28a(+) encoded 6xHis tag and thrombin cleavage site and will amplify *cjj81176_0638* starting after the signal sequence predicted by SignalP 4.1. Primer 0638-His-NR is designed with an *EcoRI* restriction site for cloning into the MCS and contains the originally coded TAA stop codon. Primer 0638-His-CF was designed with an *NcoI* restriction site, that contains an AUG start codon and will amplify *cjj81176_0638* starting after the signal sequence predicted by SignalP 4.1. Primer 0638-His-CR is designed with an *EcoRI* restriction site for cloning into the MCS and does not encode a stop codon allowing for translation through to the 6xHis tag followed by a TGA stop codon encoded in the pET28a(+) expression vector.

2.4. PG Isolation and Assessment of O-Acetylation Levels

PG isolation for O-acetylation analysis was performed as previously described with modifications (133,148). Strains were streaked onto MH-TV agar (supplemented with antibiotics as necessary) from freezer cultures, and passed once to two MH-TV plates (to ensure there is a sufficient amount of bacteria for the next passage) in parallel. From the two MH-TV plates,

strains were then passed to ~60 MH-T (supplemented with Km or Cm as necessary) plates and grown for ~18-20 hrs. Cells were harvested by suspension in cold MH-TV broth followed by centrifugation. Strains were assessed by differential interference contrast (DIC) microscopy for contamination, and the absence of coccoid cells to ensure that cultures had not grown into stationary phase. Cells were harvested by centrifugation (8 000 x g, 15 min, 4°C) and resuspended in 50 mL of 25 mM sodium phosphate buffer pH~6.5. The cell suspension was added drop-wise to an equal volume of boiling 8% SDS in 25 mM sodium phosphate buffered at pH~6.5 and boiled for three hours under reflux with stirring. Samples were centrifuged (8 000 x g, 10 min, 25°C) and the lysate supernatant containing PG was stored at -20°C until needed.

SDS-insoluble PG was recovered by ultracentrifugation (160 000 x g, 1 hr, 25°C) of lysate supernatant (Optima L-90K with 70 Ti Rotor, Beckman Coulter). PG pellets were washed with sterile ddH₂O to remove SDS (tested using methylene blue/chloroform test on supernatant from washes) (155), after which they were frozen at -20°C and lyophilized (FreeZone 2.5 Liter Benchtop Freeze Dry System, Labconco). Lyophilized PG was resuspended in 2 mL of 10 mM Tris-HCl, 10 mM NaCl, buffered at pH~6.5 and sonicated (Misonix XL 2020, Mandel Scientific) on ice with a microtip for 2 mins continuously at 35 % power. The suspension was treated with 100 µg/ml α -amylase (Fluka Biochemika), 10 µg/ml DNase I (Invitrogen), 50 µg/ml RNase A (ThermoScientific), and 20 mM MgSO₄ overnight at 37°C. Protease (from *Streptomyces griseus*, Sigma-Aldrich), heat-treated at 60°C for 2 hrs, was added to a final concentration of 200 µg mL⁻¹ and the suspension incubated overnight at 37°C. The samples were then added to an equal volume of boiling 8% SDS in 25 mM sodium phosphate buffer pH~6.5 and boiled under reflux for 3 hrs. SDS-insoluble PG was recovered by ultracentrifugation (160 000 x g, 1 hr, 25°C), washed with sterile ddH₂O, frozen at 20°C, lyophilized and stored at -20°C until needed.

O-acetylation levels were assessed by David Sychantha and Anthony Clarke at the University of Guelph. Purified PG were resuspended in 10 mM sodium phosphate buffer pH 6.5 (10 mg mL⁻¹) and homogenized by sonication on ice with a microtip for 2 min continuously at 45% power. Homogenized PG solutions were adjusted to 100 mM NaOH to release O-linked acetate, or 100 mM sodium phosphate buffer pH~6.5 as controls, and incubated at 40°C for 4 hr with agitation. Insoluble material was removed by centrifugation (21 000 x g, 10 min, room temperature) and the supernatants were filtered through Millex-HV 0.45 µm-pore-size membranes. The concentration of acetate was quantified by HPLC (7.8 × 300 mm Rezex ROA-Organic Acid column, Phenomenex) operated with 0.005 M H₂SO₄ as eluent at 0.6 mL min⁻¹ and with a column temperature of 45°C. Elution of acetate was monitored using UV absorbance at 205 nm (5). The total MurNAc content was determined by acid hydrolysis of homogenized PG (50 µL) in 6 M HCl at 100°C for 1.5 hrs *in vacuo*. Samples were dried at 50°C *in vacuo* over solid NaOH to neutralize excess HCl and the hydrolysate was dissolved in 300 µL Mili-Q water. MurNAc quantification was performed using high-performance anion-exchange chromatography with pulsed amperometric detection (Dionex ICS-5000+ LC system, 3 × 150 mm Dionex CarboPac PA20) (4).

2.5. PG Isolation and Muropeptide Analysis

PG was prepared from strains pulled from freezer culture and grown overnight under standard conditions, passed once to an MH-TV plate and grown overnight, and then passed to ~20-25 MH-T plates (supplemented with Km as required) and grown for ~18-20 hr. Cells were harvested by suspension in cold MH-TV broth followed by centrifugation. Strains were assessed by differential interference contrast microscopy (DICM) for contamination and to ensure cells did not grow into stationary phase (appearance of coccoid cells). Cells were lysed using the

boiling SDS technique as previously described (70) and PG was purified from the cell lysate as described. (3) The PG was digested with the muramidase cellosyl (kindly provided by Hoechst, Frankfurt, Germany), the muropeptides were reduced with sodium borohydride treatment, and subsequently separated by HPLC as described (3). Muropeptide structures were assigned (i) based on comparison with retention times of known muropeptides from *C. jejuni* (1,70) and (ii) by mass spectrometry (MS). For MS analysis, muropeptide fractions were collected, concentrated by SpeedVac, acidified by addition of trifluoroacetic acid to 1%, and analyzed by offline electrospray mass spectrometry on a Finnigan LTQ-FT mass spectrometer (ThermoElectron, Bremen, Germany) at the Newcastle University Pinnacle facility as described (2).

2.6. Expression, Purification, and Biochemical Assays of Apel

Cjj81176_0638 was PCR amplified (Appendix B) without the predicted 21 amino acid signal peptide (as identified by SignalP 4.1 Server) (156) and cloned into the pET28a(+) (Novagen) expression vector in-frame with the encoded 6xHis-tag at either the N- or C-terminal codon of the gene, giving rise to pHis₆-0638 and p0638-His₆ respectively (Appendix A). Expression constructs were transformed into *E. coli*-BL21 via heat shock and selected for resistance to Km (3'-aminoglycoside phosphotransferase type III) encoded on pET28a (+). Constructs were confirmed by PCR and DNA sequencing.

Expression vectors were transformed into *E. coli* BL21 for expression. BL21-pET28a(+), BL21 - pHis₆-0638, and BL21 - p0638-His₆ were grown overnight under standard conditions in the presence of Km, as required. Overnight cultures were subcultured to an OD₆₀₀ of 0.2 and grown to OD₆₀₀ of ~0.5-0.6 before induction with 1 mM IPTG at room temperature for 3 hrs. Bacterial lysates were prepared by sonication for 2 mins (10s On/ 10 s OFF) in Lysis Buffer 1

(50 mM sodium phosphate buffer pH~8.0, 300 mM NaCl, 10 mM imidazole) and recombinant Ape1 was purified by Ni-NTA agarose (Qiagen) affinity chromatography. The sample was washed twice with 4 mL of Wash Buffer 1 (20 mM imidazole, 50 mM sodium phosphate buffer pH 8.0, 300 mM NaCl), once with 4 mL of Wash Buffer 2 (35 mM imidazole, 50 mM sodium phosphate buffer pH 8.0, 300 mM NaCl), and eluted with elution buffer (200 mM imidazole, 50 mM sodium phosphate buffer pH 8.0, 300 mM NaCl). Purified protein was dialyzed against 250 x sample volume of dialysis buffer (50 mM sodium phosphate buffer pH 8.0, 30 mM NaCl) using Slide-A-Lyzer (ThermoScientific) at 4 °C. The dialysis buffer was changed twice over 36 hrs. The sample was recovered and any precipitate present was removed via centrifugation. Quantification of total soluble protein was performed with Bio-Rad Dc Protein Assay Kit or by measuring the absorbance at 280 nm on a Nanodrop (ND-1000, ThermoScientific). Samples were concentrated using 3 kD MWCO (Millipore) as directed and concentrated samples were flash frozen in liquid N₂ as 10 µL aliquots for storage at -80°C until required.

Acetylcholinesterase activity was measured using *p*-nitrophenylacetate (*p*NPAc) as a colorimetric substrate as previously described (147) by tracking the production of *p*-nitrophenol as a change in absorbance at 405 nm. Assays were performed with 2.5 µg mL⁻¹ of purified Ape1-His₆ in 50 mM sodium phosphate buffer pH~6.5 and 2 mM *p*NPAc. Reactions were monitored over a minimum of 5 mins and specific activity calculated with an experimentally determined molar absorptivity of 3.416 mM⁻¹cm⁻¹ for *p*-nitrophenol (room temperature and in 50 mM sodium phosphate buffer pH~6.5).

PG-O-acetylcholinesterase activity was measured using purified PG (as in **PG Isolation and Assessment of O-Acetylation** Levels above). Lyophilized PG was resuspended in sodium phosphate buffer pH~6.5 to a concentration of 5 mg mL⁻¹ and sonicated on ice with a microtip

for 2 mins (10 s pulses 10 s break) at 35% PWR (Misonix XL 2020). A 500 μL sample of PG suspension was supplemented with Ape1-His₆ to a concentration of 10 $\mu\text{g mL}^{-1}$ (buffer only for negative control). Samples were incubated at 37°C in a water bath for 24 hrs after which samples were centrifuged (10 000 x g, 10 mins, 4°C) to pellet PG. Acetate content in supernatant was assessed with Acetic Acid Assay Kit (Megazyme International) as directed.

2.7. Microscopy and Celltool Shape Analysis

Overnight MH-TV log-phase broth cultures were standardized to 10 mL of OD₆₀₀ of 0.05 and incubated for 4 hrs and 7 hrs at 38°C with 200 rpm shaking. At each time point, the OD₆₀₀ was recorded, the concentration of cells in the culture quantified by drop-plating 10-fold serial dilutions, and the samples were processed for microscopy using agarose slabs for DICM and prepared for transmission electron microscopy (TEM) in parallel.

For TEM, samples were prepared as previously described (1). Cells were fixed with 2.5 % (v/v) of glutaraldehyde on ice for 2 hr. Fixed samples were harvested by centrifugation at 8,000 x g for 5 min and resuspended in an equal volume of Ultrapure H₂O (Invitrogen). To prepare samples for visualization, 2 μL of fixed cells were mixed with 4 μL of 1% uranyl acetate (w v^{-1}) on parafilm, and left for 1 min. A formvar-carbon film on 300 mesh copper grid (Canemco-Marivac, Lakefield, QC, Canada) was placed on the suspension. Grids were removed from the suspension, dried, washed 10 times in ddH₂O, dried again, and visualized on a Hitachi H7600 TEM equipped with a side mount AMT Advantage (1 mega-pixel) CCD camera (Hamamatsu ORCA) at the UBC Bioimaging facility (The University of British Columbia, Vancouver, BC, Canada).

Several representative fields of live cells were imaged on agarose slabs for each strain using DICM (Nikon Eclipse TE2000-U equipped with Hamamatsu C4742-95 digital camera) for

Celltool analysis. (157) Images were processed by thresholding to generate binary images in Adobe Photoshop ®. Images were thresholded to generate white cells on a black background such that the outcomes of the cell shapes were true to the original DICM image. Similar thresholding levels were maintained for each set of images and different image sets were thresholded such that the background pixilation was similar. Artifacts and cells that were clumped or ill-represented based on lighting effects were manually removed. The Celltool program was used to extract the contours of each cell. The contours of the wild-type population were aligned to one another to generate an average shape and principal components analysis (PCA) was performed to generate a "Shape Model" to describe 95% of the variation in the wild-type population (the default percentage) based on different principal components called "shape modes". Contours of other strains were then aligned to this wild-type PCA Shape Model as a reference. Kolmogorov-Smirnov tests were used on 1D smooth histograms of each shape mode to determine whether there was a statistically significant difference between the strains based on this wild-type Shape Model (157).

2.8. Phenotypic Characterization of OAP Mutants: Motility, Biofilm, Cell Surface Hydrophobicity, and Minimum Inhibitory/Bactericidal Concentrations

Phenotypic assays were performed on log-phase broth cultures as described in **Strains and growth conditions** above. Motility and biofilm assays were performed as previously described (70,158). For motility assays in soft agar, overnight cultures were resuspended to an OD₆₀₀ of ~0.2 in MH-TV broth and 2 µL was point inoculated in MH-TV agar (0.4% w v⁻¹). Halo formation was measured after overnight growth. Biofilm formation was assayed as standing cultures in MH-TV broth at a starting OD₆₀₀ of ~0.05 from overnight log-phase cultures grown

for 24 hours in borosilicate test-tubes. Biofilms were quantified with crystal violet staining and absorbance measured at 570 nm.

Cell surface hydrophobicity was assessed using the hexadecane partitioning method as previously described (159,160) with the following adjustments. Cells were harvested at 8,000 x g for 10 mins and washed three times with PBS, and resuspended to an OD₆₀₀ ~0.5. Hexadecane was added in a ratio of 1:4 (hexadecane:aqueous solution) by volume, the mixture vortexed for 5 min and incubated at 38°C for 30 min. The aqueous layer was removed, aerated by bubbling N₂ gas through the aqueous layer for 30 seconds and left open to the air for 10 minutes to ensure removal of all traces of hexadecane, and the OD₆₀₀ measured. Cell surface hydrophobicity was expressed as follows where OD_{600*i*} and OD_{600*f*} refer to the optical densities before and after extraction respectively.

$$\% \text{ Hydrophobicity} = \left(\frac{\text{OD}_{600i} - \text{OD}_{600f}}{\text{OD}_{600i}} \right) \times 100\%$$

Minimum inhibitory concentration/bactericidal concentration (MIC/BC) experiments were performed as previously described. In a 96-well plate, 100 µL of inoculum (log-phase overnight cultures standardized to OD₆₀₀ ~0.0002 [10⁶ CFU mL⁻¹]) and 11 µL of 10X concentrated test compound (in 2X-serial dilutions) were added to each well. A list of compounds tested and the range of concentrations can be found in Table 3. OD₆₀₀ was measured for each well using the Varioskan Flash Multimode Plate Reader (Thermo Scientific). MIC was recorded as the lowest concentration of compound that reduced OD₆₀₀ by 50% relative to a positive control (no-test compound) after 24-hours of growth. The MBC was defined as the lowest concentration of a compound required to kill bacteria after 24-hours, and was determined

by spot plating 5 μL from each well onto MH-TV agar free of test compounds and was assessed as the lowest concentration of compound that resulted in no growth (zero colonies).

2.9. Chick Colonization Studies

Chick colonization was assessed by Michael E. Taveirne and Victor J. DiRita under protocol 10462 approved by the University of Michigan Committee on Care and Use of Animals as previously described (6,70). Day-old chicks were inoculated with 1×10^4 CFU of *C. jejuni* strains by oral gavage. Chicks were sacrificed 7 days post-inoculation and cecal contents were recovered, diluted in PBS, and plated on a *Campylobacter* selective medium (MH supplemented with $40 \mu\text{g mL}^{-1}$ V, $10 \mu\text{g mL}^{-1}$ T, $4 \mu\text{g mL}^{-1}$ cefoparazone, and $100 \mu\text{g mL}^{-1}$ of cyclohexamide) and incubated at 42°C under 6% O_2 , 12% CO_2 , 82% air for 2-3 days. Colonies were counted and expressed as CFU g^{-1} of cecal contents.

2.10. Gentamicin Protection Assay

Gentamicin protection assays were performed as previously described (69). Strains were grown under standard laboratory conditions to obtain log-phase broth cultures. INT-407 cells were seeded into 24-well tissue culture plates at $\sim 1.25 \times 10^5$ cells in Minimum Essential Medium (MEM) supplemented with 10% fetal bovine serum (FBS) and 1X penicillin/streptomycin (pen/strep) (Gibco, Life Technologies) 24 hrs before infection. INT-407 cells were washed twice with 1 mL of MEM. Bacterial strains in log-phase were standardized to $\text{OD}_{600} \sim 0.002$ in MEM for infection at a multiplicity of infection (MOI) of ~ 80 . Spot plating of 10-fold serial dilutions was used to enumerate the initial inoculum (on MH-TV agar supplemented with 20 mM Na_2SO_3). At three hours post-inoculation, 3 hr-wells were washed twice with MEM before lysis and enumeration on MH-TV agar supplemented with 20 mM Na_2SO_3 (representing bacteria that have both adhered to and invaded INT-407 cells) and 5 hr- and 8 hr-wells had inoculum replaced

with MEM supplemented with $150 \mu\text{g mL}^{-1}$ of gentamicin. At five hours post-inoculation, 5 hr-wells were washed and enumerated as described above for the three hour time-point (invasion) and 8 hr-wells had gentamycin removed and replaced with MEM supplemented with 3 % FBS (v^{-1}) and $10 \mu\text{g mL}^{-1}$ gentamicin. At eight hr post-inoculation, wells were washed and enumerated as described above (short term intracellular survival).

2.11. Interleukin-8 Quantification

The concentration of IL-8 secreted by INT407 human epithelial cells infected with *C. jejuni* strains was assayed using the human IL-8 ELISA kit (Invitrogen) as described previously (1). INT407 cells were seeded into 24-well tissue culture plates at $\sim 10^5$ cells per well in 1 mL of Minimum Essential Medium (MEM) supplemented with 10% fetal bovine serum (FBS) and 1X penicillin/streptomycin (pen/strep) (Gibco, Life Technologies) 24 hrs before infection. INT407 samples were washed twice with 1 mL of MEM. Bacterial strains in log-phase were standardized to $\text{OD}_{600} \sim 0.002$ in MEM for infection at a multiplicity of infection (MOI) of ~ 100 . At 24 hr post-inoculation, media overtop the cells were harvested, centrifuged for 10 minutes to pellet cellular debris and bacteria, and frozen and stored at -20°C until assayed. The samples were assayed for IL-8 concentration using the human IL-8 ELISA kit as directed (Thermo Fischer Scientific).

3. RESULTS

3.1. *C. jejuni* OAP Gene Homologs were Identified by BLAST and Insertion/Deletion

Mutations were Generated with Complementation of Single Mutants

The OAP gene cluster was identified in *C. jejuni* 81-176 wild type by BLAST analysis using the *N. gonorrhoeae* OAP gene sequences. The loci identified were *cjj81176_0640*, *cjj81176_0639*, and *cjj81176_0638* for *patA*, *patB*, and *ape1*, respectively (Fig. 2A). The predicted amino acid sequence identity/similarity of these gene products to *N. gonorrhoeae* homologues are 35/53% for PatA, 39/57% for PatB, and 26/44% for Ape1.

To investigate the role of OAP in *C. jejuni*, the *patA*, *patB*, and *ape1* homologs, as well as the entire gene cluster, were inactivated by insertion/deletion mutagenesis with the non-polar Km^{R} cassette (*aphA-3*) from pUC18K-2 lacking a transcription termination site (153) (Fig. 2B). Complementation was achieved using the pRRC integration vector (154). The coding region of each OAP gene plus upstream sequence containing the ribosomal binding site was inserted into the genome of the corresponding mutant at ribosomal intergenic regions along with a Cm^{R}

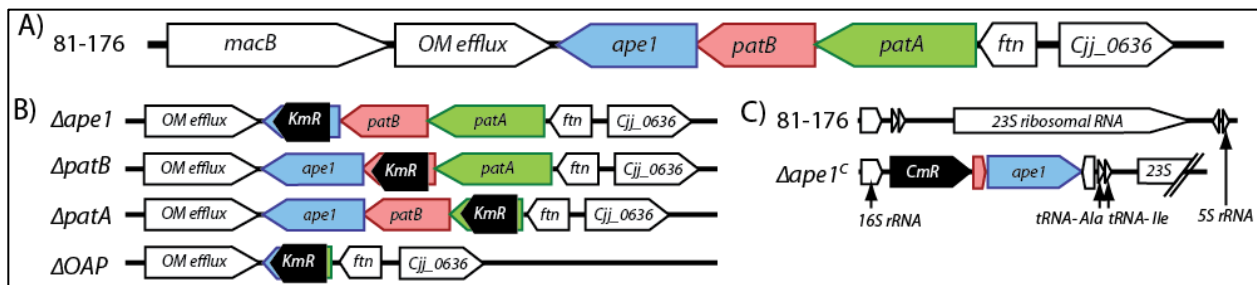


Figure 2. OAP gene cluster in *C. jejuni* and design for deletion and complementation.

A) The genomic organization of the *C. jejuni* OAP gene cluster. B) OAP mutants were generated by deletion of a portion of each gene (or entire cluster) and replaced with a non-polar Km^{R} cassette (*aphA3*) (153). Resistance to Km was used as a selective marker for successful homologous recombination. C) Complement construction (with Δape1 used as an example). Each OAP gene, with 50-100bp of upstream sequence, was cloned into the pRRC vector that contains homologous regions to three ribosomal intergenic regions downstream of the Cm^{R} cassette for selection of successful transformants. Complement constructs were transformed into their respective mutant backgrounds. MacB, macrolide specific efflux pump; OM efflux, outer membrane efflux; ftn, ferritin; 23S, 23S ribosomal RNA (154).

cassette (*ape1* complement construct shown in Fig. 2C as an example). Complementation was driven from the promoter of the Cm^R cassette.

3.2. O-Acetylation Levels of Purified PG from Deletion Mutants Reflect the Putative Functions of the *C. jejuni* OAP Gene Cluster

To determine whether the *C. jejuni* OAP gene homologs are involved in OAP, PG O-acetylation levels were determined for the mutants of the three putative OAP genes ($\Delta patA$, $\Delta patB$, and $\Delta ape1$) and for the mutant lacking the entire cluster (Δoap) (Fig. 2B). PG was isolated from all strains using an established protocol that minimizes spontaneous O-linked acetate hydrolysis (see Methods) and assessed for O-acetylation levels by quantifying base-catalyzed release of acetate and MurNAc by HPLC (4,5).

The O-acetylation levels for the wild-type 81-176 strain were determined to be $12.5 \pm 0.7\%$ O-acetylated PG relative to MurNAc content. O-acetylation levels among the mutants varied according to their predicted function (Table 1). Deletion of *patA* and *patB* resulted in a modest reduction in O-acetylation levels at $2.4 \pm 0.1\%$ and $3.0 \pm 0.2\%$, respectively, relative to MurNAc content. Deletion of the entire gene cluster in Δoap resulted in a decrease in O-acetylation levels to 2.1 ± 0.2 , similar to that of $\Delta patA$ and $\Delta patB$. O-acetylation was not completely lost in $\Delta patA$, $\Delta patB$, nor Δoap mutants, unlike in *N. meningitidis* where OAP is exclusively mediated by *patA/B* (144). This suggests that *patA/B* contribute to the overall O-acetylation levels of the PG sacculus in *C. jejuni*, but their absence is not sufficient to abolish OAP. Deletion of *ape1* led to an increase in O-acetylation at $35.6 \pm 2.2\%$ relative to total MurNAc content. These results are in accordance with the functions described for homologs in *N. gonorrhoeae* and *N. meningitidis*. O-acetylation levels were restored to wild-type levels in the $\Delta ape1$ complement ($11.8 \pm 0.5\%$). Analysis of the O-acetylation levels for $\Delta patA$ and $\Delta patB$

complements were not performed as, unlike the $\Delta ape1$ mutant, phenotypic differences between these mutants, Δoap and wild type were, in almost every case, not statistically significant or extremely minimal (see Table 1).

Table 1. O-Acetylation levels of PG of *C. jejuni* 81-176, Δape , $\Delta ape1$ complement ($\Delta ape1^C$), $\Delta patB$, $\Delta patA$ and Δoap (a mutant in which the entire cluster was deleted: Δape , $\Delta patB$ and $\Delta patA$), as determined by base-catalyzed hydrolysis reported as a % of O-acetylation relative to MurNAc content.

Strain	81-176	$\Delta ape1$	$\Delta ape1^C$	$\Delta patB$	$\Delta patA$	Δoap
% O-acetylation ¹	12.5	35.6	11.8	3.0	2.4	2.1
Standard deviation	0.7	2.2	0.5	0.2	0.1	0.2

¹Results shown are of one representative biological replicate measured in triplicate \pm standard deviation.

3.3. *C. jejuni* OAP Mutants Exhibit Altered PG Muropeptide Profiles, with $\Delta ape1$

Displaying the Most Dramatic Changes from Wild Type

O-acetylation has been described as a maturation event during PG biosynthesis occurring after transglycosylation and transpeptidation in the periplasm (149). Cleavage of PG by bacterial lytic transglycosylases (LytTG) is inhibited by PG O-acetylation, whereas removal of O-linked acetate at the C6 of MurNAc is needed for LytTG activity. Thus, O-acetylation may impact PG maturation events in *C. jejuni*, affecting aspects such as muropeptide profiles and glycan chain length. (140). We hypothesized that without the OAP gene cluster, not only is the level of O-acetylation affected, but also the muropeptide composition. To investigate this, PG was isolated from the wild type and each of the mutant and complemented strains, and the muropeptide composition was determined (Fig. 3). HPLC analysis of muropeptides is shown in Fig. 3; Table 2 shows summaries of the muropeptide analysis; Appendices 3 and 4 show raw data corresponding to the area under each peak in Fig. 3. For these experiments, a change in the relative abundance of a muropeptide species greater than 20% was considered significant.

This HPLC method used for muropeptide analysis does not preserve all of the O-acetyl groups on PG due to the alkaline conditions of the borohydride reduction and the unbuffered

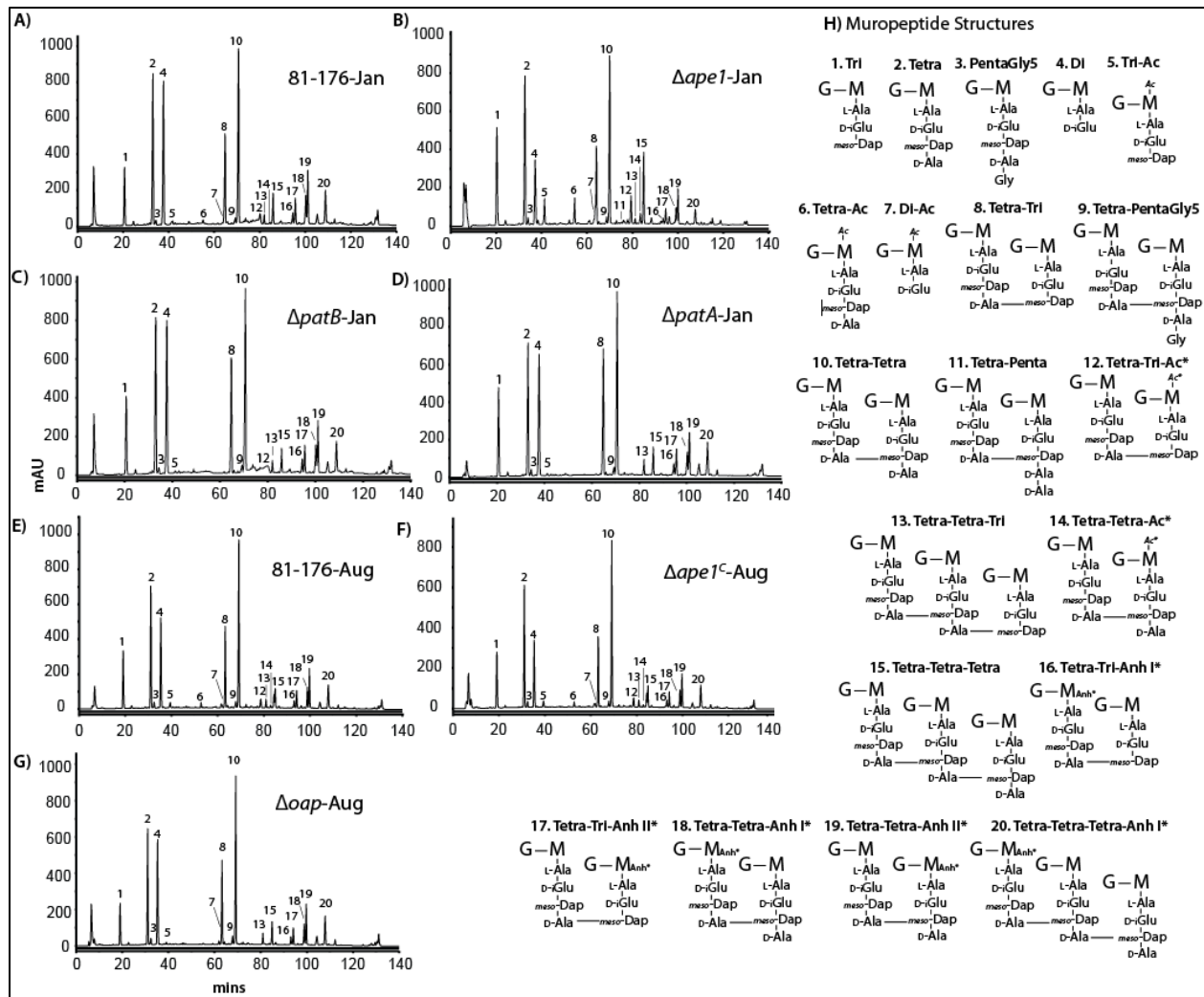


Figure 3. HPLC chromatograms of *C. jejuni* muropeptides and proposed structures.

Purified PG was digested with cellosyl and the resulting muropeptides were reduced with sodium borohydride and separated on a Prontosil 120-3-C18 AQ reverse-phase column. HPLC profiles are shown for wild-type strain 81-176, (A & E), Δ *ape1* (B), Δ *patB* (C), Δ *patA* (D), Δ *ape1*^C (F), and Δ *oap* (G). The muropeptide structure represented by each peak was determined previously by mass spectroscopy (1), and proposed muropeptide structures of each peak corresponding to the peak number in the chromatogram are shown in H. The summary of the muropeptide composition is shown in Tables 2, Appendix 3, and Appendix 4. G, N-acetylglucosamine; M, reduced N-acetylmuramic acid; l-ala, l-alanine; D-iGlu, D-isoglutamic acid; meso-Dap, meso-diaminopimelic acid; D-ala, D-alanine Ac, O-acetyl groups at MurNac C6 position; Anh, 1, 6-anhydro group of MurNac; *, it is not known on which MurNac residue the modification occurs.

conditions during PG isolation (133) and is thus less precise than the methodology used above.

Nonetheless, similar trends were observed, further supporting putative gene product function. PG

O-acetylation levels were reduced in Δ *patA*, Δ *patB*, and Δ *oap*, and increased in Δ *ape1* relative to wild-type 81-176. Monomeric O-acetylated tetrapeptide species, and O-acetylated tetra-tetra

dimeric species were absent in $\Delta patB$, $\Delta patA$, and Δoap . The abundance of all O-acetylated muropeptide species was increased in the $\Delta ape1$ mutant.

A decreased level of anhMPs in $\Delta ape1$ relative to the wild-type control corroborates the observed O-acetylation levels. A reverse correlation should exist between the concentration of O-acetylated muropeptides and anhMP as the presence of O-acetylation precludes the activity of LyTGs. In $\Delta patA$, $\Delta patB$, or Δoap , the relative abundance of anhMP species does not appear to be significantly different from wild type. Conversely, $\Delta ape1$ exhibited a 42.5% decrease in total anhMP species. As the anhMP represents the end of a glycan chain, the less chain ends, the greater the lengths of PG chains. Taking a ratio of the total abundance of muropeptides divided by the relative abundance of anhMPs will provide an indication as to the length of the glycan chains. Based on this, $\Delta ape1$ exhibits nearly 73.5% increase in average glycan chain length compared to wild type. Both these observations are similar to observations made in *N. meningitides* (144) and are consistent with the observed O-acetylation levels, as de-O-acetylation must precede LytTG

In addition to changes in O-acetylated muropeptides and anhMPs, changes were also observed in other muropeptide species between wild type and the OAP mutants, with the greatest number of changes and greatest degree of change observed in $\Delta ape1$ (Table 2). In $\Delta ape1$, notable changes of $\geq 30\%$ difference compared to wild-type were seen in monomeric dipeptides, tripeptides and pentapeptide-gly species; tetra-penta dimeric species, and tetra-tetra-tri trimeric species. In summary, total dipeptide species decreased by 38%, total tripeptides increased by 53%, and total pentapeptides increased by 62% in $\Delta ape1$ relative to wild-type. The majority of the muropeptide changes were restored to near wild-type levels in the $\Delta ape1$ complemented strain ($\Delta ape1^C$). Fewer changes reached $\geq 30\%$ difference compared to wild-type in $\Delta patA$ and

Table 2. Summary of PG muropeptide composition for *C. jejuni* 81-176, Δ *ape*, Δ *patB*, Δ *patA*, Δ *apeI*^C, Δ *patB*^C, Δ *patA*^C, and Δ *oap*

Muropeptide Species	Percentage of Peak Area ¹								
	Sample Set #1				Sample Set #2				
	<i>81-176</i>	Δ <i>apeI</i>	Δ <i>patB</i>	Δ <i>patA</i>	<i>81-176</i>	Δ <i>apeI</i> ^C	Δ <i>patB</i> ^C	Δ <i>patA</i> ^C	Δ <i>oap</i>
Monomers (Total)	43.5	49.1	44.9	41.7	42.2	41.5	39.6	41.2	40.0
Dipeptide	17.8	11.0*	18.0	15.0	13.6	11.0	11.2	17.2	16.4
Tripeptide	6.7	16.4*	8.5	10.2*	10.1	11.1	9.7	6.6*	6.7*
Tetrapeptide	18.3	20.9	17.6	15.8	17.2	18.1	17.1	16.1	15.5
Pentapeptides-Gly	0.6	0.9*	0.7	0.7	0.8	1.0	1.3*	0.9	1.0
O-Acetylated	1.0	8.0*	0.3*	0.3*	1.9	2.4	1.7	1.1*	0.8*
Dimers (Total)	47.7	40.7	47.6	49.4	48.8	49.4	49.5	48.5	48.1
TetraTri	16.8	14.2	18.4	18.5	16.0	15.5	15.2	15.7	15.2
TetraTetra	30.5	25.6	28.6	29.9	32.0	33.0	33.2	32.0	31.7
TetraPentaGly	0.4	0.9*	0.6*	1.0*	0.8	0.9	1.1*	0.8	1.2*
Anhydro-Dimers	13.5	8.2*	12.7	12.1	11.8	11.3	11.6	12.6	12.4
O-Acetylated	2.2	4.9*	1.7	0*	3.2	3.7	2.3	0.4*	0*
Trimers (Total)	8.8	10.2	7.5	8.8	7.8	8.1	9.5	8.9	10.2*
TetraTetraTri	0.9	0.5*	1.0	1.5*	1.0	0.9	1.3*	1.3*	1.4*
TetraTetraTetra	8.0	9.7	6.5	7.3	6.8	7.2	8.2	7.6	8.8
Dipeptides (Total)	17.8	11.0*	18.0	15.0	13.6	11.0	11.2	17.2	16.4
Tripeptides (Total)	15.4	23.6*	18.0	19.9	18.4	19.1	17.7	14.9	14.7
Tetrapeptides (Total)	65.9	64.0	62.9	63.9	65.1	67.1	67.6	64.8	65.1
Pentapeptides (Total)	0.8	1.3*	1.0	1.2*	1.2	1.5	1.9	1.3	1.6*
O-Acetylated (Total)	2.1	10.4*	1.2*	0.3*	3.5	4.3	2.9	1.3*	0.8*
Anhydromuropeptides	8.3	4.8*	7.8	7.5	7.7	7.4	7.9	8.3	8.6
Average Chain Length	12.0	20.8*	12.8	13.3	13.0	13.5	12.6	12.0	11.6
Degree of Cross-linkage	29.7	27.2	28.8	30.6	29.6	30.1	31.1	30.2	30.9
% Peptide Cross-links	56.5	50.9	55.1	58.3	57.8	58.5	60.4	58.8	60.0

¹Values represent the percentage area of each muropeptide from Appendices 4 and 5 calculated to give a total of 100%. Bolded numbers represent a change in relative abundance of $\geq 20\%$ from wild type. Bolded numbers with an asterisk (*) represent $\geq 30\%$ change from wild type. Percentages shown are calculated from values rounded to the nearest 0.1%. Samples were compared to the wild-type 81-176 muropeptide profile that was analyzed in the same experiment. Raw data is summarized in Appendices 4 and 5.

ΔpatB. For *ΔpatB*, the only muropeptide species with a $\geq 30\%$ difference, with the exception of the acetylated and the anhMPs, is the dimeric tetra-penta species with a 46% increase which led to an increase of 27% in total levels of pentapeptide species. For *ΔpatA*, a $\geq 30\%$ increase in monomeric tripeptides, tetra-penta dipeptides, and tetra-tetra-tri tripeptides was observed which led to a 50% increase in total pentapeptides compared to wild-type, although the change in total tripeptides did not reach $\geq 30\%$. The *Δoap* mutant exhibited some differences from wild type that followed the same trend as those from *ΔpatA*: an increase in tetra-penta dipeptides and tetra-tetra-tri tripeptides; and some peptides that were unique to *Δoap*: an increase in dipeptides and a decrease in tripeptides. *Δape1* also appeared to have a slight decrease of 10% in cross-linked muropeptides, which may be significant because the number of muropeptides in cross-links in *ΔpatA*, *ΔpatB*, *Δoap*, and *Δape1^C* exhibited differences no greater than 4% from wild-type. Analyses of PG muropeptide profiles for *ΔpatA* and *ΔpatB* complemented strains *ΔpatA^C* and *ΔpatB^C* showed minimal changes from wild type with restored O-acetylation levels for *ΔpatB^C*, but not *ΔpatA^C*.

3.4. Recombinant Ape1 Exhibits Acetyltransferase Activity *In Vitro* on Artificial Substrate *p*-Nitrophenylacetate and Natural Substrate O-Acetylated PG

Based on phenotypic data shown below as well as the more striking muropeptide data observed for *Δape1* compared to the other OAP mutants, the acetyltransferase activity of Ape1 was confirmed biochemically. Ape1 was expressed with a 6x-His tag at either the N- (His₆-Ape1) or C-terminus (Ape1-His₆) of the protein without the predicted 21 amino acid signal peptide (Fig. 4A) and purified. Details of the expression and purification conditions can be found in the experimental procedures (Fig. 4B). Purification of both recombinant proteins produced approximately 3 ml of 0.9 to 1.2 mg/ml of protein after dialysis from a starting culture of

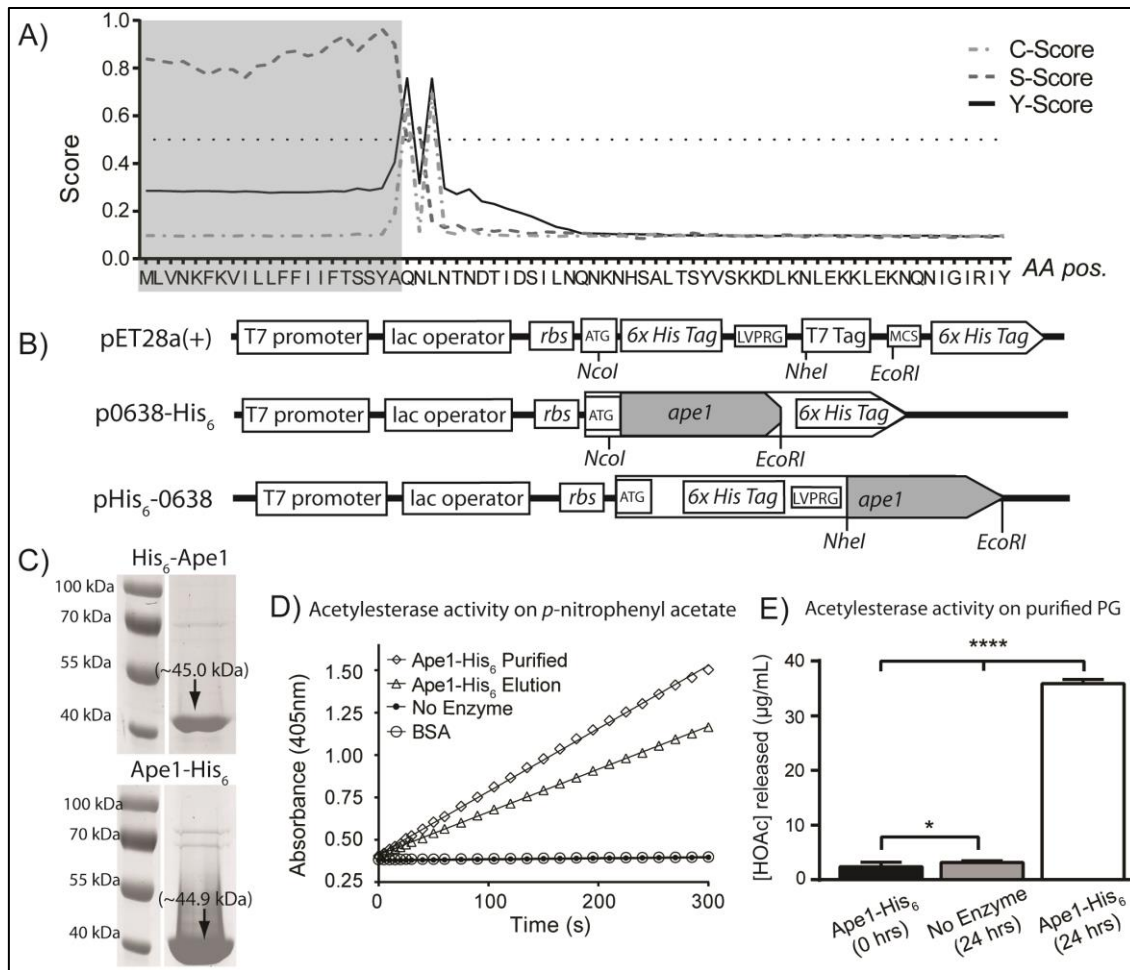


Figure 4. Design of Ape1 expression construct and assays for acetyltransferase activity.

A) SignalP 4.1 Server (156) output for signal peptide prediction of in-frame translation of *Cjj-81-176_0638*. C-score (the predicted first amino acid of the mature protein), S-score (the likelihood that the amino acid is in the signal peptide), and Y-score (amino acid with a high C-score exhibiting a large change in the S-score) predicted the cleavage site to be between the 21st and 22nd amino acids. B) *Cjj81-176_0638* was cloned without the signal peptide into pET28a(+) protein expression vectors. Top, map of cloning sites in pET28a(+) commercial expression vector. Middle, NcoI and EcoRI were used to produce a C-terminal His₆-tagged Ape1 protein that uses ATG start and TGA stop codons encoded in the vector. Bottom, NheI and EcoRI were used to produce an N-terminal His-tagged protein that uses ATG start codon encoded by the vector and the original stop codon from *Cjj81-176_0638*. rbs, ribosome binding site; LVPRG, thrombin cleavage site; MCS, multiple cloning sites. C) SDS-PAGE of Ape1 after Ni-NTA agarose purification shows protein of the approximate predicted size in eluted fractions. D) Purified Ape1-His₆ exhibits acetyltransferase/ deacetylase activity using pNPAc as a substrate (147). Reactions were monitored over five minutes as a change in the absorbance at 405 nm (formation of p-nitrophenol). The negative control and BSA control do not show acetyltransferase activity. Results shown are from one protein purification experiment. Results are reproducible for each purification experiment and activity is routinely assessed before performing enzymatic assays on PG. E) Ape1-His₆ has acetyltransferase activity using PG mucopeptides as a substrate. Determination of acetic acid concentration after treatment of Δ *ape1* PG with Ape1-His₆ for 24 hours was performed using Megazyme Acetic Acid Assay Kit. Treatment and no enzyme control were compared to acetic acid concentration at 0 h of treatment using student's t-test with * and **** indicating p-value < 0.05 and < 0.0001 respectively. Results are from one representative experiment of two biological replicates performed in triplicate.

100 mL. The expected sizes of the recombinant proteins are 45.0 and 44.9 kDa for His₆-Ape1 and Ape1-His₆, respectively. Using SDS-PAGE, a band of the appropriate size (~45 kDa) was present for both constructs (Fig. 4C) but not in an empty vector control (not shown). The specific activity of purified Ape1-His₆ was determined using *p*-nitrophenylacetate (*p*NPAc). This is a common substrate used to test for esterase activity (148,152). Specific activity for Ape1-His₆ ranged between 26.1 to 38.9 μmol/min/mg of protein among different protein preparations, suggesting that the recombinant protein exhibits acetylcysteine esterase activity (Fig. 4D). His₆-Ape1 exhibits similar specific activity as Ape1-His₆ with *p*NPAc (not shown).

Ape1-His₆ was also assayed for acetylcysteine esterase activity on its native substrate (Fig. 3C): O-acetylated PG. PG isolated from Δ *ape1* was used as the substrate due to the increased PG O-acetylation levels in this strain. Cleavage of O-acetyl groups was assessed using a commercial acetic acid assay kit (Megazyme) as an endpoint experiment. At 0 h, the average acetate concentration in the sample was 2.4 ± 0.3 μg/ml. Incubation of Δ *ape1* PG for 24 h in the absence of enzyme resulted in an average acetate concentration of 3.1 ± 0.1 μg/ml, and an average concentration of 35.9 ± 0.7 μg/ml of acetate after incubation with Ape1-His₆. Due to the insoluble nature of PG, data from this assay cannot be expressed in the classical definitions of enzyme kinetics using the native substrate. A second experiment showed similar trends but with higher acetate concentrations in the negative control and at 0 h. However, the concentrations of acetate in both were still significantly lowered (~3-fold less) than the Ape1 treated PG (not shown). The difference in acetate concentrations for the controls over the same time may represent spontaneous background hydrolysis and also suggests that the Acetic Acid Assay Kit may be detecting background or interference in reading.

3.5. Microscopy and Celltool Analyses of *C. jejuni* Δ *ape1* Population Morphology Reveal Shape pleomorphism

Since a number of changes were observed in the muropeptide profiles of these mutants, it was hypothesized that these changes may result in changes in cell shape (70). To assess this, the morphology was examined first by DICM and TEM to search for differences in the cell shape of the mutants (Fig. 5). Whereas the wild type strain exhibited the classic *C. jejuni* helical shape, the Δ *ape1* mutant exhibited primarily ‘comma-shaped’ cells and expressed differential curvature (greater wave amplitude and wavelength) (Fig. 5B). Wild-type helical morphology was restored upon complementation (Fig. 5C). A distinct change in morphology was not observed for the other OAP mutant populations (Fig. 5D-F).

The open-source shape analysis program called Celltool (157) was utilized to quantify these changes in shape in the OAP mutants. The program contains a set of tools used to extract shapes from binary images which can be used to assess and compare population morphology of strains using a variety of metrics. Extracted shapes from the wild-type population were aligned to one another, and principal component analysis (PCA) was performed to generate a baseline model for variation within the wild-type population (see **Materials and Methods** above). Visual representations of each shape mode are shown in Figs. 6 and 7. At early log phase (4 h after a starting OD₆₀₀ of ~0.05), the wild-type shape model consisted of two shape modes that together describe 95% of the variation in a *C. jejuni* wild-type strain 81-176 population (Fig. 6A). At mid log phase (7 h after a starting OD₆₀₀ of ~0.05), three shape modes described 95% of the morphological variation in the population (Fig. 7A). In both cases, the primary shape variability appears to be the length of the cell (>90% of the variance). This is to be expected since a

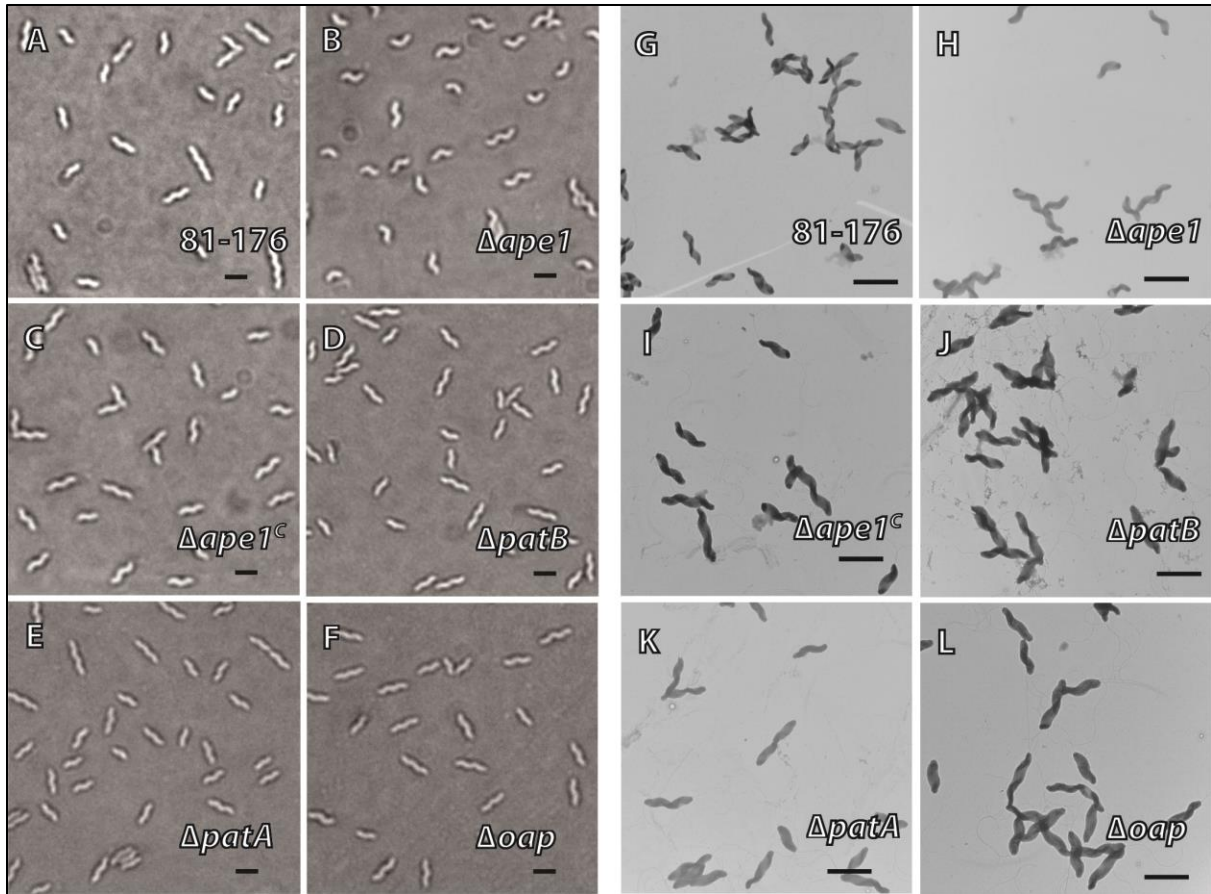


Figure 5. DICM and TEM reveal shape heterogeneity in $\Delta ape1$.

The *C. jejuni* $\Delta ape1$ mutant has a pleomorphic cell shape while other OAP mutants display unaltered cell morphology. DICM showing the morphology of wild-type 81-176 (A), $\Delta ape1$ (B), $\Delta ape1^C$ (C), $\Delta patB$ (D), $\Delta patA$ (E), and Δoap (F). Cells were harvested after 7 h of growth in MH-TV broth at an early-log phase of growth. Scale is 2 μ m (black bar). Negatively stained TEM images of (G) wild-type *C. jejuni* strain 81-176, (H) the hyper-curved $\Delta ape1$ strain, (I) the complemented strain $\Delta ape1^C$ with restored morphology, (J) $\Delta patB$, (K) $\Delta patA$, and (L) Δoap . Scale (black bar) is 2 μ m.

population of growing cells would have cells at different points of growth and division and thus length. Shape mode 2 at early log phase and late log phase explains 2.5% and 1.9% of the variation in their respective populations, and both appear to have some relation to the curvature/wavelength of the cell. A third shape mode was identified at mid log phase explaining 1.7% of the variation in that population, and appears to result from the width of the cell. Extracted contours of mutant strains were then aligned to these wild-type shape models as references and a measurement was generated for each representing their deviation from the mean

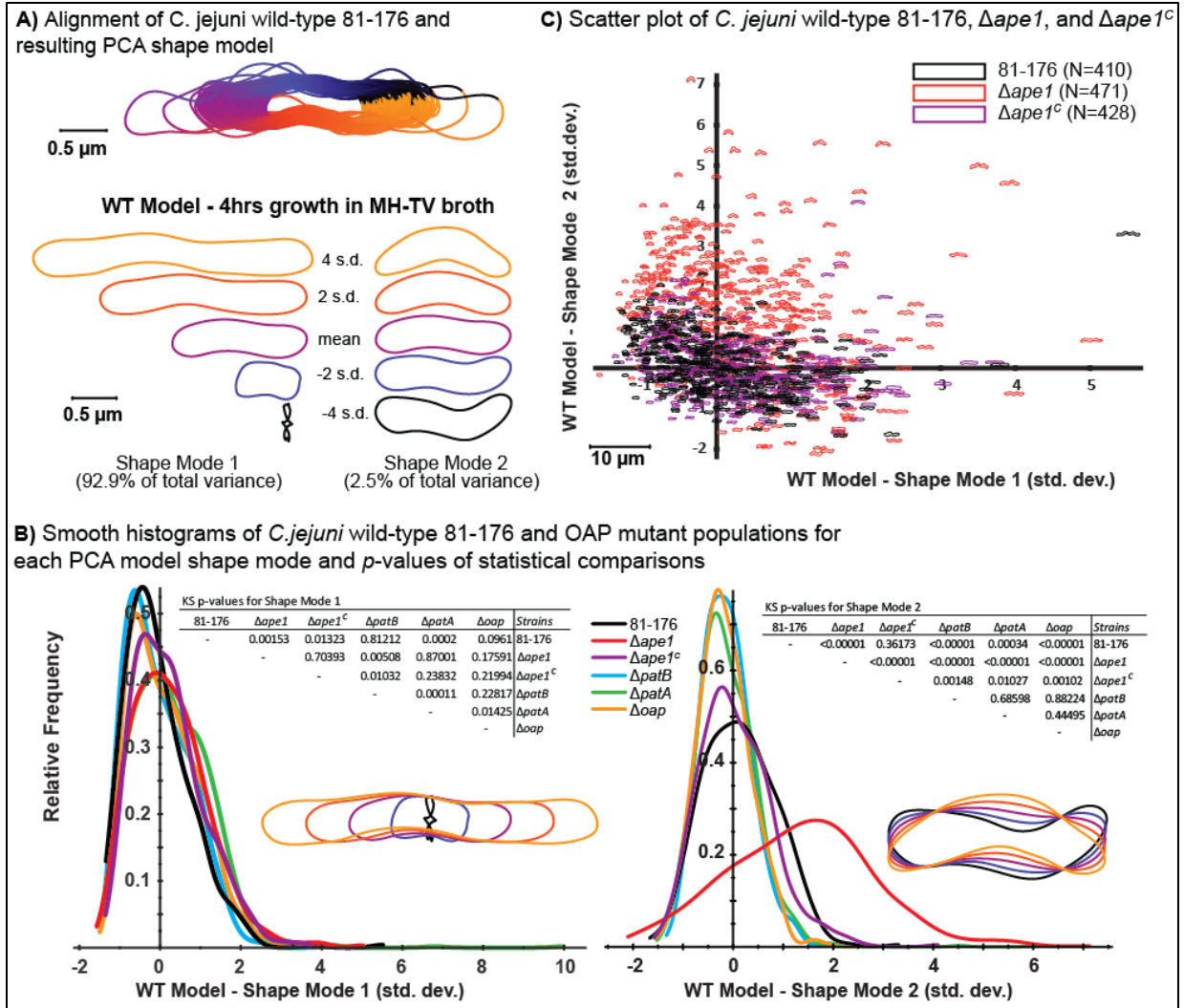


Figure 6. Celltool analysis of wild-type strain 81-176, $\Delta ape1$, $\Delta ape1^C$, $\Delta patB$, $\Delta patA$, and Δoap population morphology at early-log phase.

Several representative images were taken using DICM. Images were converted to binary format (white cells on a black background) and lumps and artifacts were manually removed from images before processing through Celltool “extract contours function” to generate contours representing each cell (157). A) Contour extraction, alignment and generation of the PCA shape model. The Celltool “align contours” function was used to align the contours of the wild-type population to one another. Principal component analysis was performed to generate a wild-type shape model that explains 95% variation in the population in principal components called “shape modes”. The extracted contours of the mutant populations were then aligned to the wild-type shape model and a measurement representing the normalized standard deviation from the wild-type mean in each shape mode was generated. Based on the visual representations, shape modes 1 and 2 represent variation in length and curvature respectively. B) Kolmogorov-Smirnov tests were performed for each shape mode between each population. C) Measurements of wild-type, $\Delta ape1$, and $\Delta ape1^C$ were plotted with shape mode 1 along the x-axis and shape mode 2 along the y-axis.

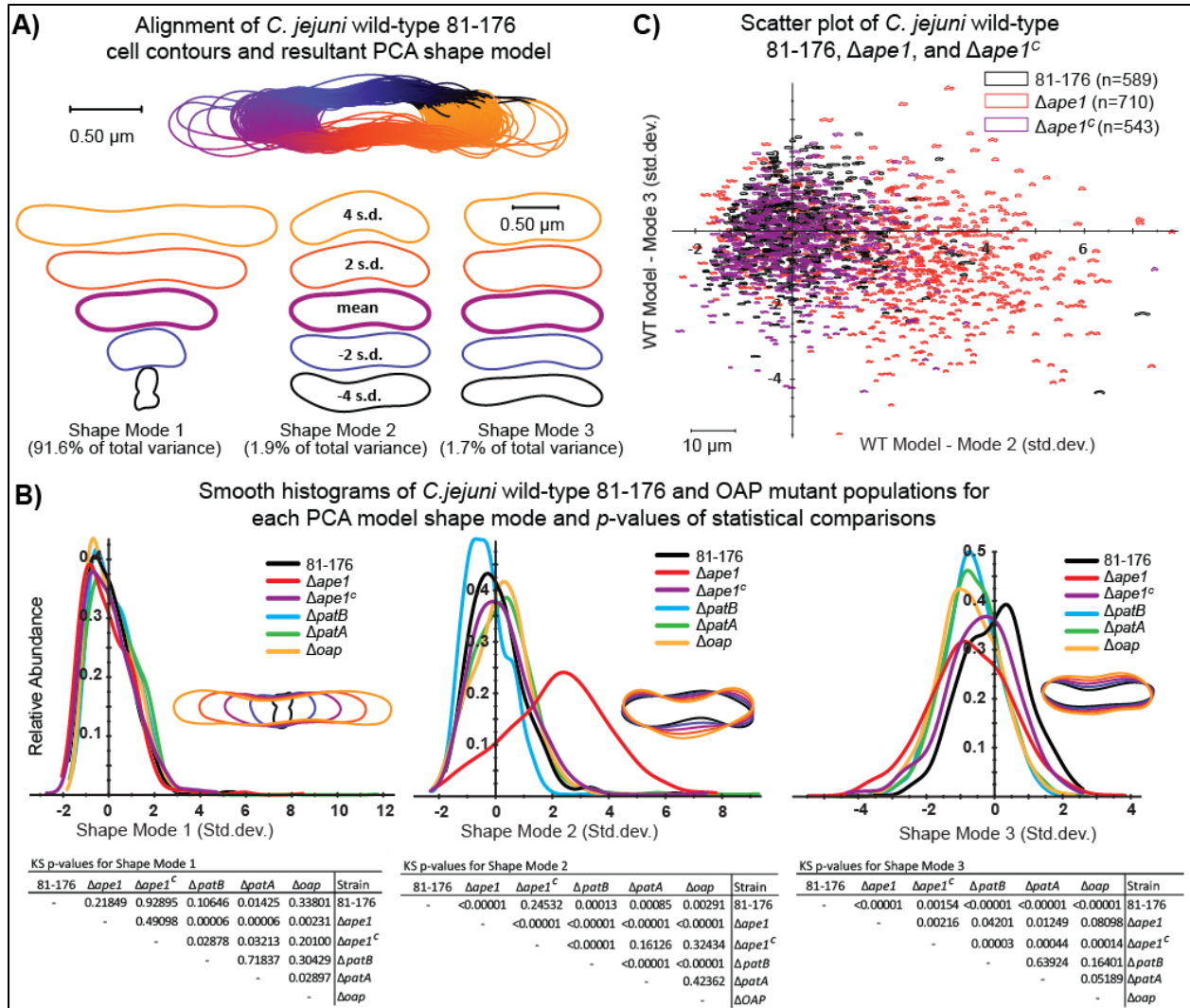


Figure 7. Celltool analysis of wild-type strain 81-176, $\Delta ape1$, $\Delta ape1^C$, $\Delta patB$, $\Delta patA$, and Δoap population morphology at mid-log phase.

DICM images were taken of strains grown for 7 h in MH-TV broth at a starting OD600 of 0.05 (to mid-log phase). Images were converted to binary format (white cells on a black background), and lumps and artifacts were manually removed before processing with Celltool (157) “extract contours function” to generate contours representing each cell. A) Contour extraction, alignment and generation of the principal component analysis (PCA) shape model for *C. jejuni* wild-type strain 81-176. Celltool “align contours” function was used to align the contours of the wild-type population to one another. B) PCA was performed to generate a wild-type shape model that explains 95% variation in the population in principal components called “shape modes”. Shape modes 1, 2, and 3 represent variation in length, curvature, and width, respectively. The extracted contours of the mutant populations were then aligned to the wild-type shape model, and a measurement representing the normalized standard deviation from the wild-type mean in each shape mode was generated and depicted graphically. Kolmogorov-Smirnov (KS) tests were performed for each shape mode between each population and are summarized below the plots. C) Measurements of wild type, $\Delta ape1$, and $\Delta ape1^C$ were plotted with shape mode 2 along the x-axis and shape mode 3 along the y-axis to create a scatter plot showing the variation in the different populations.

in standard deviations. Kolmogorov-Smirnov (KS) statistical tests were used to compare sample probability distribution. Based on the large population of bacterial cells assessed and conditions required for KS analysis, a p-value of 0.00001 was used as a cut-off for significance and the graphical representations were used to infer any important observations (Fig. 6B and 7B) (161).

In mid-log phase cells, no strains were significantly different from the wild-type population in shape mode 1 (cell length) or from each other, with the graphical output also showing that the population distributions overlay each other very closely. In shape mode 2 (cell curvature), the $\Delta ape1$ population was significantly different from wild type, $\Delta ape1^C$, $\Delta patA$, $\Delta patB$, and Δoap populations. Some of the differences in population distribution in shape mode 2 between wild type and $\Delta ape1^C$, $\Delta patA$, $\Delta patB$, and Δoap were also significant by the KS cut-off utilized. However, the graphical output showed that these strains were fairly similar to wild type, whereas $\Delta ape1$ exhibited a dramatic shift in the population distribution maximum (approximately 2.2 standard deviations from the wild-type mean) compared to all other strains. Shape mode 3 (cell width) was significantly different in all strains compared to wild type (with the exception of $\Delta ape1^C$), and each exhibited a shift of approximately one standard deviation in the population maximum towards a reduced width compared to the wild-type mean as reflected in the graphical output. Early-log phase bacteria exhibited similar population shifts as observed for mid-log phase bacteria (with the exception of shape mode 3, as cell width was not captured as major contributor to the variation in shape for wild type at this time point). As with mid-log bacteria, the most notable shift in shape was observed for cell curvature (shape mode 2) in $\Delta ape1$ (Fig. 7). 2-D scatterplots of measurements for each individual contour of wild type, $\Delta ape1$, and $\Delta ape1^C$ populations for shape modes 2 against shape modes 1 or 3 (Fig. 5C) likewise shows that

there was a clear difference in shape for the $\Delta ape1$ population compared to wild type and $\Delta ape1^C$.

3.6. Phenotypic Analyses Reveal the Importance of O-Acetylpeptidoglycan Esterase Activity on Various Aspects of *C. jejuni* Physiology.

The OAP mutants were assessed for different phenotypes serving as indicators of transmission and/or colonization efficiency: motility, biofilm formation, hydrophobicity, and sensitivity to a variety of common inhibitory compounds.

Motility is a major colonization determinant for *C. jejuni* (75). While all strains exhibited decreased motility compared to wild type in soft agar plates as measured by halo formation after point inoculation (Fig. 8A), the motility of $\Delta ape1$ was $68 \pm 5\%$ of wild type. The mutant strains $\Delta patB$, $\Delta patA$, and Δoap were modestly defective, with motility levels at $92 \pm 4\%$, $91 \pm 4\%$ and $87 \pm 5\%$, respectively, of wild type. Complementation of $\Delta ape1$ restored the motility of the mutant to 90% of wild type and was significantly different from that of $\Delta ape1$. In addition, $\Delta ape1$ formed aberrant halos on soft agar with rough perimeters as opposed to the relatively circular halos formed by wild type. This phenotype was absent in the other mutants tested and was rescued by complementation.

The ability to form biofilms is an important attribute in *C. jejuni* persistence and transmission. *C. jejuni* has been shown to survive up to 28 days in a biofilm state (162). The ability of our OAP mutants to form biofilms was assessed in borosilicate test tubes by crystal violet (CV) staining of 24 h standing cultures (158). The $\Delta ape1$ mutant exhibited a hyper-biofilm formation phenotype, producing 5.5-fold more biofilms than wild type (Fig. 8B). $\Delta ape1$ biofilm cultures also developed flocs of bacteria suspended in the broth (84), which were not observed for wild type nor were included in the crystal violet quantification of surface-adhered biofilms

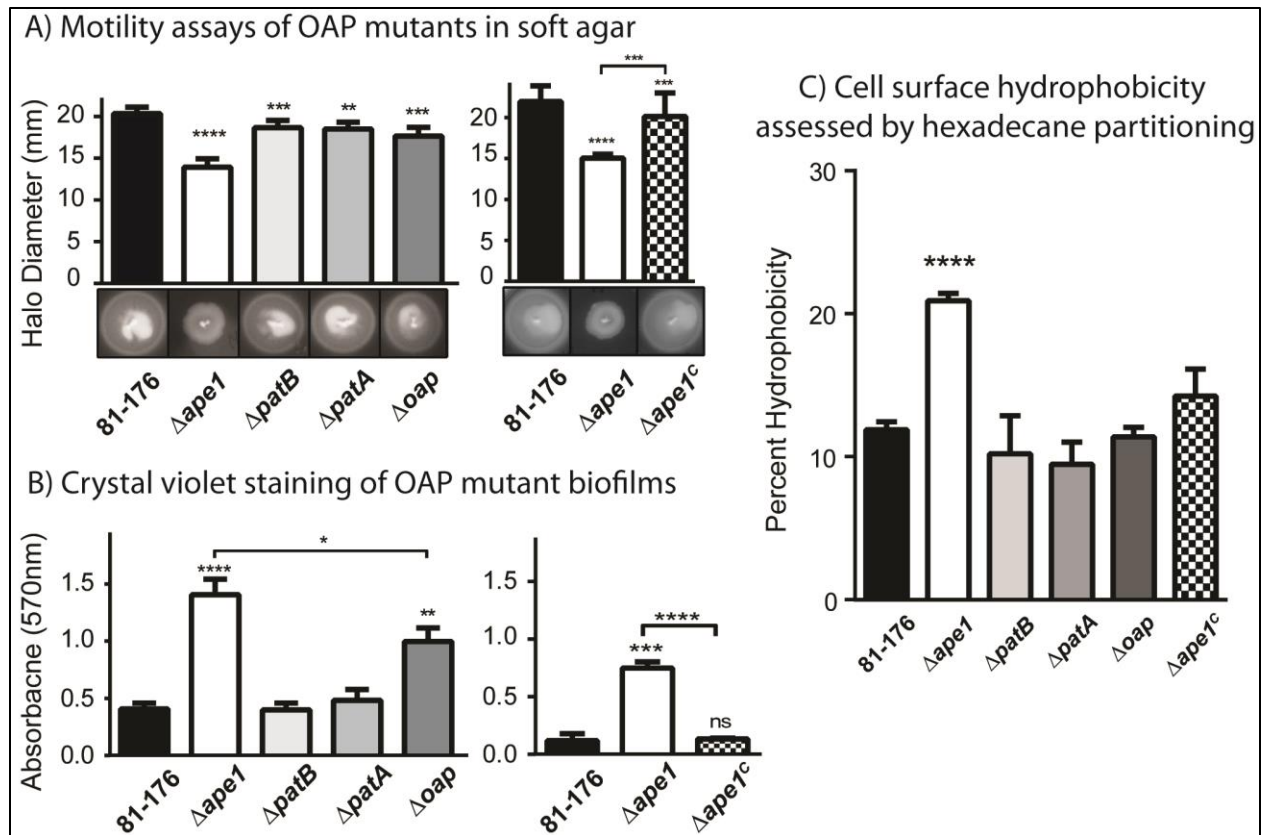


Figure 8. Motility, biofilm formation, and cell surface hydrophobicity of OAP mutants.

Motility, biofilm formation, and cell surface hydrophobicity of OAP mutants and wild-type strain 81-176. **A**, Δ ape1 exhibits a 30% decrease in motility and abnormal halo formation (rough edges). Motility was assessed by measuring the halo diameter after 24 h of strains point inoculated in 0.4% semi-solid agar. Representative images of halos are shown below each graph. Results shown are representative of one of three independent experiments with 6 replicates. Each strain was compared to wild-type using a paired Student's *t* test, with **, ***, and **** indicating $p < 0.01$, $p < 0.001$, and $p < 0.0001$. **B**, Δ ape1 and Δ oap exhibit 5.5 and 2.5 fold enhanced biofilm formation, respectively at 24 hours. Biofilm formation was assessed after 24 h by crystal violet staining of standing cultures in borosilicate tubes and spectrophotometric quantification of dissolved crystal violet at 570nm. Results shown for the mutants (left) are representative of one of three independent experiments carried out in triplicate. The results for the complements (right) are representative of one of two experiments performed in triplicate. **C**, Δ ape1 increased to 2.0-fold in hydrophobicity relative to wild-type, as assessed by hexadecane partitioning. Results are representative of one of three independent experiments performed in triplicate. For biofilm and hydrophobicity, strains were compared using an unpaired Student's *t* test, with *, **, ***, and **** indicating $p < 0.05$, $p < 0.01$, $p < 0.001$, and $p < 0.0001$. Error bars represent standard deviation.

(not shown). Complementation of Δ ape1 restored biofilm formation to wild-type levels. Biofilms formed from both the Δ patB and Δ patA mutants were indistinguishable from wild type, but the Δ oap mutant produced ~2.5-fold more biofilm material than the wild type. Characterization of Δ ape1 biofilms by microscopy was unsuccessful, as Δ ape1 forms biofilms poorly on glass

coverslips, unlike wild type. This possibly is an indication of altered cell surface properties, and so cell surface hydrophobicity was assessed using hexadecane partitioning (Fig. 8C) (160). The percentage hydrophobicity value of *Δape1* was significantly higher (2.0-fold) than wild type and was restored to wild-type levels upon complementation.

The sensitivity of the OAP mutants to detergents, salts, and antimicrobial compounds was tested by determining the minimum inhibitory concentration (MIC) (Table 3). Only *Δape1* exhibited an increased susceptibility to any of the compounds tested: the amphipathic bile salt/detergent sodium deoxycholate (DOC) and MgCl₂. For *Δape1*, an MIC range for DOC of 0.16 to 0.31 mg/ml was observed, whereas the MIC for wild type was greater than the highest concentration of DOC tested (>10 mg/ml). *Δape1* exhibited a 4 to 8-fold reduction in MIC for MgCl₂ compared to wild type. Complementation of *Δape1* restored wild type sensitivity profiles.

3.7. Ape1 is Required for Efficient *C. jejuni* Bacterial-Host Interaction

Due to the altered physiology of *Δape1*, the contribution of OAP to *C. jejuni* bacterial-host interactions was examined by determining the recovery of the mutants during chick colonization and host cell infections, as well as the ability to elicit IL-8 secretion *in vitro* in human epithelial cell infections.

Chickens are an avian reservoir for *C. jejuni* and a common source of human infection. The *Δape1* mutant exhibited a significant 4.4-log decrease in colonization, although there was also a significant difference in the variance between *Δape1* and wild type. Recovery ranged between 1.90x10⁷ CFU/g to 100 CFU/g (below the detectable limit). Surprisingly, *ΔpatB*, *ΔpatA*, and *Δoap* mutants did exhibit significant differences in chick colonization as *ΔpatB*, *ΔpatA*, and *Δoap* were recovered at wild-type levels (approximately 10⁹ CFU/g of cecal content) (Fig. 9A).

Table 3. MIC₅₀ of *C. jejuni* OAP mutants determined by broth dilution.¹

Compound	MIC ₅₀					
	<i>81-176</i>	<i>ΔapeI</i>	<i>ΔpatB</i>	<i>ΔpatA</i>	<i>Δoap</i>	<i>ΔapeI^C</i>
<u>Detergents</u>						
Deoxycholate (mg/mL)	>10	0.16-0.31	5->10	1.3->10	1.3->10	1.3->10
SDS (mg/ml)	10-12.5	2.5-6.25	10-12.5	2.5-12.5	5-6.25	12.5
Triton (% v/v)	0.05	0.02-0.05	0.02-0.05	0.02-0.05	0.05	0.05
<u>Antimicrobial</u>						
Ampicillin (μg/ml)	2.4-4.9	1.2-4.9	4.9	4.9	2.4-4.9	2.4
Lysozyme (mg/ml)	>5	>5	>5	>5	>5	>5
Polymyxin B (μg/ml)	20	10	10	10	10	10-20
*Protamine (μg/ml)	31.3	15.6-31.3	-	-	-	31.3-62.5
<u>Chelating Agent</u>						
EDTA (μM)	78-156	1.2-156	156	156	156	156
<u>Salts</u>						
NaCl (mM)	62.5-250	31.3-62.5	62.5-125	125	62.5-125	62.5-125
MgCl ₂ (mM)	62.5-125	15.6	62.5-125	62.5-125	62.5-125	62.5-125
CaCl ₂ (mM)	125	125-250	125-250	125-500	500	125
KCl (mM)	62.5	31.3-62.5	62.5	31.3-62.5	125	31.3-62.5

¹Measurements indicated with a ‘-’ were not tested. Measurements in **bold and highlighted** were consistently ≥4-fold different from wild type over three experiments. SDS, sodium dodecyl sulfate. MIC, minimum inhibitory concentration to reduce growth by 50% as assessed by optical density.

Due to the defect in chick colonization, the ability of the *C. jejuni* OAP mutants to adhere to, invade, and survive inside the human epithelial cell line INT407 was assessed by a gentamicin (Gm) protection assay. Despite being inoculated with similar CFU counts, the recovery of *ΔapeI* was significantly reduced at the adherence, invasion, and intracellular survival time points in comparison to wild type (Fig. 9B). *ΔapeI^C*, *ΔpatB*, *ΔpatA*, and *Δoap* displayed wild-type INT407 infection profiles (Fig. 9C-F).

As $\Delta ape1$ was the only OAP mutant to demonstrate reduced invasion of the INT407 cells, its ability to elicit IL-8 secretion from in INT407 cells was assessed by ELISA. Cells infected with $\Delta ape1$ reproducibly exhibited statistically significant lower levels (60-79%) of IL-8 secretion compared to cells infected with wild type. $\Delta ape1^C$ did not complement IL-8 induction defects (Fig. 9G).

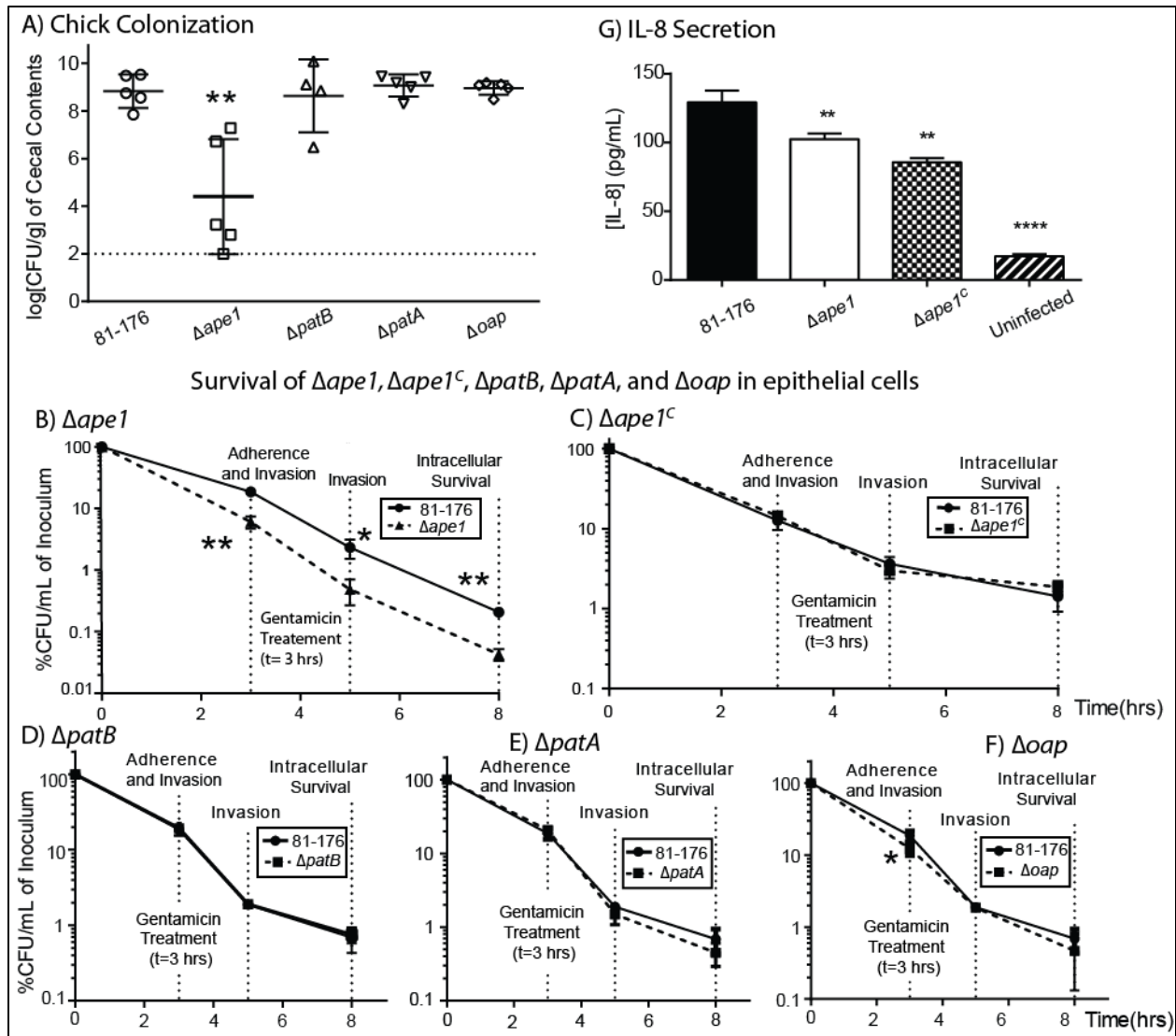


Figure 9. The effect of OAP levels on *C. jejuni* host-bacterial interactions. Complete figure caption can be found on page 55.

Figure 9. The effect of OAP levels on *C. jejuni* host-bacterial interactions.

A) $\Delta ape1$ shows reduced chick colonization compared to wild-type strain 81-176, while $\Delta patB$, $\Delta patA$, and Δoap mutants display wild-type colonization. Each point represents the recovery of *C. jejuni* strains in log CFU/g of cecal contents from individual day-old chicks 6 days post-colonization with 1×10^4 CFU/ml of the indicated strain. The geometric mean is denoted by a black bar. Error bars represent 95% confidence intervals. Adherence, invasion, and intracellular survival of *C. jejuni* in INT407 epithelial cells were assessed by a gentamicin (Gm) protection assay and OAP mutant strains. $\Delta ape1$ (B) shows a reduced ability to adhere to, invade and survive in INT407 epithelial cells which was restored upon complementation (C). $\Delta patB$ (D), $\Delta patA$ (E), and Δoap (F), exhibit near wild-type adherence, invasion, and intracellular survival properties. INT407 cells were infected with *C. jejuni* at an MOI of ~80. Adherence and invasion was quantified at 3 h post-infection. At this point the media in the remaining wells was replaced with MEM containing gentamicin (150 $\mu\text{g}/\text{mL}$) and incubated for 2 h, after which the amount of bacterial cells which had invaded the epithelial cells was measured (5 h invasion time point). The Gm in the remaining wells was washed off, and the cells were incubated with fresh MEM containing 3% FBS and a low dose of Gm (10 $\mu\text{g}/\text{mL}$) for an additional 3 h (8 h ST intracellular survival time point). CFU/mL was determined for each well by lysing the cells with water and plating the dilutions onto MH-TV plates. Results for B and C are representatives of three independent experiments performed in biological triplicate. The data in D, E, and F are representatives of two independent experiments performed with three biological replicates. G, INT407 epithelial cells secrete less IL-8 upon infection with $\Delta ape1$ than wild-type. Results are from one representative experiment of three independent experiments performed in triplicate. Error bars represent the standard deviation. *, denotes statistically significant difference using the unpaired Student's *t* test, with *, **, ***, and **** indicating $p < 0.05$, $p < 0.01$, $p < 0.0001$, and $p < 0.00001$ respectively.

4. DISCUSSION AND CONCLUSIONS

PG plays a role in multiple facets of bacterial physiology. A number of PG modifications have been shown to influence pathogenic properties in several bacterial species [for reviews, see (105) and (131)]. O-acetylation of PG is believed to be a maturation event occurring soon after transpeptidation and incorporation of muropeptides. Muropeptides need to be de-O-acetylated for LytTG activity to ensue. The full extent and influence of OAP is unknown in *C. jejuni* but based on its impact on pathogenesis in many bacterial species (136,141,142,144) and the importance of cell shape in *C. jejuni* pathogenesis (1,70,81), it was hypothesized that OAP affects PG biochemistry and that this extends into the fitness of *C. jejuni*. Here, the OAP genes in *C. jejuni* were shown to contribute to PG O-acetylation/deacetylation, consistent with their predicted functions. These genes were also important for several key physiological and pathogenic properties. This was most notable for *ape1*, encoding an esterase involved in PG O-deacetylation, which was the only OAP gene significantly required for every phenotype examined.

Analyses of the OAP levels in $\Delta patA$, $\Delta patB$ and $\Delta ape1$ support their predicted functions. Deletion of *patA* and *patB*, which act together to O-acetylate MurNAc, is non-lethal as found in several other bacterial species (136,144,163). This suggests that O-acetyl groups added by PatA/B play a non-essential role for growth of *C. jejuni* in the laboratory. However, since the O-acetylation levels were not reduced to 0% in $\Delta patA$ and $\Delta patB$, this indicates the presence of alternative PG O-acetylation machinery or compensation by other acetyltransferases (151). There are conflicting results for the essentiality of *ape1* in *N. gonorrhoeae* (145,163). In *C. jejuni*, *ape1* was not essential in *C. jejuni*. Deletion of *ape1* resulted in an increase in O-acetylation levels that was almost triple that of wild type, supporting the role of Ape1 in *C. jejuni* PG de-O-

acetylation. Ape1 acetyltransferase activity was confirmed *in vitro* with recombinant enzyme using the artificial substrate pNPAc as well as its natural substrate, O-acetylated PG from Δ *ape1*. It should be noted that the OAP levels of wild-type *C. jejuni* 81-176 described here were lower than those reported in a previous study for ATCC 700819 and NCTC 11168 (146). In addition to the strains, the growth conditions used also differed between the studies. As such, there is potential that these differences in O-acetylation can be strain differences and/or differences in culture growth phase. *C. jejuni* O-acetylation levels have not yet been assessed over different growth stages but some preliminary data from our research group suggests that O-acetylation levels may decrease as the culture gets older (unpublished data) but that is beyond the focus of this study. A direct comparison of how these and other potential factors might affect *C. jejuni* PG O-acetylation will be the topic of future work.

As with the OAP analyses described above, the muropeptide profiles also showed differences in PG O-acetylation levels between the 81-176 wild type, OAP mutant, and complemented strains used in this study. Since the PG isolation protocol used for muropeptide analysis leaves the O-linked acetate prone to spontaneous hydrolysis, these values are not quantitative representations of total O-acetylation levels. Nonetheless, the trends in O-acetylation levels in the OAP mutants were found to be similar between the two methods of PG preparation utilized, thus the muropeptide data offer additional qualitative support for the role of these OAP genes in PG O-acetylation. Unlike what was reported for *N. meningitidis*, in which Ape1 exhibited specific esterase activity to O-acetylated muropeptides with a tri-peptide stem (144), the muropeptide analysis here suggests that Ape1 may act on multiple muropeptide species, as the proportion of all O-acetylated muropeptides increased in Δ *ape1*. Previous observations with *N. gonorrhoeae* PatB O-acetyltransferase using *in vitro* assays showed specificity of PatB

towards O-acetylation of tetrapeptides (149). A decrease in O-acetylated tetrapeptide species was observed for the *C. jejuni* $\Delta patA$ and $\Delta patB$ mutants (Appendix 3); however, as this could have been due to hydrolysis during the preparation procedure, further in-depth biochemical analysis will be required and is a topic for future research.

A reverse correlation should exist between the concentration of O-acetylated muropeptides and anhMP, because the presence of O-acetylation precludes the activity of LytTGs. As expected, $\Delta ape1$, which harbors higher O-acetylation than wild type, also exhibited a 42.1% decrease in relative anhMP levels (presumably due to impaired LytTG activity) and a greater average chain length compared to wild type. Although chain length was not directly measured, these data support previous findings that Ape1 regulates PG chain length in *N. meningitidis* (144). Surprisingly, the anhMP levels changed only marginally in $\Delta patA$, $\Delta patB$, and Δoap . Thus, another mechanism for O-acetylation may exist in *C. jejuni*, consistent with our OAP analyses, may compensate sufficiently to control LytTG activity. Alternatively, O-acetylation itself may not be an essential or the only control/regulatory mechanism for chain length or LytTG activity in *C. jejuni*. Other LytTG control mechanisms, in addition to MurNAc O-acetylation, have been proposed in other organisms. LytTGs in *E. coli* and *Pseudomonas aeruginosa* have been found in complexes with peripheral membrane-bound lipoproteins and PBPs, and are thought to be controlled spatially as well as having their activity coupled with PG synthesis to prevent autolysis (140). For *C. jejuni*, our observations do suggest a role for OAP in regulating LytTG activity, although other control mechanisms likely exist.

As PG O-acetylation is believed to be a maturation process, occurring soon after incorporation into the sacculus via transglycosylation and transpeptidation (164), differences in the muropeptide composition could be possible if O-acetyl groups influences substrate

recognition by PG remodeling enzymes. Changes from wild type with >20% difference in relative abundance were indicated in Table 2. However, care must be taken in interpreting how % differences in relative abundance actually affect overall PG composition. For instance, small changes in muropeptides of low abundance can result in changes >20% (i.e., total PentaGly5 species, which were 0.8% in wild type and 1.3% for $\Delta ape1$; Table 2). Conversely, larger changes in muropeptides of high abundance can produce changes <20% yet may still be considered significant. For instance, dimeric species constituted 47.7% of the muropeptides in wild type and 40.7% in $ape1$; this degree of change may be meaningful, as it affects 7% of the total muropeptides, is unique compared to other mutants tested, and would be considered significant using a the 10% cut-off described for *H. pylori* (121). Regardless, it is clear that a defect in removing the O-linked acetate affects the PG muropeptide profile more than a diminishment in O-acetylation of PG. In addition to the increased O-acetylation and decreased anhMPs, $\Delta ape1$ exhibits the greatest change in both the number of muropeptide species and, in most cases, the greatest magnitude of change (Table 2, Fig. 3). One working hypothesis is that the increased O-acetylation in $\Delta ape1$ may alter the PG affecting substrate recognition and PG trimming by PG hydrolases, resulting in changes in the muropeptide profile.

C. jejuni Ape1-His₆ exhibits acetyltransferase activity on both the pNPAc (colourimetric determination of activity) and O-acetylated PG from $\Delta ape1$ *in vitro* (Fig 4D and E). As such, the accumulation of O-linked acetate in $\Delta ape1$ is directly related to the loss of O-acetylpeptidoglycan esterase activity *in vivo*. Whether this manifests as an altered PG muropeptide profile will require further investigation using the recombinant protein. *N. meningitidis* Ape1 showed preference for O-acetylated tripeptide substrates *in vivo* (144). The crystal structure for *N. meningitidis* Ape1 has been solved but the putative PG binding domain in

the N-terminal lobe and its interaction with PG have yet to be described (150). As *N. meningitidis* Ape1 was active against various O-acetylated muropeptides *in vitro*, specificity may be due to regulation of activity through unknown interaction partners. This portion of the enzyme may contain regulatory domains for this purpose (144) (Table 3) and may differ between the two organisms. Alternatively, these interaction partners may simply be absent in *C. jejuni*.

One of *C. jejuni*'s defining characteristics is its helical shape, a trait that is defined by the cytoskeletal-like components that co-ordinate the PG biosynthetic machinery to generate a PG structure of a particular shape (165). In addition to PG hydrolase activity (1,70), OAP was also found to be important in *C. jejuni* shape generation. Alterations in OAP also affected *C. jejuni* bacterial physiology and host-pathogen interactions, and Δ *ape1* exhibited a quantifiable change in shape. Previous work showed that muropeptide composition was altered in *C. jejuni/H. pylori* mutants in periplasmic PG hydrolases – i.e., Δ *pgp1*/ Δ *csd4* and Δ *pgp2*/ Δ *csd6*, which also exhibit a straight rod vs. helical morphology (1,70,122,166). Deletion of *C. jejuni ape1* also resulted in altered muropeptide composition, but the changes in shape were pleomorphic and not as dramatic as in the abovementioned straight-rod mutants. Thus, Celltool was employed for shape quantitation, using a PCA-based approach to provide insight into which metrics would best describe the variance amongst wild type and OAP mutant strains. Each shape mode represented an observable metric (length, curvature, and width) (Fig. 6 and 7). This analysis showed that Δ *ape1* was significantly different from the wild-type population in curvature in that it had both a hyper-curved average shape compared to wild type and a greater variance of curvature within the population. This was also observable by microscopy (Fig. 5). Ape1 was shown to affect cell size in *N. meningitidis* (144). Here, there was a significant increase in total area of Δ *ape1* cells when

compared to wild type at early-log phase, but not at mid-log phase (data not shown). One explanation could be that Ape1 activity varies at different growth stages in *C. jejuni*.

Multi-protein flagellar complexes span the PG layer, with some proteins of the complex proposed to directly interact with PG residues. These proteins include FlgI, which makes up the P-ring of the periplasmic rod-structure in the hook-basal body and is proposed to be anchored to the PG layer (75,167,168), and MotB in *H. pylori*, that makes up part of the flagellar stator responsible for generating torque and interacts with MurNAc residues (169). Accumulation of MurNAc O-acetylation may affect the anchoring of these flagellar structures, which is a possible explanation for the reduced motility of Δ *ape1*. In soft agar, Δ *ape1* also formed atypical halos with an irregular perimeter (Fig. 8A). This may reflect a chemotaxis defect. In *Salmonella enterica*, the switch protein FliG of the C-ring, which acts as the rotary component of the flagella responds to chemotactic signals and interacts with MotA of the stator that in turn interacts with PG-bound MotB (170). In *E. coli*, CheY is the response regulator that interacts with FliG to alter rotational direction of the flagella (171). Homologs of all these flagellar components are found in *C. jejuni* (75). However, mutants in *C. jejuni cheY* appear immotile on soft-agar but not by microscopy (172,173). Thus, the atypical halo morphology of Δ *ape1* does not support a complete loss in the ability to alter rotational direction but may still suggest an impaired response.

In *H. pylori*, the loss of the membrane bound LytTG, MltD, was shown to impact motility without affecting the localization or number of flagella; this was hypothesized to be a result of the inability of MotA/B to generate torque due to impaired PG/MotB interactions (143). In Δ *ape1*, flagella were still localized to the poles of the bacteria as assessed by TEM and the cells were still motile when viewed in DICM. An improperly assembled or unstable stator may impair the ability of the flagella to alter rotational direction in response to chemotactic signals.

Similarly, the accumulation of O-acetylation in $\Delta ape1$ and the subsequent effect on LytTG activity could reduce motility in $\Delta ape1$. However, the $\Delta pgp1$ and $\Delta pgp2$ straight mutants were also defective for motility, so the changes in $\Delta ape1$ morphology could also account for the observed motility defects.

Biofilm formation is a general stress response in *C. jejuni* that requires flagella-mediated motility and attachment to a surface, lysis, and release of extracellular DNA to form the biofilm matrix. $\Delta ape1$ was defective for motility in soft agar, but not immotile. Despite this, $\Delta ape1$ exhibited a hyper- rather than hypo-biofilm formation phenotype. Envelope stress was recently shown in *C. jejuni* as a potential trigger for biofilm formation (83). In that study, a mutant exhibiting envelope stress was hyper-biofilm, with the presence of DOC at 0.5 mg/ml promoting biofilm formation in *C. jejuni* 81-176 wild type by inducing bacterial cell lysis and release of extracellular DNA for the biofilm matrix (83). In the current study, DOC concentrations below 0.5 mg/ml inhibited $\Delta ape1$ growth (MIC 0.16-0.31; Table 3). This, together with the hyper-biofilm phenotype and increased cell surface hydrophobicity, suggests that the accumulation of OAP results in altered membrane properties and may contribute to a state of persistent membrane stress in $\Delta ape1$.

In *E. coli*, PG-associated lipoprotein (Pal) is associated with the inner leaflet of the outer membrane and the peptidoglycan layer, and is often found in protein complexes that span the cellular envelope. One of the functions of Pal in the Tol-Pal complexes is believed to be in maintaining integrity of the cellular envelope. The phenotypes of some *E. coli tol-pal* deletion mutants share similarities to *C. jejuni* $\Delta ape1$, including increased sensitivity to bile salts and altered motility (107). In addition, the PG binding domain (PGBD) of *E. coli* MotB and *E. coli* Pal are interchangeable (174) and both interact with MurNAc. Therefore the phenotype of $\Delta ape1$

that we observed could be a result of the presence of excess of O-acetyl groups on the PG MurNAc residues preventing stabilizing interactions between multi-protein structures and the PG sacculus. Further investigation would be needed to demonstrate a direct link between OAP and cell envelope stability.

These results also suggest that the proper O-acetylation levels in the sacculus are required for proper host-pathogen interaction. Two important colonization factors of *C. jejuni* for commensalism in chickens are motility and chemotaxis (6). As expected, our motility assessment was consistent with the finding that the ability to colonize chicks was significantly impaired in Δ *ape1*. Similar to the other phenotypes, colonization was not impaired by deletion of *patA*, *patB* or the entire OAP gene cluster. Studies have shown *C. jejuni*'s ability to invade and survive in non-phagocytic intestinal epithelial cell lines is by avoiding phagosome-lysosome fusion, and that this property is implicated in pathogenesis (88). Δ *ape1* also exhibited an impaired recovery from INT-407 epithelial cell infections in a gentamycin protection assay. O-acetylation is believed to confer lysozyme resistance. This is believed to be more important for Gram-positive bacteria as the PG is exposed to the environment unlike Gram-negative bacteria. Given our analysis of O-acetylation levels in our mutant strains and the chick colonization study, it would appear that the O-acetylation machinery is not necessary for colonization and host-cell interaction, and under the conditions examined thus far, offers no fitness advantage in a host system. However, the accumulation of the O-linked acetate in the PG sacculus is detrimental for host-interaction. It would appear that O-acetylation plays more of a regulatory role in PG synthesis than a protective one.

Compared to Gram-positive bacteria, Gram-negative bacteria are intrinsically resistant to many antibiotics because of the presence of the outer membrane that acts as a permeability

barrier. This leads to additional challenges in developing effective antibiotic treatment regimens. Nonetheless, the need for novel antibiotic targets warrants investigation into PG metabolism. The periplasmic nature of Ape1 and proposed role in control of LytTG activity make it a more appropriate target for the design of novel antimicrobial compounds compared to a cytoplasmic target. Because $\Delta ape1$ exhibited dysfunctional PG biosynthesis, adverse effects on *C. jejuni* physiology, and defective interactions with a host, Ape1 would be a more appropriate target for the design of antimicrobials than the transferase machinery for which most of these defects were not observed. Our initial protein studies and biochemical analyses on isolated PG indicate that Ape1 has O-acetyl esterase activity *in vitro* and *in vivo*. This initial protein characterization and mutant phenotypic analysis provides a foundation for future studies, which may include adapting the previously identified inhibitors (152) of *N. meningitidis* Ape1 as a mechanism of *C. jejuni* control in poultry, or for development of novel antibiotics (given the wide range of Gram negative bacteria that harbor homologs of this gene cluster).

4.1 Future Directions

The work presented here indicates a need to continue research on OAP in *C. jejuni*. A better understanding of the roles of PG in cell shape and its effect on pathogenicity has potential for the development of novel treatments of *C. jejuni* infection. The work described here focuses on the biological outcomes of removing this OAP system from *C. jejuni*. The ability to O-acetylate PG appears to be less important for infection than the inability to remove the O-linked acetate. The dysregulation of OAP through accumulation of O-linked acetate affects multiple aspects of PG biochemistry and affects factors associated with pathogenesis and virulence potential. This initial characterization lays out the ground work for further studies.

If OAP affects the interaction of PG-associated structure (such as flagella or lipoproteins), it may be beneficial to assess if there is a change in the proportion of PG-associated structures between Ape1 and mutant PG. Stable Isotope Labelling by Amino Acid (SILAC) is a method used to assess the changes in the proteome under two distinct populations (grown in the presence of amino acids labelled with light and heavy nitrogen isotopes in auxotrophic backgrounds) by comparing the ratio of light to heavy peptide fragments by MS (175). The SDS isolation protocol uses the insoluble nature of PG to separate it from the lysate by centrifugation. PG and tightly bound components will pellet under high speed centrifugation. The PG of wild type and $\Delta ape1$ can then be lysed using Cellosyl (which can lyse O-acetylated PG as well) to free proteinaceous components for proteomic analysis. This may provide insights into the role of OAP on the affinity of PG-associated proteins. Conversely, a SILAC based pull down approach may also be used to assess the differences in binding capabilities of PG-associated proteins with both purified wild-type PG and purified $\Delta ape1$ PG (176).

Because $\Delta ape1$ exhibits differences in the muropeptide profile in addition to the expected changes in OAP, it would be of interest to try and characterize the influence of O-acetylation on the PG sacculus. OAP is a maturation process and occurs after incorporation of new muropeptides into the PG sacculus, but when does de-O-acetylation happen? Is the change in muropeptide profile really a result of only accumulated O-acetylation levels, or does Ape1 interact with other PG remodeling enzymes to affect the biochemical structure in a fashion independent of its de-O-acetylase activity? Confirmation that Ape1 lacks a secondary function could be accomplished via an *in vitro* complementation by treating $\Delta ape1$ PG with Ape1 and performing a muropeptide analysis. If the change in muropeptide composition is due to the accumulation of OAP in a viable organism and not directly by Ape1 activity, the *in vitro* de-O-

acetylated PG should only differ in muropeptide composition from the non-treated PG in the levels of O-acetylation and the total (stem peptide) abundances should remain the same. A difference in the total stem levels between Δ *ape1* PG and wild-type PG should remain before and after treatment with Ape1 *in vitro*. This would support that OAP affects the muropeptide only under viable conditions and would support that OAP plays a regulatory role in PG metabolism.

OAP in *C. jejuni* differed greatly between our analysis and previous publications (146). From our current data, it cannot be determined if this difference is due to sample preparation methods or strain differences. Further work would be required to explain the differences. One explanation could be differences in expression levels. Because the cells were grown under different conditions, key genes could be expressed differently. An extensive transcriptomic analysis of time course experiments and corresponding OAP analysis under varying growth conditions could determine if there are cultivation or strain differences that result in differing regulatory mechanisms for OAP.

Another possible explanation of why the OAP levels of our study are lower than those previously reported (146) is that OAP is spatially regulated, active only in areas that require lytic activity of endogenous muramidases. Localization studies may provide us with a wider picture of where the modification occurs (e.g. at the cell poles or at the division site) and thus, where downstream regulation of LytTG activity is important. A GFP-Ape1 fusion protein may be of use for such cellular localization.

Another difference between our results and those previously described is the substrate specificity of Ape1 (144). Ape1 of *N. meningitidis* exhibits substrate specificity, because a difference in only O-acetylated tripeptides was observed in an *ape1* mutant. Our data demonstrate that O-acetylated dipeptides, tripeptides, and tetrapeptides all increase in abundance

in a $\Delta ape1$ background. One manner to assess this could be to use a preparatory HPLC column and collect eluted fractions containing O-acetylated mucopeptides. Using this, we could assess the elution profile Ape1 activity, which could appear as one or two peaks. Alternatively, as we have already generated an Ape 1 protein expression construct, crystallization studies could be performed to describe the PGBD. The *N. meningitides* Ape1 has been crystallized but the PGBD of the N-lobe has yet to be described (150), and considering the differences in observed substrate specificity, crystallization may identify a novel class of PGBD or help to identify PG-/Ape1-interacting partners.

REFERENCES

1. Firdich, E., Biboy, J., Adams, C., Lee, J., Ellermeier, J., Gielda, L. D., DiRita, V. J., Girardin, S. E., Vollmer, W., and Gaynor, E. C. (2012) Peptidoglycan-Modifying Enzyme Pgp1 Is Required for Helical Cell Shape and Pathogenicity Traits in *Campylobacter jejuni*. *PLoS Path.* **8**
2. Bui, N. K., Gray, J., Schwarz, H., Schumann, P., Blanot, D., and Vollmer, W. (2009) The Peptidoglycan Sacculus of *Myxococcus xanthus* Has Unusual Structural Features and Is Degraded during Glycerol-Induced Myxospore Development. *J. Bacteriol.* **191**, 494-505
3. Glauner, B. (1988) Separation and Quantification of Muropeptides with High-Performance Liquid-Chromatography. *Anal. Biochem.* **172**, 451-464
4. Clarke, A. J. (1993) Compositional analysis of peptidoglycan by high-performance anion-exchange chromatography. *Anal. Biochem.* **212**, 344-350
5. Clarke, A. J. (1993) Extent of Peptidoglycan-O Acetylation in the Tribe Proteaceae. *J. Bacteriol.* **175**, 4550-4553
6. Hendrixson, D. R., and DiRita, V. J. (2004) Identification of *Campylobacter jejuni* genes involved in commensal colonization of the chick gastrointestinal tract. *Mol. Microbiol.* **52**, 471-484
7. Jacobs, B. C., Rothbarth, P. H., van der Meche, F. G., Herbrink, P., Schmitz, P. I., de Klerk, M. A., and van Doorn, P. A. (1998) The spectrum of antecedent infections in Guillain-Barre syndrome: a case-control study. *Neurology* **51**, 1110-1115
8. Yuki, N., and Hartung, H. P. (2012) Guillain-Barre syndrome. *N Engl J Med* **366**, 2294-2304
9. Kist, M. (1986) [Who discovered *Campylobacter jejuni/coli*? A review of hitherto disregarded literature]. *Zentralbl Bakteriol Mikrobiol Hyg A* **261**, 177-186
10. Debruyne, L., Gevers, D., and Vandamme, P. (2008) Taxonomy of the Family *Campylobacteraceae*. in *Campylobacter* (Nachamkin, I., Szymanski, C. M., and Blaser, M. J. eds.), 3rd Ed., ASM Press, Washington, DC. pp 3-26, 716 p.
11. Penner, J. L. (1988) The genus *Campylobacter*: a decade of progress. *Clin. Microbiol. Rev.* **1**, 157-172
12. Man, S. M. (2011) The clinical importance of emerging *Campylobacter* species. *Nature Reviews Gastroenterology & Hepatology* **8**, 669-685
13. Silva, J., Leite, D., Fernandes, M., Mena, C., Gibbs, P. A., and Teixeira, P. (2011) *Campylobacter* spp. as a foodborne pathogen: a review. *Frontiers in Microbiology* **2**
14. Coker, A. O., Isokpehi, R. D., Thomas, B. N., Amisu, K. O., and Obi, C. L. (2002) Human campylobacteriosis in developing countries. *Emerg Infect Dis* **8**, 237-244
15. Blaser, M. J., and Enberg, J. (2008) Clinical aspects of *Campylobacter jejuni* and *Campylobacter coli* Infections. in *Campylobacter* (Nachamkin, I., Szymanski, C. M., and Blaser, M. J. eds.), 3rd Ed., ASM Press, Washington, DC. pp 99-121, 716 p.
16. Robinson, D. A. (1981) Infective dose of *Campylobacter jejuni* in milk. *Br Med J (Clin Res Ed)* **282**, 1584
17. Black, R. E., Levine, M. M., Clements, M. L., Hughes, T. P., and Blaser, M. J. (1988) Experimental *Campylobacter jejuni* infection in humans. *J. Infect. Dis.* **157**, 472-479
18. Tee, W., and Mijch, A. (1998) *Campylobacter jejuni* bacteremia in human immunodeficiency virus (HIV)-infected and non-HIV-infected patients: comparison of clinical features and review. *Clin. Infect. Dis.* **26**, 91-96

19. Perlman, D. M., Ampel, N. M., Schiffman, R. B., Cohn, D. L., Patton, C. M., Aguirre, M. L., Wang, W. L., and Blaser, M. J. (1988) Persistent *Campylobacter jejuni* infections in patients infected with the human immunodeficiency virus (HIV). *Ann Intern Med* **108**, 540-546
20. de Boer, R. F., Ott, A., Guren, P., van Zanten, E., van Belkum, A., and Kooistra-Smid, A. M. (2013) Detection of *Campylobacter* species and *Arcobacter butzleri* in stool samples by use of real-time multiplex PCR. *J. Clin. Microbiol.* **51**, 253-259
21. Vencia, W., Nogarol, C., Bianchi, D. M., Gallina, S., Zuccon, F., Adriano, D., Gramaglia, M., and Decastelli, L. (2014) Validation according to ISO 16140:2003 of a commercial real-time PCR-based method for detecting *Campylobacter jejuni*, *C. coli*, and *C. lari* in foods. *Int. J. Food Microbiol.* **177**, 78-80
22. Zautner, A. E., Johann, C., Strubel, A., Busse, C., Tareen, A. M., Masanta, W. O., Lugert, R., Schmidt-Ott, R., and Gross, U. (2014) Seroprevalence of campylobacteriosis and relevant post-infectious sequelae. *Eur. J. Clin. Microbiol. Infect. Dis.* **33**, 1019-1027
23. Jacobs, B. C., van Belkum, A., and Endtz, H. P. (2008) Guillain-Barré Syndrome and *Campylobacter* Infection. in *Campylobacter* (Nachamkin, I., Szymanski, C. M., and Blaser, M. J. eds.), 3rd Ed., ASM Press, Washington, DC. pp 245-261, 716 p.
24. Caudie, C., Quittard Pinon, A., Taravel, D., Sivadon-Tardy, V., Orlikowski, D., Rozenberg, F., Sharshar, T., Raphael, J. C., and Gaillard, J. L. (2011) Preceding infections and anti-ganglioside antibody profiles assessed by a dot immunoassay in 306 French Guillain-Barre syndrome patients. *J Neurol* **258**, 1958-1964
25. Poropatich, K. O., Walker, C. L., and Black, R. E. (2010) Quantifying the association between *Campylobacter* infection and Guillain-Barre syndrome: a systematic review. *J Health Popul Nutr* **28**, 545-552
26. Godschalk, P. C., Kuijf, M. L., Li, J., St Michael, F., Ang, C. W., Jacobs, B. C., Karwaski, M. F., Brochu, D., Moterassed, A., Endtz, H. P., van Belkum, A., and Gilbert, M. (2007) Structural characterization of *Campylobacter jejuni* lipooligosaccharide outer cores associated with Guillain-Barre and Miller Fisher syndromes. *Infect. Immun.* **75**, 1245-1254
27. Islam, Z., Gilbert, M., Mohammad, Q. D., Klaij, K., Li, J., van Rijs, W., Tio-Gillen, A. P., Talukder, K. A., Willison, H. J., van Belkum, A., Endtz, H. P., and Jacobs, B. C. (2012) Guillain-Barre syndrome-related *Campylobacter jejuni* in Bangladesh: ganglioside mimicry and cross-reactive antibodies. *PLoS One* **7**, e43976
28. Ajene, A. N., Walker, C. L. F., and Black, R. E. (2013) Enteric Pathogens and Reactive Arthritis: A Systematic Review of *Campylobacter*, *Salmonella* and *Shigella*-associated Reactive Arthritis. *Journal of Health Population and Nutrition* **31**, 299-307
29. Selmi, C., and Gershwin, M. E. (2014) Diagnosis and classification of reactive arthritis. *Autoimmun. Rev.* **13**, 546-549
30. Mortensen, N. P., Kuijf, M. L., Ang, C. W., Schiellerup, P., Krogfelt, K. A., Jacobs, B. C., van Belkum, A., Endtz, H. P., and Bergman, M. P. (2009) Sialylation of *Campylobacter jejuni* lipo-oligosaccharides is associated with severe gastro-enteritis and reactive arthritis. *Microb. Infect.* **11**, 988-994
31. Kalischuk, L. D., and Buret, A. G. (2010) A role for *Campylobacter jejuni*-induced enteritis in inflammatory bowel disease? *American Journal of Physiology-Gastrointestinal and Liver Physiology* **298**, G1-G9

32. Elia, P. P., Tolentino, Y. F., Bernardazzi, C., and de Souza, H. S. (2015) The Role of Innate Immunity Receptors in the Pathogenesis of Inflammatory Bowel Disease. *Mediators Inflamm* **2015**, 936193
33. Lone, A. G., Selinger, L. B., Uwiera, R. R., Xu, Y., and Inglis, G. D. (2013) *Campylobacter jejuni* colonization is associated with a dysbiosis in the cecal microbiota of mice in the absence of prominent inflammation. *PLoS One* **8**, e75325
34. Kalischuk, L. D., Inglis, G. D., and Buret, A. G. (2009) *Campylobacter jejuni* induces transcellular translocation of commensal bacteria via lipid rafts. *Gut Pathog* **1**, 2
35. Kalischuk, L. D., Leggett, F., and Inglis, G. D. (2010) *Campylobacter jejuni* induces transcytosis of commensal bacteria across the intestinal epithelium through M-like cells. *Gut Pathog* **2**, 14
36. Backert, S., Boehm, M., Wessler, S., and Tegtmeyer, N. (2013) Transmigration route of *Campylobacter jejuni* across polarized intestinal epithelial cells: paracellular, transcellular or both? *Cell Commun Signal* **11**, 72
37. Boehm, M., Hoy, B., Rohde, M., Tegtmeyer, N., Baek, K. T., Oyarzabal, O. A., Brondsted, L., Wessler, S., and Backert, S. (2012) Rapid paracellular transmigration of *Campylobacter jejuni* across polarized epithelial cells without affecting TER: role of proteolytic-active HtrA cleaving E-cadherin but not fibronectin. *Gut Pathog* **4**, 3
38. Bouwman, L. I., Niewold, P., and van Putten, J. P. (2013) Basolateral invasion and trafficking of *Campylobacter jejuni* in polarized epithelial cells. *PLoS One* **8**, e54759
39. Kaakoush, N. O., Mitchell, H. M., and Man, S. M. (2014) Role of Emerging *Campylobacter* Species in Inflammatory Bowel Diseases. *Inflammatory Bowel Diseases* **20**, 2189-2197
40. Ternhag, A., Asikainen, T., Giesecke, J., and Ekdahl, K. (2007) A meta-analysis on the effects of antibiotic treatment on duration of symptoms caused by infection with *Campylobacter* species. *Clin. Infect. Dis.* **44**, 696-700
41. Zhang, Q., and Plummer, P. J. (2008) Mechanisms of Antibiotic resistance in *Campylobacter*. in *Campylobacter* (Nachamkin, I., Szymanski, C. M., and Blaser, M. J. eds.), 3rd Ed., ASM Press, Washington, DC. pp 263-276, 716 p.
42. Luangtongkum, T., Jeon, B., Han, J., Plummer, P., Logue, C. M., and Zhang, Q. (2009) Antibiotic resistance in *Campylobacter*: emergence, transmission and persistence. *Future Microbiol* **4**, 189-200
43. Ruiz-Palacios, G. M. (2007) The health burden of *Campylobacter* infection and the impact of antimicrobial resistance: playing chicken. *Clin. Infect. Dis.* **44**, 701-703
44. Wagenaar, J. A., Jacobs-Reitsma, W., Hofshagen, M., and Newell, D. (2008) Poultry colonization with *Campylobacter* and its control at the primary production level in *Campylobacter* (Nachamkin, I., Szymanski, C. M., and Blaser, M. J. eds.), 3rd Ed., ASM Press, Washington, DC. pp 667-678, 716 p.
45. Sears, A., Baker, M. G., Wilson, N., Marshall, J., Muellner, P., Campbell, D. M., Lake, R. J., and French, N. P. (2011) Marked campylobacteriosis decline after interventions aimed at poultry, New Zealand. *Emerg Infect Dis* **17**, 1007-1015
46. Baker, M. G., Kvalsvig, A., Zhang, J., Lake, R., Sears, A., and Wilson, N. (2012) Declining Guillain-Barre syndrome after campylobacteriosis control, New Zealand, 1988-2010. *Emerg Infect Dis* **18**, 226-233

47. Saxena, M., John, B., Mu, M., Van, T. T. H., Taki, A., Coloe, P. J., and Smooker, P. M. (2013) Strategies to reduce *Campylobacter* colonisation in chickens. *6th Vaccine & Isv Congress* **7**, 40-43
48. Thomas, M. K., Murray, R., Flockhart, L., Pintar, K., Pollari, F., Fazil, A., Nesbitt, A., and Marshall, B. (2013) Estimates of the burden of foodborne illness in Canada for 30 specified pathogens and unspecified agents, circa 2006. *Foodborne Pathog Dis* **10**, 639-648
49. Crim, S. M., Iwamoto, M., Huang, J. Y., Griffin, P. M., Gilliss, D., Cronquist, A. B., Cartter, M., Tobin-D'Angelo, M., Blythe, D., Smith, K., Lathrop, S., Zansky, S., Cieslak, P. R., Dunn, J., Holt, K. G., Lance, S., Tauxe, R., and Henao, O. L. (2014) Incidence and trends of infection with pathogens transmitted commonly through food--Foodborne Diseases Active Surveillance Network, 10 U.S. sites, 2006-2013. *MMWR Morb Mortal Wkly Rep* **63**, 328-332
50. EDEC. (2014) Annual epidemiological report 2014: Food- and waterborne diseases and zoonoses. Stockholm
51. Murray, C. J., Vos, T., Lozano, R., Naghavi, M., Flaxman, A. D., Michaud, C., Ezzati, M., Shibuya, K., Salomon, J. A., Abdalla, S., Aboyans, V., Abraham, J., Ackerman, I., Aggarwal, R., Ahn, S. Y., Ali, M. K., Alvarado, M., Anderson, H. R., Anderson, L. M., Andrews, K. G., Atkinson, C., Baddour, L. M., Bahalim, A. N., Barker-Collo, S., Barrero, L. H., Bartels, D. H., Basanez, M. G., Baxter, A., Bell, M. L., Benjamin, E. J., Bennett, D., Bernabe, E., Bhalla, K., Bhandari, B., Bikbov, B., Bin Abdulhak, A., Birbeck, G., Black, J. A., Blencowe, H., Blore, J. D., Blyth, F., Bolliger, I., Bonaventure, A., Boufous, S., Bourne, R., Boussinesq, M., Braithwaite, T., Brayne, C., Bridgett, L., Brooker, S., Brooks, P., Brugh, T. S., Bryan-Hancock, C., Bucello, C., Buchbinder, R., Buckle, G., Budke, C. M., Burch, M., Burney, P., Burstein, R., Calabria, B., Campbell, B., Canter, C. E., Carabin, H., Carapetis, J., Carmona, L., Cella, C., Charlson, F., Chen, H., Cheng, A. T., Chou, D., Chugh, S. S., Coffeng, L. E., Colan, S. D., Colquhoun, S., Colson, K. E., Condon, J., Connor, M. D., Cooper, L. T., Corriere, M., Cortinovis, M., de Vaccaro, K. C., Couser, W., Cowie, B. C., Criqui, M. H., Cross, M., Dabhadkar, K. C., Dahiya, M., Dahodwala, N., Damsere-Derry, J., Danaei, G., Davis, A., De Leo, D., Degenhardt, L., Dellavalle, R., Delossantos, A., Denenberg, J., Derrett, S., Des Jarlais, D. C., Dharmaratne, S. D., Dherani, M., Diaz-Torne, C., Dolk, H., Dorsey, E. R., Driscoll, T., Duber, H., Ebel, B., Edmond, K., Elbaz, A., Ali, S. E., Erskine, H., Erwin, P. J., Espindola, P., Ewoigbokhan, S. E., Farzadfar, F., Feigin, V., Felson, D. T., Ferrari, A., Ferri, C. P., Fevre, E. M., Finucane, M. M., Flaxman, S., Flood, L., Foreman, K., Forouzanfar, M. H., Fowkes, F. G., Fransen, M., Freeman, M. K., Gabbe, B. J., Gabriel, S. E., Gakidou, E., Ganatra, H. A., Garcia, B., Gaspari, F., Gillum, R. F., Gmel, G., Gonzalez-Medina, D., Gosselin, R., Grainger, R., Grant, B., Groeger, J., Guillemin, F., Gunnell, D., Gupta, R., Haagsma, J., Hagan, H., Halasa, Y. A., Hall, W., Haring, D., Haro, J. M., Harrison, J. E., Havmoeller, R., Hay, R. J., Higashi, H., Hill, C., Hoen, B., Hoffman, H., Hotez, P. J., Hoy, D., Huang, J. J., Ibeanusi, S. E., Jacobsen, K. H., James, S. L., Jarvis, D., Jasrasaria, R., Jayaraman, S., Johns, N., Jonas, J. B., Karthikeyan, G., Kassebaum, N., Kawakami, N., Keren, A., Khoo, J. P., King, C. H., Knowlton, L. M., Kobusingye, O., Koranteng, A., Krishnamurthi, R., Laden, F., Lalloo, R., Laslett, L. L., Lathlean, T., Leasher, J. L., Lee, Y. Y., Leigh, J., Levinson, D., Lim, S. S., Limb, E., Lin, J. K., Lipnick, M., Lipshultz, S. E., Liu, W., Loane, M., Ohno, S. L., Lyons, R.,

- Mabweijano, J., MacIntyre, M. F., Malekzadeh, R., Mallinger, L., Manivannan, S., Marcenes, W., March, L., Margolis, D. J., Marks, G. B., Marks, R., Matsumori, A., Matzopoulos, R., Mayosi, B. M., McAnulty, J. H., McDermott, M. M., McGill, N., McGrath, J., Medina-Mora, M. E., Meltzer, M., Mensah, G. A., Merriman, T. R., Meyer, A. C., Miglioli, V., Miller, M., Miller, T. R., Mitchell, P. B., Mock, C., Mocumbi, A. O., Moffitt, T. E., Mokdad, A. A., Monasta, L., Montico, M., Moradi-Lakeh, M., Moran, A., Morawska, L., Mori, R., Murdoch, M. E., Mwaniki, M. K., Naidoo, K., Nair, M. N., Naldi, L., Narayan, K. M., Nelson, P. K., Nelson, R. G., Nevitt, M. C., Newton, C. R., Nolte, S., Norman, P., Norman, R., O'Donnell, M., O'Hanlon, S., Olives, C., Omer, S. B., Ortblad, K., Osborne, R., Ozgediz, D., Page, A., Pahari, B., Pandian, J. D., Rivero, A. P., Patten, S. B., Pearce, N., Padilla, R. P., Perez-Ruiz, F., Perico, N., Pesudovs, K., Phillips, D., Phillips, M. R., Pierce, K., Pion, S., Polanczyk, G. V., Polinder, S., Pope, C. A., 3rd, Popova, S., Porrini, E., Pourmalek, F., Prince, M., Pullan, R. L., Ramaiah, K. D., Ranganathan, D., Razavi, H., Regan, M., Rehm, J. T., Rein, D. B., Remuzzi, G., Richardson, K., Rivara, F. P., Roberts, T., Robinson, C., De Leon, F. R., Ronfani, L., Room, R., Rosenfeld, L. C., Rushton, L., Sacco, R. L., Saha, S., Sampson, U., Sanchez-Riera, L., Sanman, E., Schwebel, D. C., Scott, J. G., Segui-Gomez, M., Shahraz, S., Shepard, D. S., Shin, H., Shivakoti, R., Singh, D., Singh, G. M., Singh, J. A., Singleton, J., Sleet, D. A., Sliwa, K., Smith, E., Smith, J. L., Stapelberg, N. J., Steer, A., Steiner, T., Stolk, W. A., Stovner, L. J., Sudfeld, C., Syed, S., Tamburlini, G., Tavakkoli, M., Taylor, H. R., Taylor, J. A., Taylor, W. J., Thomas, B., Thomson, W. M., Thurston, G. D., Tleyjeh, I. M., Tonelli, M., Towbin, J. A., Truelsens, T., Tsilimbaris, M. K., Ubeda, C., Undurraga, E. A., van der Werf, M. J., van Os, J., Vavilala, M. S., Venketasubramanian, N., Wang, M., Wang, W., Watt, K., Weatherall, D. J., Weinstock, M. A., Weintraub, R., Weisskopf, M. G., Weissman, M. M., White, R. A., Whiteford, H., Wiebe, N., Wiersma, S. T., Wilkinson, J. D., Williams, H. C., Williams, S. R., Witt, E., Wolfe, F., Woolf, A. D., Wulf, S., Yeh, P. H., Zaidi, A. K., Zheng, Z. J., Zonies, D., Lopez, A. D., AlMazroa, M. A., and Memish, Z. A. (2012) Disability-adjusted life years (DALYs) for 291 diseases and injuries in 21 regions, 1990-2010: a systematic analysis for the Global Burden of Disease Study 2010. *Lancet* **380**, 2197-2223
52. Hoffmann, S., Batz, M. B., and Morris, J. G., Jr. (2012) Annual cost of illness and quality-adjusted life year losses in the United States due to 14 foodborne pathogens. *J. Food Prot.* **75**, 1292-1302
53. Olsen, C. K. E., S., van Pelt, W., and Tauxe, R. V. (2008) Epidemiology of *Campylobacter jejuni* Infections in Industrialized Nations. in *Campylobacter* (Nachamkin, I., Szymanski, C. M., and Blaser, M. J. eds.), 3rd Ed., ASM Press, Washington, DC. pp 163-189, 716 p.
54. Meldrum, R. J., Griffiths, J. K., Smith, R. M., and Evans, M. R. (2005) The seasonality of human campylobacter infection and *Campylobacter* isolates from fresh, retail chicken in Wales. *Epidemiol. Infect.* **133**, 49-52
55. Patrick, M. E., Christiansen, L. E., Waino, M., Ethelberg, S., Madsen, H., and Wegener, H. C. (2004) Effects of climate on incidence of *Campylobacter* spp. in humans and prevalence in broiler flocks in Denmark. *Appl. Environ. Microbiol.* **70**, 7474-7480
56. Platts-Mills, J. A., and Kosek, M. (2014) Update on the burden of *Campylobacter* in developing countries. *Curr. Opin. Infect. Dis.* **27**, 444-450

57. Kotloff, K. L., Nataro, J. P., Blackwelder, W. C., Nasrin, D., Farag, T. H., Panchalingam, S., Wu, Y., Sow, S. O., Sur, D., Breiman, R. F., Faruque, A. S., Zaidi, A. K., Saha, D., Alonso, P. L., Tamboura, B., Sanogo, D., Onwuchekwa, U., Manna, B., Ramamurthy, T., Kanungo, S., Ochieng, J. B., Omere, R., Oundo, J. O., Hossain, A., Das, S. K., Ahmed, S., Qureshi, S., Quadri, F., Adegbola, R. A., Antonio, M., Hossain, M. J., Akinsola, A., Mandomando, I., Nhampossa, T., Acacio, S., Biswas, K., O'Reilly, C. E., Mintz, E. D., Berkeley, L. Y., Muhsen, K., Sommerfelt, H., Robins-Browne, R. M., and Levine, M. M. (2013) Burden and aetiology of diarrhoeal disease in infants and young children in developing countries (the Global Enteric Multicenter Study, GEMS): a prospective, case-control study. *Lancet* **382**, 209-222
58. Newell, D. G. (2001) Animal models of *Campylobacter jejuni* colonization and disease and the lessons to be learned from similar *Helicobacter pylori* models. *J. Appl. Microbiol.* **90**, 57s-67s
59. Stahl, M., Ries, J., Vermeulen, J., Yang, H., Sham, H. P., Crowley, S. M., Badayeva, Y., Turvey, S. E., Gaynor, E. C., Li, X., and Vallance, B. A. (2014) A novel mouse model of *Campylobacter jejuni* gastroenteritis reveals key pro-inflammatory and tissue protective roles for Toll-like receptor signaling during infection. *PLoS Pathog* **10**, e1004264
60. Centers for Disease, C., and Prevention. (2013) Recurrent outbreak of *Campylobacter jejuni* infections associated with a raw milk dairy--Pennsylvania, April-May 2013. *MMWR Morb Mortal Wkly Rep* **62**, 702
61. Clark, C. G., Price, L., Ahmed, R., Woodward, D. L., Melito, P. L., Rodgers, F. G., Jamieson, F., Ciebin, B., Li, A., and Ellis, A. (2003) Characterization of waterborne outbreak-associated *Campylobacter jejuni*, Walkerton, Ontario. *Emerg Infect Dis* **9**, 1232-1241
62. Dasti, J. I., Tareen, A. M., Lugert, R., Zautner, A. E., and Gross, U. (2010) *Campylobacter jejuni*: a brief overview on pathogenicity-associated factors and disease-mediating mechanisms. *Int. J. Med. Microbiol.* **300**, 205-211
63. Gundogdu, O., Bentley, S. D., Holden, M. T., Parkhill, J., Dorrell, N., and Wren, B. W. (2007) Re-annotation and re-analysis of the *Campylobacter jejuni* NCTC11168 genome sequence. *BMC Genomics* **8**, 162
64. Parkhill, J., Wren, B. W., Mungall, K., Ketley, J. M., Churcher, C., Basham, D., Chillingworth, T., Davies, R. M., Feltwell, T., Holroyd, S., Jagels, K., Karlyshev, A. V., Moule, S., Pallen, M. J., Penn, C. W., Quail, M. A., Rajandream, M. A., Rutherford, K. M., van Vliet, A. H., Whitehead, S., and Barrell, B. G. (2000) The genome sequence of the food-borne pathogen *Campylobacter jejuni* reveals hypervariable sequences. *Nature* **403**, 665-668
65. Apel, D., Ellermeier, J., Pryjma, M., Dirita, V. J., and Gaynor, E. C. (2012) Characterization of *Campylobacter jejuni* RacRS reveals roles in the heat shock response, motility, and maintenance of cell length homogeneity. *J. Bacteriol.* **194**, 2342-2354
66. Gaynor, E. C., Wells, D. H., MacKichan, J. K., and Falkow, S. (2005) The *Campylobacter jejuni* stringent response controls specific stress survival and virulence-associated phenotypes. *Mol. Microbiol.* **56**, 8-27
67. Svensson, S. L., Davis, L. M., MacKichan, J. K., Allan, B. J., Pajaniappan, M., Thompson, S. A., and Gaynor, E. C. (2009) The CprS sensor kinase of the zoonotic pathogen *Campylobacter jejuni* influences biofilm formation and is required for optimal chick colonization. *Mol. Microbiol.* **71**, 253-272

68. Pajaniappan, M., Hall, J. E., Cawthraw, S. A., Newell, D. G., Gaynor, E. C., Fields, J. A., Rathbun, K. M., Agee, W. A., Burns, C. M., Hall, S. J., Kelly, D. J., and Thompson, S. A. (2008) A temperature-regulated *Campylobacter jejuni* gluconate dehydrogenase is involved in respiration-dependent energy conservation and chicken colonization. *Mol. Microbiol.* **68**, 474-491
69. Pryjma, M., Apel, D., Huynh, S., Parker, C. T., and Gaynor, E. C. (2012) FdhTU-modulated formate dehydrogenase expression and electron donor availability enhance recovery of *Campylobacter jejuni* following host cell infection. *J. Bacteriol.* **194**, 3803-3813
70. Frirdich, E., Vermeulen, J., Biboy, J., Soares, F., Taveirne, M. E., Johnson, J. G., DiRita, V. J., Girardin, S. E., Vollmer, W., and Gaynor, E. C. (2014) Peptidoglycan LD-carboxypeptidase Pgp2 influences *Campylobacter jejuni* helical cell shape and pathogenic properties and provides the substrate for the DL-carboxypeptidase Pgp1. *J. Biol. Chem.* **289**, 8007-8018
71. Bacon, D. J., Alm, R. A., Burr, D. H., Hu, L., Kopecko, D. J., Ewing, C. P., Trust, T. J., and Guerry, P. (2000) Involvement of a plasmid in virulence of *Campylobacter jejuni* 81-176. *Infect. Immun.* **68**, 4384-4390
72. Abuoun, M., Manning, G., Cawthraw, S. A., Ridley, A., Ahmed, I. H., Wassenaar, T. M., and Newell, D. G. (2005) Cytolethal distending toxin (CDT)-negative *Campylobacter jejuni* strains and anti-CDT neutralizing antibodies are induced during human infection but not during colonization in chickens. *Infect. Immun.* **73**, 3053-3062
73. Louwen, R. P., van Belkum, A., Wagenaar, J. A., Doorduyn, Y., Achterberg, R., and Endtz, H. P. (2006) Lack of association between the presence of the pVir plasmid and bloody diarrhea in *Campylobacter jejuni* enteritis. *J. Clin. Microbiol.* **44**, 1867-1868
74. Tracz, D. M., Keelan, M., Ahmed-Bentley, J., Gibreel, A., Kowalewska-Grochowska, K., and Taylor, D. E. (2005) pVir and bloody diarrhea in *Campylobacter jejuni* enteritis. *Emerg Infect Dis* **11**, 838-843
75. Lertsethtakarn, P., Ottemann, K. M., and Hendrixson, D. R. (2011) Motility and chemotaxis in *Campylobacter* and *Helicobacter*. *Annu. Rev. Microbiol.* **65**, 389-410
76. Grant, C. C., Konkel, M. E., Cieplak, W., Jr., and Tompkins, L. S. (1993) Role of flagella in adherence, internalization, and translocation of *Campylobacter jejuni* in nonpolarized and polarized epithelial cell cultures. *Infect. Immun.* **61**, 1764-1771
77. Mertins, S., Allan, B. J., Townsend, H. G., Koster, W., and Potter, A. A. (2013) Role of motAB in adherence and internalization in polarized Caco-2 cells and in cecal colonization of *Campylobacter jejuni*. *Avian Dis.* **57**, 116-122
78. Newell, D. G., McBride, H., and Dolby, J. M. (1985) Investigations on the role of flagella in the colonization of infant mice with *Campylobacter jejuni* and attachment of *Campylobacter jejuni* to human epithelial cell lines. *J Hyg (Lond)* **95**, 217-227
79. Guerry, P. (2007) *Campylobacter* flagella: not just for motility. *Trends Microbiol.* **15**, 456-461
80. Andersen-Nissen, E., Smith, K. D., Strobe, K. L., Barrett, S. L., Cookson, B. T., Logan, S. M., and Aderem, A. (2005) Evasion of Toll-like receptor 5 by flagellated bacteria. *Proc Natl Acad Sci U S A* **102**, 9247-9252
81. Young, K. D. (2006) The selective value of bacterial shape. *Microbiol. Mol. Biol. Rev.* **70**, 660-703

82. Sulaeman, S., Hernould, M., Schaumann, A., Coquet, L., Bolla, J. M., De, E., and Tresse, O. (2012) Enhanced adhesion of *Campylobacter jejuni* to abiotic surfaces is mediated by membrane proteins in oxygen-enriched conditions. *PLoS One* **7**, e46402
83. Svensson, S. L., Pryjma, M., and Gaynor, E. C. (2014) Flagella-mediated adhesion and extracellular DNA release contribute to biofilm formation and stress tolerance of *Campylobacter jejuni*. *PLoS One* **9**, e106063
84. Joshua, G. W. P., Guthrie-Irons, C., Karlyshev, A. V., and Wren, B. W. (2006) Biofilm formation in *Campylobacter jejuni*. *Microbiology-Sgm* **152**, 387-396
85. Konkel, M. E., Monteville, M. R., Rivera-Amill, V., and Joens, L. A. (2001) The pathogenesis of *Campylobacter jejuni*-mediated enteritis. *Curr Issues Intest Microbiol* **2**, 55-71
86. Eucker, T. P., and Konkel, M. E. (2012) The cooperative action of bacterial fibronectin-binding proteins and secreted proteins promote maximal *Campylobacter jejuni* invasion of host cells by stimulating membrane ruffling. *Cell. Microbiol.* **14**, 226-238
87. Monteville, M. R., Yoon, J. E., and Konkel, M. E. (2003) Maximal adherence and invasion of INT 407 cells by *Campylobacter jejuni* requires the CadF outer-membrane protein and microfilament reorganization. *Microbiology* **149**, 153-165
88. Watson, R. O., and Galan, J. E. (2008) *Campylobacter jejuni* survives within epithelial cells by avoiding delivery to lysosomes. *PLoS Path.* **4**
89. Boehm, M., Krause-Gruszczynska, M., Rohde, M., Tegtmeyer, N., Takahashi, S., Oyarzabal, O. A., and Backert, S. (2011) Major host factors involved in epithelial cell invasion of *Campylobacter jejuni*: role of fibronectin, integrin beta1, FAK, Tiam-1, and DOCK180 in activating Rho GTPase Rac1. *Front Cell Infect Microbiol* **1**, 17
90. Krause-Gruszczynska, M., Boehm, M., Rohde, M., Tegtmeyer, N., Takahashi, S., Buday, L., Oyarzabal, O. A., and Backert, S. (2011) The signaling pathway of *Campylobacter jejuni*-induced Cdc42 activation: Role of fibronectin, integrin beta1, tyrosine kinases and guanine exchange factor Vav2. *Cell Commun Signal* **9**, 32
91. Buelow, D. R., Christensen, J. E., Neal-McKinney, J. M., and Konkel, M. E. (2011) *Campylobacter jejuni* survival within human epithelial cells is enhanced by the secreted protein CiaI. *Mol. Microbiol.* **80**, 1296-1312
92. Christensen, J. E., Pacheco, S. A., and Konkel, M. E. (2009) Identification of a *Campylobacter jejuni*-secreted protein required for maximal invasion of host cells. *Mol. Microbiol.* **73**, 650-662
93. Neal-McKinney, J. M., and Konkel, M. E. (2012) The *Campylobacter jejuni* CiaC virulence protein is secreted from the flagellum and delivered to the cytosol of host cells. *Front Cell Infect Microbiol* **2**, 31
94. Samuelson, D. R., Eucker, T. P., Bell, J. A., Dybas, L., Mansfield, L. S., and Konkel, M. E. (2013) The *Campylobacter jejuni* CiaD effector protein activates MAP kinase signaling pathways and is required for the development of disease. *Cell Commun Signal* **11**, 79
95. Iwata, T., Chiku, K., Amano, K., Kusumoto, M., Ohnishi-Kameyama, M., Ono, H., and Akiba, M. (2013) Effects of lipooligosaccharide inner core truncation on bile resistance and chick colonization by *Campylobacter jejuni*. *PLoS One* **8**, e56900
96. Naito, M., Fridrich, E., Fields, J. A., Pryjma, M., Li, J., Cameron, A., Gilbert, M., Thompson, S. A., and Gaynor, E. C. (2010) Effects of sequential *Campylobacter jejuni*

- 81-176 lipooligosaccharide core truncations on biofilm formation, stress survival, and pathogenesis. *J. Bacteriol.* **192**, 2182-2192
97. van Mourik, A., Steeghs, L., van Laar, J., Meiring, H. D., Hamstra, H. J., van Putten, J. P., and Wosten, M. M. (2010) Altered linkage of hydroxyacyl chains in lipid A of *Campylobacter jejuni* reduces TLR4 activation and antimicrobial resistance. *J. Biol. Chem.* **285**, 15828-15836
 98. Cullen, T. W., O'Brien, J. P., Hendrixson, D. R., Giles, D. K., Hobb, R. I., Thompson, S. A., Brodbelt, J. S., and Trent, M. S. (2013) EptC of *Campylobacter jejuni* mediates phenotypes involved in host interactions and virulence. *Infect. Immun.* **81**, 430-440
 99. Karlyshev, A. V., Linton, D., Gregson, N. A., Lastovica, A. J., and Wren, B. W. (2000) Genetic and biochemical evidence of a *Campylobacter jejuni* capsular polysaccharide that accounts for Penner serotype specificity. *Mol. Microbiol.* **35**, 529-541
 100. Karlyshev, A. V., Champion, O. L., Churcher, C., Brisson, J. R., Jarrell, H. C., Gilbert, M., Brochu, D., St Michael, F., Li, J., Wakarchuk, W. W., Goodhead, I., Sanders, M., Stevens, K., White, B., Parkhill, J., Wren, B. W., and Szymanski, C. M. (2005) Analysis of *Campylobacter jejuni* capsular loci reveals multiple mechanisms for the generation of structural diversity and the ability to form complex heptoses. *Mol. Microbiol.* **55**, 90-103
 101. Keo, T., Collins, J., Kunwar, P., Blaser, M. J., and Iovine, N. M. (2011) *Campylobacter* capsule and lipooligosaccharide confer resistance to serum and cationic antimicrobials. *Virulence* **2**, 30-40
 102. Maue, A. C., Mohawk, K. L., Giles, D. K., Poly, F., Ewing, C. P., Jiao, Y., Lee, G., Ma, Z., Monteiro, M. A., Hill, C. L., Ferderber, J. S., Porter, C. K., Trent, M. S., and Guerry, P. (2013) The polysaccharide capsule of *Campylobacter jejuni* modulates the host immune response. *Infect. Immun.* **81**, 665-672
 103. Monteiro, M. A., Baqar, S., Hall, E. R., Chen, Y. H., Porter, C. K., Bentzel, D. E., Applebee, L., and Guerry, P. (2009) Capsule polysaccharide conjugate vaccine against diarrheal disease caused by *Campylobacter jejuni*. *Infect. Immun.* **77**, 1128-1136
 104. Guerry, P., Poly, F., Riddle, M., Maue, A. C., Chen, Y. H., and Monteiro, M. A. (2012) *Campylobacter* polysaccharide capsules: virulence and vaccines. *Front Cell Infect Microbiol* **2**, 7
 105. Firdich, E., and Gaynor, E. C. (2013) Peptidoglycan hydrolases, bacterial shape, and pathogenesis. *Curr. Opin. Microbiol.* **16**, 767-778
 106. Vollmer, W. (2008) Structural variation in the glycan strands of bacterial peptidoglycan. *FEMS Microbiol. Rev.* **32**, 287-306
 107. Godlewska, R., Wisniewska, K., Pietras, Z., and Jagusztyn-Krynicka, E. K. (2009) Peptidoglycan-associated lipoprotein (Pal) of Gram-negative bacteria: function, structure, role in pathogenesis and potential application in immunoprophylaxis. *FEMS Microbiol. Lett.* **298**, 1-11
 108. Silhavy, T. J., Kahne, D., and Walker, S. (2010) The bacterial cell envelope. *Cold Spring Harb Perspect Biol* **2**, a000414
 109. Balomenou, S., Fouet, A., Tzanodaskalaki, M., Couture-Tosi, E., Bouriotis, V., and Boneca, I. G. (2013) Distinct functions of polysaccharide deacetylases in cell shape, neutral polysaccharide synthesis and virulence of *Bacillus anthracis*. *Mol. Microbiol.* **87**, 867-883
 110. Candela, T., Balomenou, S., Aucher, W., Bouriotis, V., Simore, J. P., Fouet, A., and Boneca, I. G. (2014) N-acetylglucosamine deacetylases modulate the anchoring of the

- gamma-glutamyl capsule to the cell wall of *Bacillus anthracis*. *Microb. Drug Resist.* **20**, 222-230
111. Sobhanifar, S., King, D. T., and Strynadka, N. C. (2013) Fortifying the wall: synthesis, regulation and degradation of bacterial peptidoglycan. *Curr. Opin. Struct. Biol.* **23**, 695-703
 112. Sukhithasri, V., Nisha, N., Biswas, L., Anil Kumar, V., and Biswas, R. (2013) Innate immune recognition of microbial cell wall components and microbial strategies to evade such recognitions. *Microbiol. Res.* **168**, 396-406
 113. Sham, L. T., Butler, E. K., Lebar, M. D., Kahne, D., Bernhardt, T. G., and Ruiz, N. (2014) Bacterial cell wall. MurJ is the flippase of lipid-linked precursors for peptidoglycan biogenesis. *Science* **345**, 220-222
 114. van Heijenoort, J. (2011) Peptidoglycan hydrolases of *Escherichia coli*. *Microbiol. Mol. Biol. Rev.* **75**, 636-663
 115. Turner, R. D., Vollmer, W., and Foster, S. J. (2014) Different walls for rods and balls: the diversity of peptidoglycan. *Mol. Microbiol.* **91**, 862-874
 116. Dworkin, J. (2014) The medium is the message: interspecies and interkingdom signaling by peptidoglycan and related bacterial glycans. *Annu. Rev. Microbiol.* **68**, 137-154
 117. Moynihan, P. J., and Clarke, A. J. (2011) O-Acetylated peptidoglycan: controlling the activity of bacterial autolysins and lytic enzymes of innate immune systems. *Int J Biochem Cell Biol* **43**, 1655-1659
 118. Dworkin, J. (2010) Form equals function? Bacterial shape and its consequences for pathogenesis. *Mol. Microbiol.* **78**, 792-795
 119. Schoonmaker, M. K., Bishai, W. R., and Lamichhane, G. (2014) Nonclassical transpeptidases of *Mycobacterium tuberculosis* alter cell size, morphology, the cytosolic matrix, protein localization, virulence, and resistance to beta-lactams. *J. Bacteriol.* **196**, 1394-1402
 120. Strating, H., Vandenende, C., and Clarke, A. J. (2012) Changes in peptidoglycan structure and metabolism during differentiation of *Proteus mirabilis* into swarmer cells. *Canadian Journal of Microbiology* **58**, 1183-1194
 121. Sycuro, L. K., Pincus, Z., Gutierrez, K. D., Biboy, J., Stern, C. A., Vollmer, W., and Salama, N. R. (2010) Peptidoglycan crosslinking relaxation promotes *Helicobacter pylori*'s helical shape and stomach colonization. *Cell* **141**, 822-833
 122. Sycuro, L. K., Wyckoff, T. J., Biboy, J., Born, P., Pincus, Z., Vollmer, W., and Salama, N. R. (2012) Multiple peptidoglycan modification networks modulate *Helicobacter pylori*'s cell shape, motility, and colonization potential. *PLoS Pathog* **8**, e1002603
 123. Royet, J., Gupta, D., and Dziarski, R. (2011) Peptidoglycan recognition proteins: modulators of the microbiome and inflammation. *Nat. Rev. Immunol.* **11**, 837-851
 124. Bertsche, U., Mayer, C., Gotz, F., and Gust, A. A. (2015) Peptidoglycan perception--sensing bacteria by their common envelope structure. *Int. J. Med. Microbiol.* **305**, 217-223
 125. Antosz, H., and Osiak, M. (2013) NOD1 and NOD2 receptors: integral members of the innate and adaptive immunity system. *Acta Biochim. Pol.* **60**, 351-360
 126. Zilbauer, M., Dorrell, N., Elmi, A., Lindley, K. J., Schuller, S., Jones, H. E., Klein, N. J., Nunez, G., Wren, B. W., and Bajaj-Elliott, M. (2007) A major role for intestinal epithelial nucleotide oligomerization domain 1 (NOD1) in eliciting host bactericidal immune responses to *Campylobacter jejuni*. *Cell. Microbiol.* **9**, 2404-2416

127. den Blaauwen, T., Andreu, J. M., and Monasterio, O. (2014) Bacterial cell division proteins as antibiotic targets. *Bioorg. Chem.* **55**, 27-38
128. Page, W. J., Huyer, G., Huyer, M., and Worobec, E. A. (1989) Characterization of the porins of *Campylobacter jejuni* and *Campylobacter coli* and implications for antibiotic susceptibility. *Antimicrob. Agents Chemother.* **33**, 297-303
129. Cordillot, M., Dubee, V., Triboulet, S., Dubost, L., Marie, A., Hugonnet, J. E., Arthur, M., and Mainardi, J. L. (2013) In Vitro Cross-Linking of Mycobacterium tuberculosis Peptidoglycan by L,D-Transpeptidases and Inactivation of These Enzymes by Carbapenems. *Antimicrobial Agents and Chemotherapy* **57**, 5940-5945
130. Correale, S., Ruggiero, A., Capparelli, R., Pedone, E., and Berisio, R. (2013) Structures of free and inhibited forms of the L,D-transpeptidase LdtMt1 from Mycobacterium tuberculosis. *Acta Crystallogr D Biol Crystallogr* **69**, 1697-1706
131. Moynihan, P. J., Sychantha, D., and Clarke, A. J. (2014) Chemical biology of peptidoglycan acetylation and deacetylation. *Bioorg. Chem.* **54**, 44-50
132. Bera, A., Biswas, R., Herbert, S., and Gotz, F. (2006) The presence of peptidoglycan O-acetyltransferase in various staphylococcal species correlates with lysozyme resistance and pathogenicity. *Infect. Immun.* **74**, 4598-4604
133. Dupont, C., and Clarke, A. J. (1991) Dependence of lysozyme-catalysed solubilization of *Proteus mirabilis* peptidoglycan on the extent of O-acetylation. *Eur. J. Biochem.* **195**, 763-769
134. Ellison, R. T., 3rd, and Giehl, T. J. (1991) Killing of gram-negative bacteria by lactoferrin and lysozyme. *J. Clin. Invest.* **88**, 1080-1091
135. Ellison, R. T., 3rd, Giehl, T. J., and LaForce, F. M. (1988) Damage of the outer membrane of enteric gram-negative bacteria by lactoferrin and transferrin. *Infect. Immun.* **56**, 2774-2781
136. Wang, G., Lo, L. F., Forsberg, L. S., and Maier, R. J. (2012) Helicobacter pylori peptidoglycan modifications confer lysozyme resistance and contribute to survival in the host. *MBio* **3**, e00409-00412
137. Fleming, T. J., Wallsmith, D. E., and Rosenthal, R. S. (1986) Arthropathic properties of gonococcal peptidoglycan fragments: implications for the pathogenesis of disseminated gonococcal disease. *Infect. Immun.* **52**, 600-608
138. Benachour, A., Ladjouzi, R., Le Jeune, A., Hebert, L., Thorpe, S., Courtin, P., Chapot-Chartier, M. P., Prajsnar, T. K., Foster, S. J., and Mesnage, S. (2012) The Lysozyme-Induced Peptidoglycan N-Acetylglucosamine Deacetylase PgdA (EF1843) Is Required for *Enterococcus faecalis* Virulence. *J. Bacteriol.* **194**, 6066-6073
139. Bernard, E., Rolain, T., Courtin, P., Guillot, A., Langella, P., Hols, P., and Chapot-Chartier, M. P. (2011) Characterization of O-acetylation of N-acetylglucosamine: a novel structural variation of bacterial peptidoglycan. *J. Biol. Chem.* **286**, 23950-23958
140. Scheurwater, E., Reid, C. W., and Clarke, A. J. (2008) Lytic transglycosylases: bacterial space-making autolysins. *Int J Biochem Cell Biol* **40**, 586-591
141. Bernard, E., Rolain, T., David, B., Andre, G., Dupres, V., Dufrene, Y. F., Hallet, B., Chapot-Chartier, M. P., and Hols, P. (2012) Dual role for the O-acetyltransferase OatA in peptidoglycan modification and control of cell septation in *Lactobacillus plantarum*. *PLoS One* **7**, e47893

142. Laaberki, M. H., Pfeffer, J., Clarke, A. J., and Dworkin, J. (2011) O-Acetylation of Peptidoglycan Is Required for Proper Cell Separation and S-layer Anchoring in *Bacillus anthracis*. *J. Biol. Chem.* **286**, 5278-5288
143. Roure, S., Bonis, M., Chaput, C., Ecobichon, C., Mattox, A., Barriere, C., Geldmacher, N., Guadagnini, S., Schmitt, C., Prevost, M. C., Labigne, A., Backert, S., Ferrero, R. L., and Boneca, I. G. (2012) Peptidoglycan maturation enzymes affect flagellar functionality in bacteria. *Mol. Microbiol.* **86**, 845-856
144. Veyrier, F. J., Williams, A. H., Mesnage, S., Schmitt, C., Taha, M. K., and Boneca, I. G. (2013) De-O-acetylation of peptidoglycan regulates glycan chain extension and affects in vivo survival of *Neisseria meningitidis*. *Mol. Microbiol.* **87**, 1100-1112
145. Weadge, J. T., and Clarke, A. J. (2006) Identification and characterization of O-acetylpeptidoglycan esterase: a novel enzyme discovered in *Neisseria gonorrhoeae*. *Biochemistry* **45**, 839-851
146. Weadge, J. T., Pfeffer, J. M., and Clarke, A. J. (2005) Identification of a new family of enzymes with potential O-acetylpeptidoglycan esterase activity in both Gram-positive and Gram-negative bacteria. *BMC Microbiol.* **5**
147. Weadge, J. T., and Clarke, A. J. (2007) *Neisseria gonorrhoeae* O-acetylpeptidoglycan esterase, a serine esterase with a Ser-His-Asp catalytic triad. *Biochemistry* **46**, 4932-4941
148. Pfeffer, J. M., Weadge, J. T., and Clarke, A. J. (2013) Mechanism of Action of *Neisseria gonorrhoeae* O-Acetylpeptidoglycan Esterase, an SGNH Serine Esterase. *J. Biol. Chem.* **288**, 2605-2613
149. Moynihan, P. J., and Clarke, A. J. (2014) Substrate Specificity and Kinetic Characterization of Peptidoglycan O-Acetyltransferase B from *Neisseria gonorrhoeae*. *J. Biol. Chem.* **289**, 16748-16760
150. Williams, A. H., Veyrier, F. J., Bonis, M., Michaud, Y., Raynal, B., Taha, M. K., White, S. W., Haouz, A., and Boneca, I. G. (2014) Visualization of a substrate-induced productive conformation of the catalytic triad of the *Neisseria meningitidis* peptidoglycan O-acetylerase reveals mechanistic conservation in SGNH esterase family members. *Acta Crystallogr D Biol Crystallogr* **70**, 2631-2639
151. Moynihan, P. J., and Clarke, A. J. (2010) O-acetylation of peptidoglycan in gram-negative bacteria: identification and characterization of peptidoglycan O-acetyltransferase in *Neisseria gonorrhoeae*. *J. Biol. Chem.* **285**, 13264-13273
152. Pfeffer, J. M., and Clarke, A. J. (2012) Identification of the first known inhibitors of O-acetylpeptidoglycan esterase: a potential new antibacterial target. *ChemBioChem* **13**, 722-731
153. Menard, R., Sansonetti, P. J., and Parsot, C. (1993) Nonpolar mutagenesis of the ipa genes defines IpaB, IpaC, and IpaD as effectors of *Shigella flexneri* entry into epithelial cells. *J. Bacteriol.* **175**, 5899-5906
154. Karlyshev, A. V., and Wren, B. W. (2005) Development and application of an Insertional system for gene delivery and expression in *Campylobacter jejuni*. *Appl. Environ. Microbiol.* **71**, 4004-4013
155. Hayashi, K. (1975) A rapid determination of sodium dodecyl sulfate with methylene blue. *Anal. Biochem.* **67**, 503-506
156. Petersen, T. N., Brunak, S., von Heijne, G., and Nielsen, H. (2011) SignalP 4.0: discriminating signal peptides from transmembrane regions. *Nat. Methods* **8**, 785-786

157. Pincus, Z., and Theriot, J. A. (2007) Comparison of quantitative methods for cell-shape analysis. *J. Microsc.* **227**, 140-156
158. McLennan, M. K., Ringoir, D. D., Frirdich, E., Svensson, S. L., Wells, D. H., Jarrell, H., Szymanski, C. M., and Gaynor, E. C. (2008) Campylobacter jejuni biofilms up-regulated in the absence of the stringent response utilize a calcofluor white-reactive polysaccharide. *J. Bacteriol.* **190**, 1097-1107
159. Ben Abdallah, F., Lagha, R., Said, K., Kallel, H., and Gharbi, J. (2014) Detection of cell surface hydrophobicity, biofilm and fimbriae genes in salmonella isolated from tunisian clinical and poultry meat. *Iran J Public Health* **43**, 423-431
160. Rosenberg, M., Gutnick, D., and Rosenberg, E. (1980) Adherence of Bacteria to Hydrocarbons - a Simple Method for Measuring Cell-Surface Hydrophobicity. *FEMS Microbiol. Lett.* **9**, 29-33
161. Lin, M. F., Lucas, H. C., and Shmueli, G. (2013) Too Big to Fail: Large Samples and the p-Value Problem. *Information Systems Research* **24**, 906-917
162. Buswell, C. M., Herlihy, Y. M., Lawrence, L. M., McGuiggan, J. T., Marsh, P. D., Keevil, C. W., and Leach, S. A. (1998) Extended survival and persistence of Campylobacter spp. in water and aquatic biofilms and their detection by immunofluorescent-antibody and -rRNA staining. *Appl. Environ. Microbiol.* **64**, 733-741
163. Dillard, J. P., and Hackett, K. T. (2005) Mutations affecting peptidoglycan acetylation in Neisseria gonorrhoeae and Neisseria meningitidis. *Infect. Immun.* **73**, 5697-5705
164. Clarke, A. J., and Dupont, C. (1992) O-acetylated peptidoglycan: its occurrence, pathobiological significance, and biosynthesis. *Can J Microbiol* **38**, 85-91
165. Mattei, P. J., Neves, D., and Dessen, A. (2010) Bridging cell wall biosynthesis and bacterial morphogenesis. *Curr. Opin. Struct. Biol.* **20**, 749-755
166. Sycuro, L. K., Rule, C. S., Petersen, T. W., Wyckoff, T. J., Sessler, T., Nagarkar, D. B., Khalid, F., Pincus, Z., Biboy, J., Vollmer, W., and Salama, N. R. (2013) Flow cytometry-based enrichment for cell shape mutants identifies multiple genes that influence Helicobacter pylori morphology. *Mol. Microbiol.* **90**, 869-883
167. Hizukuri, Y., Kojima, S., Yakushi, T., Kawagishi, I., and Homma, M. (2008) Systematic Cys mutagenesis of FlgI, the flagellar P-ring component of Escherichia coli. *Microbiology* **154**, 810-817
168. Jones, C. J., Homma, M., and Macnab, R. M. (1989) L-, P-, and M-ring proteins of the flagellar basal body of Salmonella typhimurium: gene sequences and deduced protein sequences. *J. Bacteriol.* **171**, 3890-3900
169. Roujeinikova, A. (2008) Crystal structure of the cell wall anchor domain of MotB, a stator component of the bacterial flagellar motor: implications for peptidoglycan recognition. *Proc Natl Acad Sci U S A* **105**, 10348-10353
170. Morimoto, Y. V., Nakamura, S., Hiraoka, K. D., Namba, K., and Minamino, T. (2013) Distinct roles of highly conserved charged residues at the MotA-FliG interface in bacterial flagellar motor rotation. *J. Bacteriol.* **195**, 474-481
171. Roman, S. J., Meyers, M., Volz, K., and Matsumura, P. (1992) A chemotactic signaling surface on CheY defined by suppressors of flagellar switch mutations. *J. Bacteriol.* **174**, 6247-6255
172. Kanungpean, D., Kakuda, T., and Takai, S. (2011) False Positive Responses of Campylobacter jejuni when Using the Chemical-In-Plug Chemotaxis Assay. *J. Vet. Med. Sci.* **73**, 389-391

173. McGee, D. J., Langford, M. L., Watson, E. L., Carter, J. E., Chen, Y. T., and Ottemann, K. M. (2005) Colonization and inflammation deficiencies in Mongolian gerbils infected by *Helicobacter pylori* chemotaxis mutants. *Infect. Immun.* **73**, 1820-1827
174. Hizukuri, Y., Morton, J. F., Yakushi, T., Kojima, S., and Hommay, M. (2009) The peptidoglycan-binding (PGB) Domain of the *Escherichia coli* Pal Protein can also Function as the PGB Domain in *E. coli* Flagellar Motor Protein MotB. *Journal of Biochemistry* **146**, 219-229
175. Ong, S. E. (2012) The expanding field of SILAC. *Anal. Bioanal. Chem.* **404**, 967-976
176. Wehbi, H., Portillo, E., Harvey, H., Shimkoff, A. E., Scheurwater, E. M., Howell, P. L., and Burrows, L. L. (2011) The peptidoglycan-binding protein FimV promotes assembly of the *Pseudomonas aeruginosa* type IV pilus secretin. *J. Bacteriol.* **193**, 540-550
177. Korlath, J. A., Osterholm, M. T., Judy, L. A., Forfang, J. C., and Robinson, R. A. (1985) A point-source outbreak of campylobacteriosis associated with consumption of raw milk. *J. Infect. Dis.* **152**, 592-596
178. Gaynor, E. C., Cawthraw, S., Manning, G., MacKichan, J. K., Falkow, S., and Newell, D. G. (2004) The genome-sequenced variant of *Campylobacter jejuni* NCTC 11168 and the original clonal clinical isolate differ markedly in colonization, gene expression, and virulence-associated phenotypes. *J. Bacteriol.* **186**, 503-517
179. Glauner, B., Holtje, J. V., and Schwarz, U. (1988) The composition of the murein of *Escherichia coli*. *J Biol Chem* **263**, 10088-10095

APPENDIX 1. BACTERIAL STRAINS OR PLASMIDS USED IN THIS STUDY

Strain or Plasmid	Genotype or Description	Source
<u>C. jejuni Strains</u>		
81-176	Wild-type isolated from diarrheic patient	(177)
Δ <i>apeI</i>	81-176 <i>apeI::aphA3</i> ;Km ^R	This study
Δ <i>patB</i>	81-176 <i>patB::aphA3</i> ;Km ^R	This study
Δ <i>patA</i>	81-176 <i>patA::aphA3</i> ;Km ^R	This study
Δ <i>oap</i>	81-176 <i>oap::aphA3</i> ;Km ^R	This study
Δ <i>apeI</i> ^C	81-176 Δ <i>apeI rrn::apeI</i> (from pRRC-0638)	This study
Δ <i>patB</i> ^C	81-176 Δ <i>patB rrn::patB</i> (from pRRC-0639)	This study
Δ <i>patA</i> ^C	81-176 Δ <i>patA rrn::patA</i> (from pRRC-0640)	This study
11168-O	<i>C. jejuni</i> strain originally isolated from diarrheic feces	(178)
11168-GS	11168 that was genome sequenced after numerous passages	(64,178)
<u>E.coli Strains</u>		
DH5- α	F ⁻ , ϕ 80d <i>deoR lacZ</i> Δ <i>M15 endA1 recA1 hsdR17</i> (r _K -m _K ⁺) <i>supE44 thi-1 gyrA96 relA1</i> Δ (<i>lacZYA-argF</i>) U169	Invitrogen
BL21(λ DE3)	F ⁻ <i>ompT hsdS_B</i> (r _B ⁻ , m _B ⁻) <i>gal dcm</i> [λ DE3]	Novagen
<u>Plasmids</u>		
pGEM-T	High-copy, linearized, T-tailed, Blue/White, Ap ^R	Promega
pUC18-K2	Source of non-polar <i>aphA3</i> cassette; Ap ^R Km ^R	(153)
pGEM-T-0638	pGEM-T ligated to 0638 amplified with 0637-2 and 0639-5 (2113 bp); Ap ^R	This study
pGEM-0638:: <i>aphA-3</i>	pGEM-T-0638 inverse PCR amplified with 0638-3 and 0638-2 (4098 bp) and ligated to <i>aphA-3</i> (KpnI, HincII); Ap ^R , Km ^R	This study
pGEM-T-0639	pGEM-T ligated to 0639 amplified with 0639-1 and 0639-2 (2146 bp); Ap ^R	This study
pGEM-0639:: <i>aphA-3</i>	pGEM-T-0639 inverse PCR amplified with 0639-3 and 0639-4 (4267 bp) and ligated to <i>aphA-3</i> (KpnI, HincII); Ap ^R , Km ^R	This study
pGEM-T-0640	pGEM-T ligated to 0640 amplified with 0639-6 and 0641-4 (2396 bp); Ap ^R	This study
pGEM-0640:: <i>aphA-3</i>	pGEM-T-0640 inverse PCR amplified with 0640-1 and 0640-2 (4168 bp) and ligated to <i>aphA-3</i> (KpnI, HincII); Ap ^R , Km ^R	This study

pGEM-0638-40 ::aphA-3	pGEM-T ligated to 0637 fragment amplified with 0637-1 and 0638-1 (1483 bp), 0641 fragment amplified with 0641-1 and 0641-2 (822 bp), and <i>aphA-3</i> (KpnI, HincII); Ap ^R , Km ^R	This study
pRRC	<i>C. jejuni</i> rRNA spacer integration vector; Cm ^R	(154)
pRRC-0638	pRRC ligated to 0638 amplified with 0638-C1(NheI) and 0638-C2(MfeI) (1347 bp); Cm ^R	This study
pRRC-0639	pRRC ligated to 0639 amplified with 0639-C1(NheI) and 0639-C2(MfeI) (1276 bp); Cm ^R	This study
pRRC-0640	pRRC ligated to 0640 amplified with 0640-C1(NheI) and 0640-C2(MfeI) (1616 bp); Cm ^R	This study
pET28a(+)	Commercial vector for expression of recombinant 6x-His-tagged protein	Novagen
p0638-His ₆	pET28a(+) ligated to <i>apeI</i> amplified with 0638-eCF (NcoI) and 0638-eCR (EcoRI) (1121 bp) for expression of C-terminal 6x-His-tagged 0638; Km ^R	This study
pHis ₆ -0638	pET28a(+) ligated to <i>apeI</i> amplified with 0638-eNF (NheI) and 0638-eNR (EcoRI) (1116 bp); for expression of N-terminal 6x-His-tagged 0638 Km ^R	This study

APPENDIX 2. LIST OF PRIMERS USED WITH UNDERLINED RESTRICTION SITES IN LOWERCASE

Primer ¹ (Source)	Sequence (5' to 3')	Restriction Site
<u>ΔapeI</u>		
0637-2	GGTGGAGCATTAAGCGGAA	
0639-5	GCCACCAATAAGGCTTTTATTA AAAACTC	
0638-2*	GAA <u>ggtacc</u> TGAGTATGGAATCTATTGTGTCATTTGTATTTA	<i>KpnI</i>
0638-3*	CTATGAGCTGATGGCTAAAAAGTTACT	
<u>ΔpatB</u>		
0639-1	GGCTAGATGGCATATCAGTCTTTC	
0639-2	GACCATTTGTTAATTTGTGTAGTTCTTAACTC	
0639-3*	GAA <u>ggtacc</u> CTACAACAACCAAGCCAAGCA	<i>KpnI</i>
0639-4*	GTGGCGCAAGAGAAATGTCT	
<u>ΔpatA</u>		
0639-6	GACCAGTCAAATAGGATTTATAAGAAAGG	
0641-4	GCAGCAAACCTTATATCTTAGTATGAGTTCTT	
0640-2 *	GAA <u>ggtacc</u> GCTATCATTA AAAATACTAAATTCTAGAGAAAATA	<i>KpnI</i>
	AGTC	
0640-1*	GAATCTCCATTTTTACTAAAACCTTTTATCATAGC	
<u>Δoap</u>		
0637-1	TGCAAGAAATGCAGCAAATTTAAATCC	
0638-1	GAA <u>ggtacc</u> CTATGAGCTGATGGCTAAAAAGTTACT	<i>KpnI</i>
0641-1	GGATACACAGTCGATGAACCTG	<i>NcoI</i>
0641-2	GAA <u>ggtacc</u> A <u>cccggg</u> CCTTCAATCCAAAGCGAGATTTG	<i>KpnI, SmaI</i>
<u>Resistance Markers</u>		
cat-2 (1)	GTTTTTTGGATGAATTACAAGA	
aphA3-2 (1)	CTATTTTTTGACTTACTGGGGA	
<u>Complement</u>		
0638-C1	GCGGCG <u>gctagc</u> CGCAAGAGAAATGTCTAAACTTTTATTAGAAC	<i>NheI</i>
0638-C2	GCGGCG <u>caattg</u> CCCAGCAAGAATTTTAAAGAGCTAGATT	<i>MfeI</i>
0639-C1	GCGGCG <u>gctagc</u> CTTTTGGGGTTCTTTTATGATCTATCCTTTA	<i>NheI</i>
0639-C2	GCGGCG <u>caattg</u> TGAGTATGGAATCTATTGTGTCATTTGTATTTA	<i>MfeI</i>
0640-C1	GCGGCG <u>gctagc</u> GGTATGTAAGCGAACAACACGAA	<i>NheI</i>
0640-C2	GCGGCG <u>caattg</u> ACCAAGCCAAGCACTATAATCAAATAA	<i>MfeI</i>
<u>Ribosomal 16S Markers</u>		
ak233 (154)	GCAAGAGTTTTGCTTATGTTAGCAC	
ak234 (154)	GAAATGGGCAGAGTGATTCTCCG	
ak235 (154)	GTGCGGATAATGTTGTTTCTG	
<u>Protein Expression</u>		
0638-His-NF	GCGGCG <u>gctagc</u> CAAATTTAAATACAAATGACACAATAGATTC	<i>NheI</i>
	CATACT	
0638-His-NR	GCGGCG <u>gaattc</u> TTAATAATCAATGATATTTTTTAAATCCTCGAG	<i>EcoRI</i>
	TAACTT	

0638-His-CF	GCGGCG ccatgg GGCAAATTTAAATACAAATGACACAATAGA	<i>NcoI</i>
	TTCCATACT	
0638-His-CR	GCGGCG gaattc CCATAATCAATGATATTTTTTAAATCCTCGAGT	<i>EcoRI</i>
	AACTT	

[†] An asterisk (*) after the primer name indicates primers used for inverse PCR amplification for generating deletion constructs. The letter **C** in the primer name indicates primers used to generate complementation constructs in pRRC vectors. His in the primer name indicates primers used to amplify *Cjj81176_0638* for generating His-tagged protein expression constructs.

APPENDIX 3. MUROPEPTIDE COMPOSITION OF *C. JEJUNI* WILD-TYPE 81-176, Δ *apeI*, Δ *patB*, AND Δ *patA* SHOWING RELATIVE ABUNDANCE OF MUROPEPTIDES CORRESPONDING TO PEAKS IN HPLC CHROMATOGRAMS (FIGURE 3) OF SAMPLES ANALYZED IN JANUARY 2013.

Peaks ¹	Muropeptide	<i>81-176</i>	Δ <i>apeI</i>	Δ <i>patB</i>	Δ <i>patA</i>
1	Tri	5.8	12.3	7.3	9.5
2	Tetra	16.1	16.6	15.8	15.2
3	Penta-Gly5	0.6	0.8	0.7	0.7
4	Di	16.3	8.3	16.1	14.3
5	Tri-Ac	0.3	2.8	0.3	0.3
6	Tetra- Ac	0.6	2.6	0.0	0.0
7	Di-Ac	0.0	1.9	0.0	0.0
8	TetraTri	9.7	7.6	11.1	13.7
9	TetraPentaGly5	0.4	0.7	0.6	1.0
10	TetraTetra	19.0	17.0	18.0	21.2
11	Tetra Penta	0.0	0.1	0.0	0.0
12	TetraTri-Ac	1.8	3.4	1.6	0.0
13	TetraTetraTri	0.8	0.5	0.9	1.5
14	TetraTetra-Ac	0.3	1.1	0.0	0.0
15	TetraTetraTetra	2.9	7.0	1.9	2.8
16	TetraTriAnh I	1.2	0.5	1.3	1.3
17	TetraTriAnh II	2.6	1.6	2.5	2.7
18	TetraTetraAnh I	3.0	1.8	2.8	2.7
19	TetraTetraAnhII	5.6	3.7	4.9	4.9
20	TetraTetraTetraAnh	4.3	1.9	3.9	4.3
1 - 20	All known ²	91.2	92.3	89.5	95.9

¹ Peak numbers correspond to those from HPLC chromatograms in Figure 2. Muropeptides are named according to Glauner, Holtje and Schwarz (179) and are depicted in Fig. 2H. Di, disaccharide dipeptide (disaccharide = β 1,4-linked N-acetylglucosamine-N-acetylmuramic acid); Tri, disaccharide tripeptide; Tetra, disaccharide tetrapeptide; Penta, disaccharide pentapeptide; Gly, glycine in position 5 of a peptide side chain; Ac, O-acetyl groups at the C-6 hydroxyl group of MurNAc; Anh, 1,6-anhydromuramic acid. Disaccharides are linked to form dimers or trimers by crosslinks between amino acids 4 (D-Ala) and 3 (*meso*-DAP).

² Total abundance does not add up to 100% due to the presence of peaks for which a structure has not been assigned.

APPENDIX 4. MUROPEPTIDE COMPOSITION OF *C. JEJUNI* WILD-TYPE 81-176, Δ *apeI*^C, Δ *patB*^C, Δ *patA*^C, AND Δ *oap* SHOWING RELATIVE ABUNDANCE OF MUROPEPTIDES CORRESPONDING TO PEAKS IN HPLC CHROMATOGRAMS (FIGURE 3) OF SAMPLES ANALYZED IN AUGUST 2013

Peaks	Muropeptide	<i>81-176</i>	Δ <i>apeI</i> ^C	Δ <i>patB</i> ^C	Δ <i>patA</i> ^C	Δ <i>oap</i>
1	Tri	8.8	9.6	8.8	6.0	6.2
*	TetraGly4	0.4	0.4	0.4	0.3	0.4
2	Tetra	16.1	16.9	16.2	15.7	15.1
3	Penta-Gly5	0.8	1.0	1.2	0.9	1.0
4	Di	13.0	10.1	10.4	16.2	15.7
5	Tri-Ac	1.0	1.2	0.7	0.5	0.4
6	Tetra- Ac	0.6	0.7	0.5	0.0	0.0
7	Di-Ac	0.2	0.5	0.5	0.6	0.4
8	TetraTri	10.5	10.1	10.6	11.5	11.2
9	TetraPentaGly5	0.8	0.9	1.0	0.8	1.2
10	TetraTetra	21.4	22.4	23.0	22.4	22.5
12	TetraTri-Ac	1.5	1.7	0.9	0.0	0.0
13	TetraTetraTri	1.0	0.9	1.3	1.3	1.4
14	TetraTetra-Ac	1.7	1.8	1.4	0.4	0.0
15	TetraTetraTetra	2.5	2.8	3.1	2.9	3.4
16	TetraTriAnh I	1.1	1.0	1.1	1.3	1.2
17	TetraTriAnh II	2.4	2.1	2.2	2.5	2.5
18	TetraTetraAnh I	2.8	2.8	3.0	3.1	3.0
19	TetraTetraAnhII	5.2	5.0	5.1	5.4	5.5
*	TetraTetraTriAnh	1.1	0.9	1.3	1.4	1.7
20	TetraTetraTetraAnh	4.1	4.2	4.9	4.5	5.3
1 - 20	All known ²	96.8	97.1	97.4	97.7	97.9

¹Peak numbers correspond to those from HPLC chromatograms shown in Figure 2. A peak number designated with a “*” represents a muropeptide structure that was not previously described and therefore, the structure is not shown in Figure 2H. Muropeptides are named according to Glauner, Holtje and Schwarz (179) and are depicted in Fig. 2H. Di, disaccharide dipeptide (disaccharide = β 1,4-linked N-acetylglucosamine-N-acetylmuramic acid); Tri, disaccharide tripeptide; Tetra, disaccharide tetrapeptide; Penta, disaccharide pentapeptide; Gly, glycine in position 5 of a peptide side chain; Ac, O-acetyl groups at the C-6 hydroxyl group of MurNAc; Anh, 1,6-anhydromuramic acid. Disaccharides are linked to form dimers or trimers by DD- crosslinks between amino acids 4 (D-Ala) and 3 (*meso*-DAP).

²The total abundance does not add up to 100% due to the presence of peaks for which a structure has not been assigned.